



IDENTIFICATION OF OFFSHORE HOT SPOTS

An integrated biological oceanographic survey focusing on biodiversity, productivity and food chain relations

Scientific Report from DCE – Danish Centre for Environment and Energy

No. 357

2019



AARHUS
UNIVERSITY

DCE – DANISH CENTRE FOR ENVIRONMENT AND ENERGY

[Blank page]

IDENTIFICATION OF OFFSHORE HOT SPOTS

An integrated biological oceanographic survey focusing on biodiversity, productivity and food chain relations

Scientific Report from DCE – Danish Centre for Environment and Energy

No. 357

2019

Eva Friis Møller¹
Thomas Juul-Pedersen²
Christian Mohn¹
Mette Agersted Dalgaard³
Johnna Holding⁴
Mikael Sejr⁴
Mads Schultz¹
Signe Lemcke⁴
Norman Ratcliffe⁵
Svend Erik Garbus¹
Daniel Spelling Clausen¹
Anders Mosbech¹

¹ Aarhus University, Department of Bioscience

² Greenland Institute of Natural Resources

³ University of Oslo

⁴ Aarhus University, Arctic Research Centre

⁵ British Antarctic Survey



AARHUS
UNIVERSITY

DCE – DANISH CENTRE FOR ENVIRONMENT AND ENERGY

Data sheet

Series title and no.:	Scientific Report from DCE – Danish Centre for Environment and Energy No. 357
Title:	Identification of offshore hot spots
Subtitle:	An integrated biological oceanographic survey focusing on biodiversity, productivity and food chain relations
Authors:	Eva Friis Møller ¹ , Thomas Juul-Pedersen ² , Christian Mohn ¹ , Mette Agersted Dalgaard ³ , Johnna Holding ⁴ , Mikael Sejr ⁴ , Mads Schultz ¹ , Signe Lemcke ⁴ , Norman Ratcliffe ⁵ , Svend Erik Garbus ¹ , Daniel Spelling Clausen ¹ , Anders Mosbech ¹
Institutions:	¹ Aarhus University, Department of Bioscience, ² Greenland Institute of Natural Resources, ³ University of Oslo, ⁴ Aarhus University, Arctic Research Centre, ⁵ British Antarctic Survey
Publisher:	Aarhus University, DCE – Danish Centre for Environment and Energy ©
URL:	http://dce.au.dk/en
Year of publication:	December 2019
Editing completed:	November 2019
Referee:	David Boertmann
Quality assurance, DCE:	Kirsten Bang
Linguistic QA:	Anne van Acker. Greenlandic summary by Scantext
Financial support:	This study is part of the Northeast Greenland Environmental Study Programme. The Northeast Greenland Environmental Study Programme is a collaboration between DCE – Danish Centre for Environment and Energy at Aarhus University, the Greenland Institute of Natural Resources, and the Environmental Agency for Mineral Resource Activities of the Government of Greenland. Oil companies operating in Greenland are obliged to contribute to knowledge regarding environmental matters. The Strategic Environmental Impact Assessment and the background study programme is funded under these commitments administered by the Mineral Licence and Safety Authority and the Environment Agency for Mineral Resources Activities.
Please cite as:	Møller EF, Juul-Pedersen T, Mohn C, Dalgaard MA, Holding J, Sejr M, Schultz M, Lemcke S, Ratcliffe N, Garbus SE, Clausen DS, Mosbech A. 2019. Identification of offshore hot spots. An integrated biological oceanographic survey focusing on biodiversity, productivity and food chain relations. Aarhus University, DCE – Danish Centre for Environment and Energy, 65 pp. Scientific Report No. 357 http://dce2.au.dk/pub/SR357.pdf
	Reproduction permitted provided the source is explicitly acknowledged
Abstract:	This study provides information on the marine ecosystem in the western Greenland Sea and the shelf off Northeast Greenland. The biology in the area was clearly associated with the physical-chemical environment. Integrated phytoplankton biomass and production were highest at or outside the East Greenland shelf break. Likewise, the zooplankton biomass was highest along the shelf break area, and species composition reflected the origin of the water. As expected, the survey showed low diversity and abundance of seabirds and marine mammals. In total 22 and 9 species were observed, respectively. Little auks were the most numerous seabirds with the highest densities found along the shelf break.
Keywords:	Arctic, marine, ecosystem, seabird, marine mammals, phytoplankton, zooplankton, biogeochemistry
Layout:	Anne van Acker
Front page photo:	Eva Friis Møller
ISBN:	978-87-7156-456-3
ISSN (electronic):	2245-0203
Number of pages:	65
Internet version:	The report is available in electronic format (pdf) at http://dce2.au.dk/pub/SR357.pdf

Contents

1	Summary	5
2	Sammenfatning	7
3	Eqikkaaneq	8
4	Background	9
5	Methods	11
5.1	Physical oceanography	11
5.2	Biogeochemistry and phytoplankton	11
5.3	Zooplankton	14
5.4	Acoustic measurements	14
5.5	Seabirds and marine mammals	16
6	Results and discussion	18
6.1	Physical oceanography	18
6.2	Biogeochemistry and phytoplankton	24
6.3	Zooplankton	29
6.4	Acoustic measurements	32
6.5	Seabirds and marine mammals	34
7	References	54
	Appendix 1	57

[Blank page]

1 Summary

This study is part of the Strategic Environmental Study Plan for Northeast Greenland established to provide environmental information for planning and regulating oil exploration activities and oil spill response in the Greenland Sea and the shelf off Northeast Greenland. The aim is to provide information on the ecology and temporal and spatial sensitivity of this very little studied marine ecosystem. As a part of this, an interdisciplinary survey with R/V Dana was conducted in August/September 2017. 82 stations were sampled between 2° W and 20° W and 74.5° N and 79° N, primarily at stations on the shelf (100-400 m depth), but also at deeper stations at the shelf break and off shelf (up to 3.000 m depth).

During the survey, waters in the upper 100 m were dominated by Polar surface water, which is of Arctic origin and mainly associated with the East Greenland Current. Arctic Atlantic water, which is of Arctic origin with contributions from Atlantic waters therefore had higher salinity and dominated the water masses in the depth range 100-200 m. The warmest and most saline water was return Atlantic water or re-circulating Atlantic water, and was mainly found along the Greenland shelf break in the depth range 100-300 m. The coexistence of colder and less saline East Greenland Current waters and warmer and more saline waters from the Atlantic was clearly visible as a dynamic frontal system along the East Greenland shelf break during the cruise. A general trend in nutrient conditions throughout the study area was prevailing low concentrations in the surface waters (<20 m), particularly for nitrate at the shelf. The highest integrated levels of nitrate in the upper 50 m were recorded along the shelf break corresponding with deeper mixing of the water column.

The biology in the area was clearly associated with the physical-chemical environment. Depleted nitrate levels in the surface layer, which also has the most favourable light conditions, likely were a major factor controlling phytoplankton production. Integrated phytoplankton biomass and production within the 0-50 m depth strata across the study area revealed the highest values at or outside the East Greenland shelf break. Likewise, the mesozooplankton biomass and community composition were clearly associated with the oceanography and bathymetry of the area. The biomass was highest along the shelf break area, and species composition reflected the origin of the water. The North Atlantic *Calanus finmarchicus* was present at all stations, but much more abundant at the stations off the shelf in the Greenland Sea. The Arctic *Calanus* species *C. glacialis* and *C. hyberboreus*, on the other hand, had the opposite patterns, and were not found at all in the upper 50 m in the Greenland Sea. A large part of the dominant *Calanus* was still present in the surface water, which is important for visual predators and predators feeding from the surface, e.g. seabirds like little auk. The macrozooplankton like the mesozooplankton had elevated biomass in the shelf break area, but also at the stations near-shore. Acoustic measurements gave a high-resolution distribution of the density of organisms along the cruise track, and confirmed the pattern found by net sampling.

As expected, the survey showed low diversity and abundance of seabirds and marine mammals. 22 bird species and 9 species of marine mammals were observed. Little auks were the most numerous seabird observed at the cruise

with the highest densities observed along the shelf break, and lower densities on the shelf in the open pack ice. Fulmars (*Fulmarus glacialis*) and black-legged kittiwakes (*Rissa tridactyla*) were widespread in low numbers. Very few thick-billed murres (*Uria lomvia*) were observed during the Dana cruise. This is consistent with the records in the Greenland Seabirds at Sea database and SEA-TRACK data where thick-billed murres mainly have been observed further to the east.

2 Sammenfatning

Som en del af miljøforskningsprogrammet i Nordøstgrønland blev der i august-september 2017 gennemført et tre ugers interdisciplinært forskningstogt med det danske forskningsskib Dana. 20 forskere deltog, og der blev taget prøver på 82 stationer mellem 2° V og 20° V og 74,5° N og 79° N primært på kontinentalsoklen, hvor vanddybden var 100-400 m, men også på dybere vand. De øverste 100 m af vandsøjlen var domineret af polarvand fra nord, mens vandet dybere i vandsøjlen i højere grad var påvirket af atlantisk vand, og der var en meget dynamisk frontzone langs kanten af kontinentalsoklen. Samtidig var vandet i overfladen meget næringsfattigt. De fysiske-kemiske karakteristika i området havde stor betydning for biologien. Den højeste produktion af planteplankton fandtes, hvor der skete en opblanding af de øverste vandlag i zonen mellem kontinentalsoklen og de dybere områder. Det samme mønster afspejlede sig også i det næste led i fødekæden: dyreplankton. Samtidig var det også tydeligt, at arktiske arter dominerer i det polare vand, mens områder tættere på de dybe områder i Grønlandshavet var mere påvirket af atlantiske arter. En stor del af det dominerende dyreplankton var stadig til stede i de øverste vandlag, hvad der har stor betydning for de større dyr, der lever af dem, som fx fugle, fisk og grønlandshval. Diversiteten og antallet af fugle og havpattedyr var generelt lavt. Søkonger var de mest talrige og blev primært observeret i områder, hvor der var høj planktonproduktion på kontinentalskrænten. Mallebukker (*Fulmarus glacialis*) og rider (*Rissa tridactyla*) blev fundet spredt i området i lavt antal. Kun ganske få polarlomvier (*Uria lomvia*) blev observeret, og formodentlig trækker de primært længere mod øst.

3 Eqikkaaneq

Kalaallit Nunaata kangiani avatangiisini misissuinerup ilaattut 2017-imi august-septemberimi sapaatini akunnerni pingasuni danskit umiarsuaannik ilisimatuussutsikkut misissuummik Danamik ilisimatusartoqarpoq. Ilisimatusartut 20-t peqataapput uumasooqarfiusunilu 82-imi 2° W-imi, 20° W-imi, 74.5° N-imi 79° N-imilu, pingaartumik immap naqqata nunavimmut atasortaata killingani, imarmi 100-400-nik ititigisumi itinerusunilu misileraasoqarluni. Imaq immap qaavaniik 100 meterinut ititigisup annerpaartaa imermik avannaaneersumik akoqarpoq, itinerusorli atlantikup imertaanik annerusumik akoqarluni kiisalu immap naqqata nunavimmut atasortaata killinga atuarlugu aporaaffiusoq allanngorartuuvoq. Aammattaaq immap qaava inuussutissakitsuaraavoq. Sumiiffimmi sarfaq inuussutissallu uumassusilinnut pingaaruteqarluinnarsimavoq. Immap naqqata nunavimmut atasortaata killingata itisuullu akornanni immap qaavani akulerussuuttoqarnerani naasut tappiorannartut pingaartumik pinngortarsimapput. Nerisariaanni tullernguuttuni tassa uumasuni tappiorannartuni tamanna aamma atuussimavoq. Taamatuttaaq Issittup imartaani issittumi uumassusillit amerlanerusut illuatungaanili Kalaallit Nunaata imartaani imarmut itisuumut qaninnerusuni issittumi uumasusilinnit sunnertisimanerusut takuneqarluarsinnaasimavoq. Immap qaavani uumasut tappiorannartut pingaartumik uumapput, taakkualu uumasunut taakkuninnga nerisaqartunut soorlu timmissanut, aalisakkanut arfivinnullu pingaaruteqarluinnarput. Timmissat imaanilu miluumasut assigiinngisitaarnerat amerlassusaallu annikitsuaraasimapput. Appaliarsuit amerlanerpaasimapput sumiiffinnilu tappiorannartunik annertuumik naasoqarfiusuni siumorneqartarsimallutik. Timmiakuluit taateraallu sumiiffimmi siaruarsimapput ikitsuinnaasimallutillu. Appat ikitsuinnaat siumorneqarsimapput kangimullu ingerlaassangatinneqarlutik.

4 Background

Marine hot spots are areas with enhanced and concentrated primary production, areas with high biodiversity and areas with concentrations of biota; they will often contain all of these characteristics. Their temporal and spatial distribution, their predictability and the physical factors which may govern their presence are important issues. Information on these hot spots is essential for the oil companies which shall prepare environmental impact assessments, for preparing Net Environmental Benefit Analysis (NEBA) and for the authorities, which shall regulate the activities.

Marine Arctic regions with seasonal sea ice usually have intense periods of high pelagic production, thereby fuelling and sustaining the marine food chains throughout the year. In the assessment area, nutrient-rich Atlantic water is mixed with the nutrient-poor water from the Arctic Ocean and in these front areas high primary productivity may occur, confirmed by remote sensing (satellite studies) which indicates the presence of areas of high surface biomass. However, remote sensing alone cannot provide reliable spatial description of biomass and productivity, due to the lacking ability to identify the occurrence of subsurface biomass. Remote sensing data which has been calibrated and verified by *in situ* data can, however, assist in providing seasonal and spatial information beyond the field measurements. The long life of the secondary producers including overwintering of non-feeding stages means that they can be transported away from the areas with high primary production that supported their growth, and concentrated in other areas depending on bathymetry and currents. Thus, hot spots of primary production and secondary production may be decoupled. Earlier studies indicate a rich diversity of planktonic organisms in the coastal areas, but since the diversity has not been described in the offshore assessment area, potentially sensitive areas cannot be identified at the moment. The indicated heterogeneous distribution of biological productivity and limited understanding of the pelagic food chain in the assessment area causes significant uncertainty to environmental impact assessments of oil operations and possible oil spills. Moreover, dynamics of the pelagic-benthic coupling sustaining the offshore benthic communities remains largely unknown in the area.

Only little is known about the seabird numbers and distribution in the western Greenland Sea during autumn. Some information is available from seabirds at sea surveys using ships of opportunity, especially seismic surveys, and some information is available from tracking studies; the available information was summarized in the SEIA in 2011 (Boertmann & Mosbech 2011). Relatively few seabirds breed on the coasts of northeast Greenland (NEG), while large numbers of seabirds breed on Svalbard, including estimates of 819,000 breeding pairs of thick-billed murre, more than a million pairs of little auks (Isaksen & Bakken 1995) and 243,000 breeding pairs of black-legged kittiwakes (Fau-chald et al. 2015). The autumn migration of these Svalbard birds is assumed to pass through the Greenland Sea, and it is important to understand this migration in space and time in relation to oil activities. It is known that thick-billed murres conduct a swimming migration where the male and the chick swim together, and tracking of little auks from Svalbard and the colonies near Scoresby Sund (Fort et al. 2013; Mosbech et al. 2012) have identified a post-breeding and moulting area in the Greenland Sea region. In the NEG programme there are several studies providing further information on seabird

distribution and numbers including aerial surveys and tracking of ivory gulls and little auks. In this study, we recorded seabirds and marine mammals in an integrated marine ship-based survey with the aim of correlating the observed seabird and marine mammal distribution with the biological oceanography recorded synoptically on the cruise. Here we present results of distribution and density of seabirds and marine mammals together with supplementary information from previous surveys, and recent tracking data from the SEATRACK programme (<http://seatrack.seapop.no>) providing information on the linkage to colonies in the North Atlantic.

The assessment area is highly heterogeneous in terms of ice cover and thus also primary productivity may be highly patchy resulting in hot spots. Large parts of the area are dominated by heavy drift ice throughout most summers, leading to relatively low productivity, and causing logistical challenges for scientific studies. Previous studies have thus concentrated on three areas where the open-water season is longer and productivity is (expected to be) higher: (i) the North East Water Polynya (NEW) (Hirche et al. 1994; Bauerfeind et al. 1997; Pesant et al. 2002), (ii) the extensive fjord systems along the East Greenland coast, where only Young Sound has been subject to detailed scientific studies (Rysgaard & Glud 2007; Middelbo et al. 2018; Holding et al. 2019), and (iii) the marginal ice zone in the Greenland Sea (Richardson et al. 2005; Møller et al. 2006; Qu et al. 2016). To supplement the existing knowledge, the major activity of this project was a three-week ship-based survey around 1 September, closely integrated with synoptic aerial surveys for seabirds and marine mammals. In this report we present the data from the three-week ship survey on physical and biological oceanography, and the distribution of seabirds and marine mammals. Data on distribution of fish (including acoustic fish abundance survey) and the benthic community carried out in relation to the oceanography at the same cruise are presented in Hansen et al. 2019 and reports from Greenland Institute of Natural Resources.

5 Methods

An interdisciplinary survey with R/V Dana was conducted from 22 August to 12 September 2017. At eighty-two stations samples were collected between 2° W and 20° W and 74.5° N and 79° N, primarily at 100-400 m depth on the shelf, but also at deeper stations at the shelf break and off shelf. The cruise track was altered compared to the original planned due to the ice conditions in the area (*figure 5.1*). A full list of activities can be found in Appendix 1. Additionally, sampling of selected parameters was carried out on a succeeding cruise by R/V Dana funded by the Danish Centre for Marine Research (lead by Prof. Marit-Solveig Seidenkrantz, AU).

5.1 Physical oceanography

CTD (Conductivity-Temperature-Depth) profiles were collected at 82 stations (including repeated casts at selected biological stations) with a 24 Hz sampling rate Seabird SBE 911plus CTD system attached to a 12 5-litre bottle carousel water sampler. The CTD system was equipped with sensors for conductivity, temperature, pressure, oxygen (SBE 43), PAR (Biospherical/Licor) and Chlorophyll (Turner Cyclops). Temperature and salinity CTD data were post-processed using the Seabird Seasave data acquisition and processing software. Important processing steps included the generation of upcast bottle files to create a record of environmental data at water bottle release depths, the removal of large outliers, and depth-averaging of downcast CTD profiles over 0.5 m vertical bins. Data on currents in the area were extracted from AVISO (Archiving, Validation and Interpretation of Satellite Oceanographic data), a service for processing and distributing satellite remote sensing data from Topex/Poseidon, Jason-1, ERS-1 and ERS-2, and EnviSat (<https://aviso-data-center.cnes.fr/>).

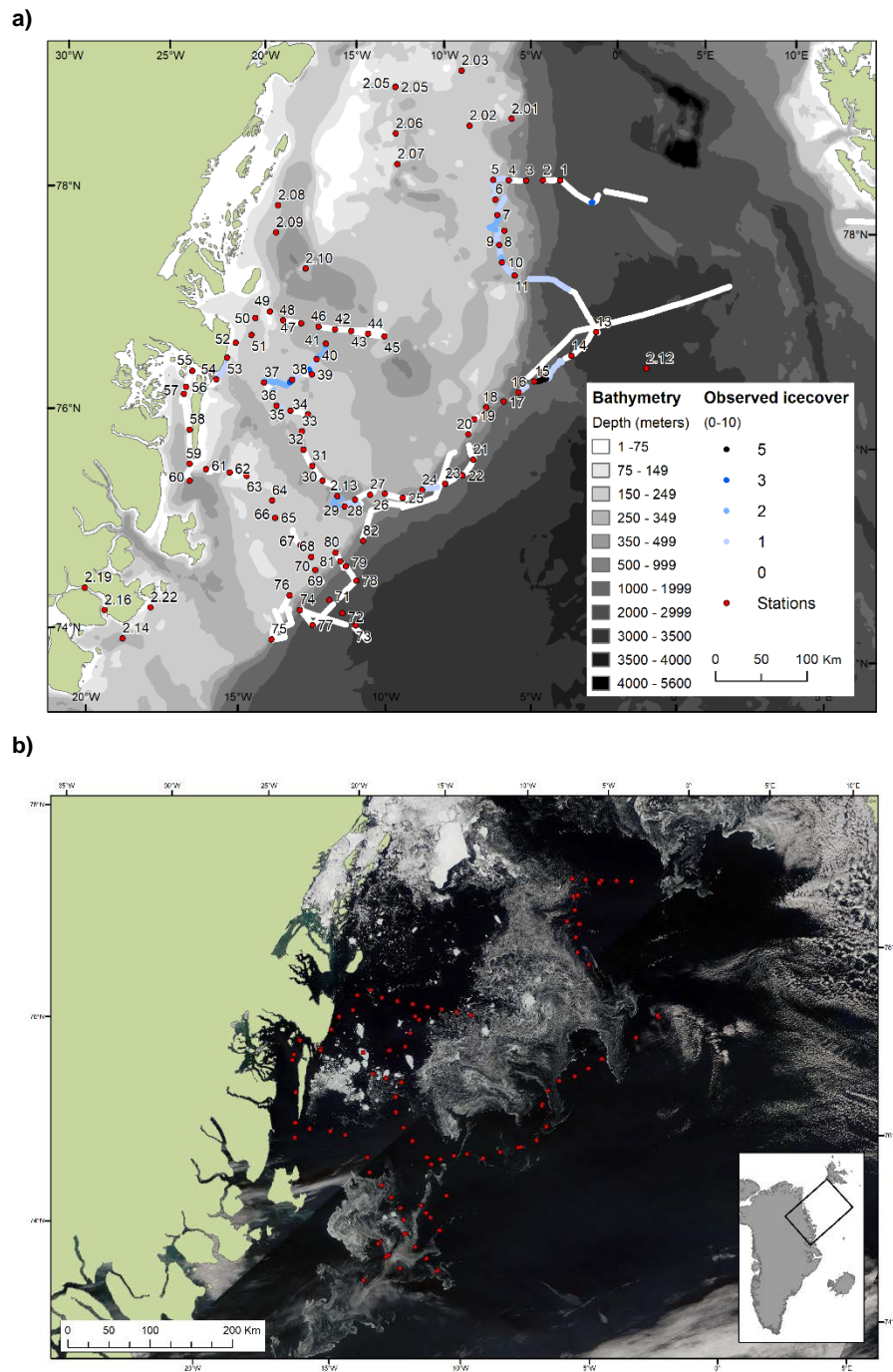
5.2 Biogeochemistry and phytoplankton

Water samples were collected at 27 stations (biological stations) using a 12-bottle Rosette water sampler (5-liter bottles) equipped with a Seabird SBE 911plus CTD system. Chlorophyll-*a* measurements were conducted with a Turner Cyclops fluorescence sensor attached to the CTD calibrated against samples measured as described below. The water samples were analysed for a range of biogeochemical and biological parameters (*table 5.1*).

Nutrient samples were frozen immediately after collection and later analysed on a flow injection autoanalyser, following Hansen & Koroleff (1999). Concentrations of nitrate, silicate, phosphate and ammonia were measured, but only results of nitrate and silicate will be presented here.

Samples for pigment analysis (250-500 ml) were filtered on 25 mm GF/F (Whatman) and 10 µm filters and extracted in 96 % ethanol for 24 h before being analysed on a fluorometer (TD-700, Turner Design) calibrated against a chlorophyll-*a* standard (Jespersen & Christoffersen 1987). Fluorometric measurements were done before and after 1 M HCl addition.

Figure 5.1. The area is characterized by a large 100-250 km wide shelf area with water depths up to 400 m, a shelf break about 75 km wide where water depth falls to 1,000-1,200 m and a deep ocean area. a) Map with station numbers. Stations numbered 1-82 are from the NEG-programme survey, while those numbered 2.01-2.22 are from a succeeding research cruise. b) The sea ice extent on 26 August 2017 together with the stations at the NEG cruise. The sea ice moved further south during the cruise, reflected in the displacement between sea ice and stations on the map.



Primary production (PP) was measured on samples from 5 m depth and the depth of chlorophyll-*a* maxima by the ^{14}C incubation technique (Steeman Nielsen 1952) using photosynthesis-irradiance curves (P-I curves). Unfiltered seawater (1.2 l) was transferred to a glass flask and 3 ml of $\text{NaH}^{14}\text{CO}_3$ ($20 \mu\text{Ci mL}^{-1}$; DHI Lab, Denmark) was added and mixed carefully before being added to 14 incubation bottles (55 ml), i.e. 11 light-incubated bottles and 3 dark-incubated bottles. The light bottles from each depth were linearly arranged in the light incubator for ca 2 hours. Photosynthetically active radiation (PAR) was measured within each incubator bottle (US-SQS/L, Submersible Spherical Micro Quantum Sensor, Heinz Walz GmbH) and was used to create P-I curves. Incubation bottle samples were filtered on 25 mm GF/F filters (Whatman) and the filters placed inside plastic scintillation vials, 100 μl of 1 M HCl was added to remove excess $\text{NaH}^{14}\text{CO}_3$ and the filters were fumigated for 24

hours in a fume hood. Samples were subsequently frozen. 10 ml scintillation cocktail (Ultima Gold, Perkin Elmer) was added to the samples before being counted on a scintillation counter (Liquid Scintillation Analyzer, Tri-Carb 2800TR, PerkinElmer). Primary production rates were calculated from the obtained P-I curves using the light attenuation coefficient from the measured PAR profile and chlorophyll-*a* concentrations of the sample water. Primary production was calculated using the equation:

$$PP \text{ (mg C m}^{-3} \text{ h}^{-1}) = (\text{DPM}_{\text{filter}} \times \text{DIC} \times 1.05) / (\text{DPM}_{\text{added}} \times \text{incubation time})$$

where $\text{DPM}_{\text{filter}}$ is the signal measured on the scintillation counter, DIC is the *in situ* dissolved inorganic carbon concentration (estimated as 2,000 μM) and $\text{DPM}_{\text{added}}$ is the activity of the added ^{14}C which is corrected for the incubation time. The constant 1.05 is the ^{14}C discrimination factor due a 5 % metabolic discrimination against the heavier ^{14}C isotope. Primary production values were divided by the chlorophyll-*a* concentration at each sample depth to produce biomass specific primary production rates ($\text{mg C mg Chl-}a^{-1} \text{ h}^{-1}$).

Underwater Photosynthetically Active Radiation (PAR) was measured using the LI-COR Biospherical PAR sensor attached to the CTD. Incoming irradiance (PAR) was obtained from the vessel's on-board meteorological station. *In situ* primary production was calculated at chlorophyll-*a* sampling depths based on the obtained biomass specific primary production rates, *in situ* chlorophyll-*a* concentration, *in situ* daily average incoming irradiance (PAR) corrected for the *in situ* light attenuation in the water column obtained from the CTD profiler. Primary production rates from 5 m and depth of chlorophyll-*a* maxima were considered representative above and below the mixed layer depth (MLD), respectively.

Table 5.1. Sample depths for biogeochemical parameters.

Depth (m)	Nutrients ¹	Pigments ²	Prim. prod.	C/N ⁵
1	X	X		
5	X	X	X	X
10	X	X		
15	X	X		
20	X	X		
30	X	X		(X)
50	X	X		(X)
100	X	X		(X)
200				X
300				(X)
Chl- <i>a</i> max ³				X
Bottom ⁴				X

¹ Nutrients: nitrate, silicate, phosphate and ammonia

² Pigments: chlorophyll-*a* and phaeopigments at GF/F and 10 μm size fractions

³ Sampling at chlorophyll-*a* maxima

⁴ Sampling at near-bottom down to a maximum of 1,000

⁵ The number of sampling depths was reduced (parenthesis) following the first nine stations due to time constraints during sample preparation

Water samples (2.5-10 l) for total particulate carbon and nitrogen concentration were filtered on pre-combusted (450 °C for 8 hours) 25 mm GF/F filters (Whatman), dried at 60 °C for 12 hours and frozen prior to analysis. The samples will be analysed on a mass spectrometer.

Trapezoid integration was used to calculate the integrated concentrations of nutrients and chlorophyll-*a* as well as primary production values for the 0-50 m depth strata, i.e. covering the photic zone at all, except two biological stations (>50 m).

5.3 Zooplankton

Zooplankton were sampled at 27 stations. Mesozooplankton were collected in four depth strata with a Hydrobios Multinet equipped with 50 μm nets. Macrozooplankton were sampled with a MIK ring net (ICES 2017) equipped with 1,500 μm black nets in the upper 100 m. Additional samples in selected depth strata were taken when the acoustic measurement suggest high concentrations of organisms.

Samples were preserved in buffered formalin (4 % final concentration). For copepods, individuals were counted, and species/genera, stage and sex were identified. *Calanus hyberboreus* were identified to species for copepodite stages CIII-CVI, while *C. finmarchicus* and *C. glacialis* were identified to species for CV and CVI based on prosome length (Swailethorp et al. 2011; Nielsen et al. 2014). All smaller stages of *Calanus* were only identified to genus. Prosome length was measured for 10 individuals in each species/stage group in all samples. Biomass of copepods was calculated using length: C-weight regressions from literature (Klein Breteler et al. 1982; Hirche & Mumm 1992; Sabatini & Kiørboe 1994; Satapoomin 1999; Hygum et al. 2000; Madsen et al. 2001). Non-copepod zooplankton groups were identified to genus or species and counted; their total lengths were measured. Biomass was calculated using length: C-weight regressions from literature.

5.4 Acoustic measurements

5.4.1 Spatial distribution of organisms

Spatial distribution of plankton and fish was measured using three scientific Simrad EK60 split beam echo sounders with frequencies of 18, 38 and 120 kHz. The transducers were hull mounted on the vessel 6 metres below the sea surface. See *table 5.2* for technical settings of the transducers.

The vessel sailed a total of 1520 nmi during the period of the cruise. Analyses of acoustic data were performed using the software system LSSS (Large Scale Survey System, Institute of Marine Research). Estimations of relative zooplankton (and fish) abundance (presented as nautical area scattering coefficient, NASC, sA ($\text{m}^2 \text{nmi}^{-2}$)) were performed using raw data from 38 kHz in 1 nmi intervals and only between stations (survey speed ~ 10 knots). Data from all three frequencies, together with net data (if/when available), were used to distinguish between fish and zooplankton. Areas with noise on either of the frequencies would be excluded from the frequency response comparison. Hence, frequency response of all three frequencies could often only be used in the upper 200 metres (depending on the noise level) as this depth was the maximal reach for 120 kHz. Also, sometimes data from 18 kHz would be noisy close to the bottom or close to the surface. Due to resonance, fish with a swim bladder would have a higher frequency response at 18 and 38 kHz (depending on size) than at 120 kHz, whereas zooplankton such as krill and copepods would have the highest response at 120 kHz. The total backscatter was divided into three different groups (i) fish and stronger scatterers, ii) macroplankton (i.e. krill-like organisms), and iii) smaller zooplankton, and mean

volume backscattering strength (S_v , dB) thresholds of -82 dB, -85 dB and -90 dB, respectively, were used to separate the three groups.

Table 5.2. EK60 and Wideband Autonomous Transceiver (WBAT) settings.

	EK60 system			WBAT system	
	18 kHz	38 kHz	120 kHz	70 kHz	200 kHz
Transducer					
Model	ES18-2013	ES38-B	ES120-7c	ES70-18CD	ES200-7CD
Equivalent beam angle $10 \log \Psi$ (dB)	-17.20	-20.60	-20.4	-13.00	-20.70
Beams					
Alongship half power opening angle (deg)	10.60	7.03	6.44	17.65	6.81
Offset along angle (deg)	-0.13	-0.03	-0.11	0.41	0.08
Athwartship half power opening angle (deg)	10.79	7.01	6.47	20.3	6.74
Offset arhward. angle (deg)	0.01	-0.08	0.05	-0.69	0.02
Survey settings					
Sound speed (m/s)	1456	1456	1456	1456	1456
Puls duration (ms)	1.024	1.024	1.024	0.256	0.256
Electrical power (W)	2000	2000	250	125	75

Analysing acoustic data is a subjective process, and as it is difficult to separate e.g. mesopelagic fish from krill, the scrutinized data have to be taken with precautions. However, as the data have been analysed in the same manner, i.e. using the same threshold values for the three groups, it is possible to compare relative sA values (proxy for abundance) across areas. sA has only been assigned to “plankton” in the upper 100 metres, both due to the fact that the main part of the zooplankton biomass was here, and that data from 120 kHz transducer, which is used to verify that it is plankton, does not reach much further.

The relative abundance (sA values) for the three different groups (plankton, krill/amphipods and “others” (stronger scatterers)) was plotted on a geographical map illustrating the spatial distribution of organisms. The relative abundance was estimated by Inverse Distance Weighted Interpolation in ArcGIS. Data have been plotted for the whole water column (sA total, although for plankton only for the upper 100 metres), and in different depth strata (0-50, 50-100, 100-150, 150-200 and 200 m-bottom).

5.4.2 Vertical distribution of organisms

At 38 stations (however not between st. 13 and 28 (see figure 4.1) due to technical problems), a WBAT (Wideband Autonomous Transceiver, Simrad) was mounted on the CTD to make vertical profiles of the backscatter in the area. Two split beam transducers (70 kHz (ES70-18CD) and 200 kHz (ES200-7CD), Simrad) were connected to the WBAT and mounted sideward on the WBAT frame and recorded acoustic data in a 100 metre range horizontally. WBAT data were used to get an idea of the vertical distribution of targets >2 mm in size (like *Calanus* spp., krill, amphipods, and fish larvae). The WBAT was programmed to ping with the 200 kHz transducer while being lowered down and to ping with 70 kHz when being heaved from bottom towards the surface. Ping interval was 0.6 s for both transducers, and the CTD/WBAT was hauled with 0.25 m s^{-1} in the upper 100 metres and 0.50 m s^{-1} below this depth. Net data, when/if available, were used to identify acoustic targets in different depth strata and also data from EK60 (18, 38 and 120 kHz) on a given station were used for target identification by using the frequency response. Here, we

only used data from 200 kHz when estimating abundance and vertical distribution. See *table 5.2* for technical settings of the two transducers.

5.4.3 Target strength (TS) measurements and abundance estimates

Due to high quality of data with minimal noise, WBAT data from the 200 kHz transducer were used to detect single targets for mean target strength (TS, dB) measurements on each station. A minimum of 100 TS measurements from single targets of different size groups, respectively, were exported and the corresponding spherical scattering cross-section σ (m²) was calculated for each target by using the formula:

$$\sigma = 4\pi \times 10^{(TS/10)}$$

where TS = single measurements of targets.

Subsequently, a mean σ was calculated and converted to a mean TS value by:

$$TS = 10 \times \log(\sigma/4\pi)$$

where σ = mean σ for the whole water column.

For small zooplankton (copepods), single targets were detected 2-10 metres away from the WBAT. For larger targets (macroplankton and fish larvae (and stronger targets)), TS measurements were detected ~30-50 and ~60-80 metres away from the WBAT, respectively, due to avoidance closer to the WBAT. TS was measured in the whole water column at each station to give a mean σ .

In the range 50-80 metres away from the WBAT, targets with a TS >-60dB (e.g. mesopelagic fish) were removed. Afterwards, copepods, macroplankton and 0-group (fish larvae and stronger targets than macroplankton) were identified by mean volume backscattering strength (Sv) thresholds of -90 dB, -85 dB and -75 dB, respectively, and assigned the corresponding sA within these threshold intervals. sA values were analysed in 10 metre depth intervals (10-20 m, 20-30 m, etc). For each station, the total sA from each 10 metre depth interval and mean σ for each station were used to calculate the vertical distribution (in 10 m depth intervals) and abundance (ind m⁻³) for each size group (copepods, macroplankton and 0-group, respectively) by:

$$Abundance (ind m^{-3}) = \frac{sA(50-80 m)}{\sigma} / 1852^2 \times z$$

where sA (50-80 m) = total sA (m² nmi⁻²) 50-80 metres away from WBAT, σ = mean σ (m²) at the given station, z = range in metres (here 30 metres (from 50-80 m)). sA is given in m² nmi⁻², and therefore, z is multiplied by 18,522 to get abundance per metre. Due to reflection from the surface, the upper 10 metres of the water column was not included in the analysis.

5.5 Seabirds and marine mammals

During the Dana cruise, 22 August to 10 September 2017, data were systematically collected on abundance and distribution of seabirds and marine mammals according to the Manual for Seabirds and Marine Mammal Survey on Seismic Vessels in Greenland, and stored accordingly in the Greenland Seabird at Sea database (Johansen et al. 2015). Supplemental observations were

collected during the subsequent survey in the area, 12 September - 1 October 2017. However, as most daylight hours during this survey were spent stationary on stations, the effort was low.

Systematic observations were conducted on transects between oceanographic stations from an observation box on top of the bridge, 12,5 m above sea level and at a typical cruising speed of 10 knots. Seabird observations were conducted using 90 degree transect type A (50, 100, 200, and 300 distance bands) with snapshots of flying birds (2 min.) and 180 degree total counting. Marine mammals were observed in 180 degree transects using distance sampling. Due to low visibility, some of the transects were truncated at 100 m width. At most transects, there were two observers supplementing each other. Bird densities were calculated using species specific Effective Search Width based on the Greenland Seabirds at Sea Database (Johansen et al. 2015) and mapped along the transects using inverse distance weighing (IDW) (IDW fixed width 15 km, power = 2). As a starting point for further analysis in the Strategic Environmental Assessment distribution maps from previous surveys in the Greenland Sea, stored in the Seabird at Sea database (surveys mainly from seismic vessels in 1994, 1995, 2006, 2007, 2009) as well as tracking data as screen dump maps from the SEATRACK programme (<http://seatrack.sea-pop.no>) are presented in the species account.

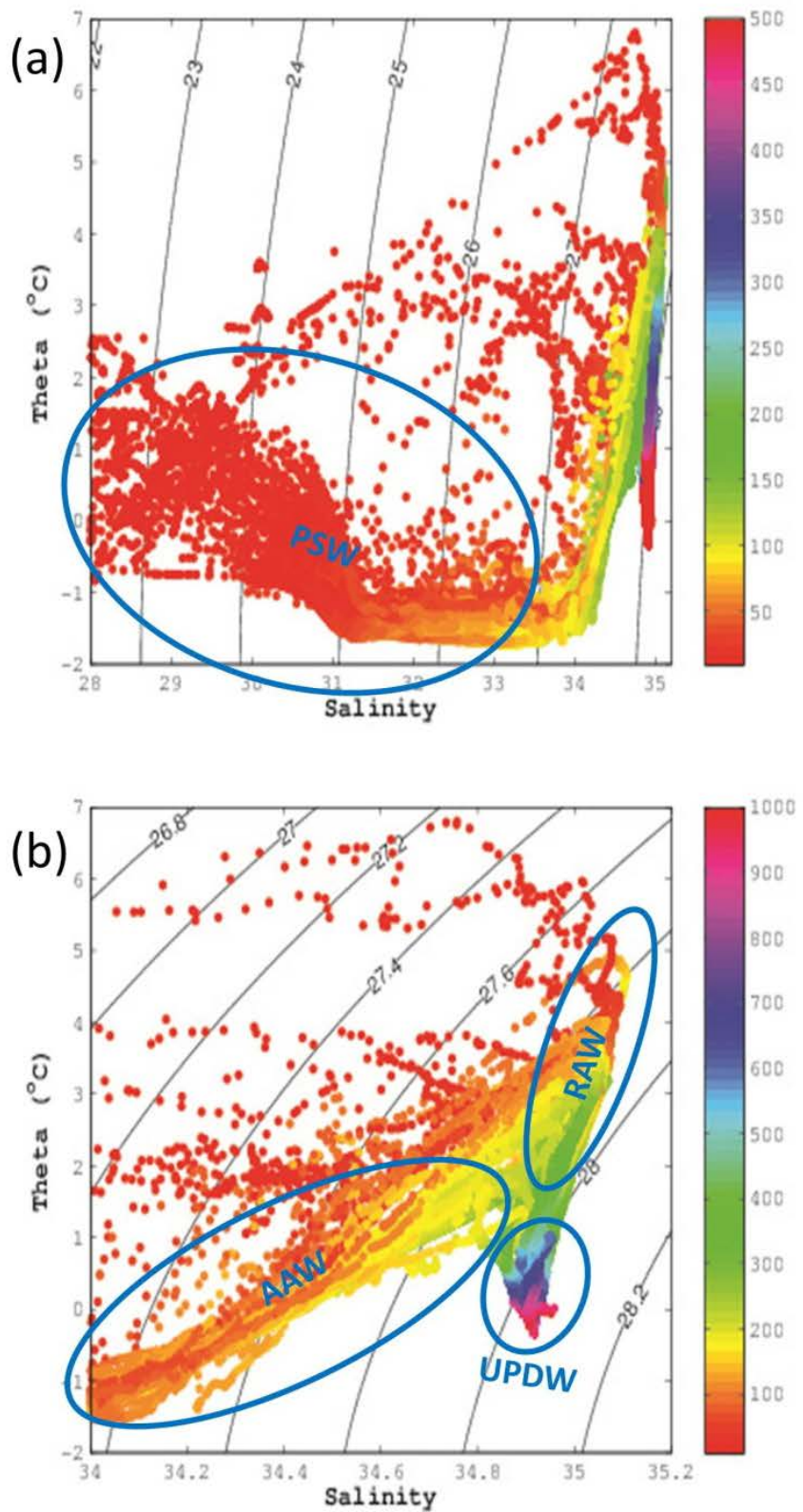
6 Results and discussion

6.1 Physical oceanography

6.1.1 Water masses

The main water masses of the East Greenland Current and surrounding waters of the East Greenland shelf and the deeper Greenland Sea in August/September between 74° and 80° N west of the Greenwich meridian are presented in *figure 6.1*. The classification of water masses follows the analysis of Rudels et al. (2002). Near-surface waters in the upper 100 m (*figure 6.1*) were dominated by Polar Surface Water (PSW). PSW is of Arctic origin and mainly associated with the East Greenland Current. South of the Fram Strait, PSW is modulated by a combination of freshwater input from river run-off and net precipitation and warmer, more saline Atlantic water. The core of the PSW was largely confined to the NE Greenland shelf between 50 and 100 m water depth and was characterized by salinities in the range 31-33 and temperatures <-1 °C. The upper part of PSW at depths <50 m is described as PSW warm (PSWw). PSWw was significantly warmer (T range -1 to +2 °C) and less saline (S range 28 to 31) due to the influence of seasonal heating and melting of sea ice. The water masses in the depth range 100-200 m are dominated by Arctic Atlantic Water (AAW). AAW is a water mass of Arctic origin with contributions from Atlantic waters. In September 2017, it was found in the salinity and temperature range $\Delta S = 34-34.8$ and $\Delta T = -1-+2$ °C respectively (*figure 6.1b*). The warmest and most saline water was Return Atlantic Water or Re-circulating Atlantic Water (RAW, *figure 6.1b*). RAW was mainly found along the Greenland shelf break in the depth range 100-300 m with salinities >35 and temperatures of up to 4 °C. RAW originates in the northward flowing West Spitsbergen Current and crosses the northern Greenland Sea at around 78° N, where it becomes entrained into the southward flowing East Greenland Current system (*figure 6.2*). The coexistence of colder and less saline East Greenland Current waters and warmer and more saline waters from the Atlantic was clearly visible as a dynamic frontal system along the East Greenland shelf break during the cruise (see *figure 6.3* for an example). The most prominent deep water mass at depths >500 m observed during the cruise was upper Polar Deep Water (uPDW). uPDW is formed in the Arctic ocean and was characterized by a narrow salinity range ($34.8 < S < 35$) and temperatures <1 °C (*figure 6.1*).

Figure 6.1. θ -S diagram of all water masses of the East Greenland Current and surrounding waters between 74° and 80° N west of the Greenwich meridian as sampled during the NEG cruise in August/September 2017. (a) All CTD stations and sampling depths. The colour scale has been set to a maximum depth of 500 m; the depth range 500-1,000 m has the same colour. (b) Zoom on water masses with salinities ≥ 34 . See explanation for water mass abbreviations in text.



6.1.2 Mixed layer depth

The ocean mixed layer is considered as a region in the upper ocean with little to no variations in temperature, salinity and density. The presence of such nearly vertically uniform oceanic regions has often been described on the basis of vertical profiles of *in situ* measurements of temperature, salinity and pressure across the global ocean. Near-surface mixed layers are generated by wind-induced turbulent mixing and heat fluxes at the ocean surface (e.g. winter cooling). There are different methods to calculate the lower boundary of the mixed layer depth (MLD). We calculated the MLD as the depth above the largest density difference along each CTD profile. MLDs varied between relatively low values (5-15 m) in Greenland coastal and inner shelf regions, where deeper MLDs (>15 m) were typically found along the outer shelf and close to the shelf break (figure 6.4). Lower coastal and shelf MLD values might have developed as a consequence of strong near surface stratification caused by the relatively warm and low-salinity surface waters due to the influence of seasonal heating and melting of sea ice (figure 6.4).

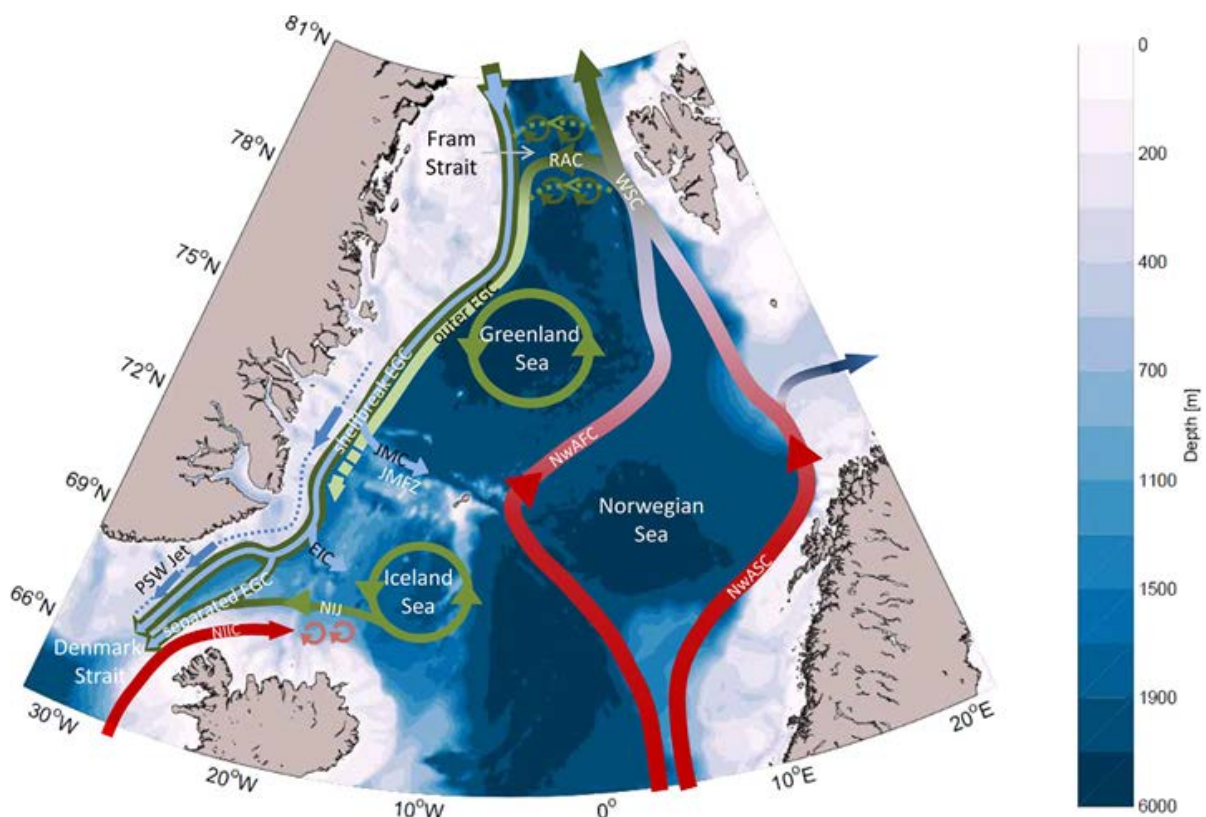


Figure 6.2. Schematic representation of the warm to cold water conversion in the Greenland Sea (from Håvik et al. 2017). See explanation in section 6.1.4.

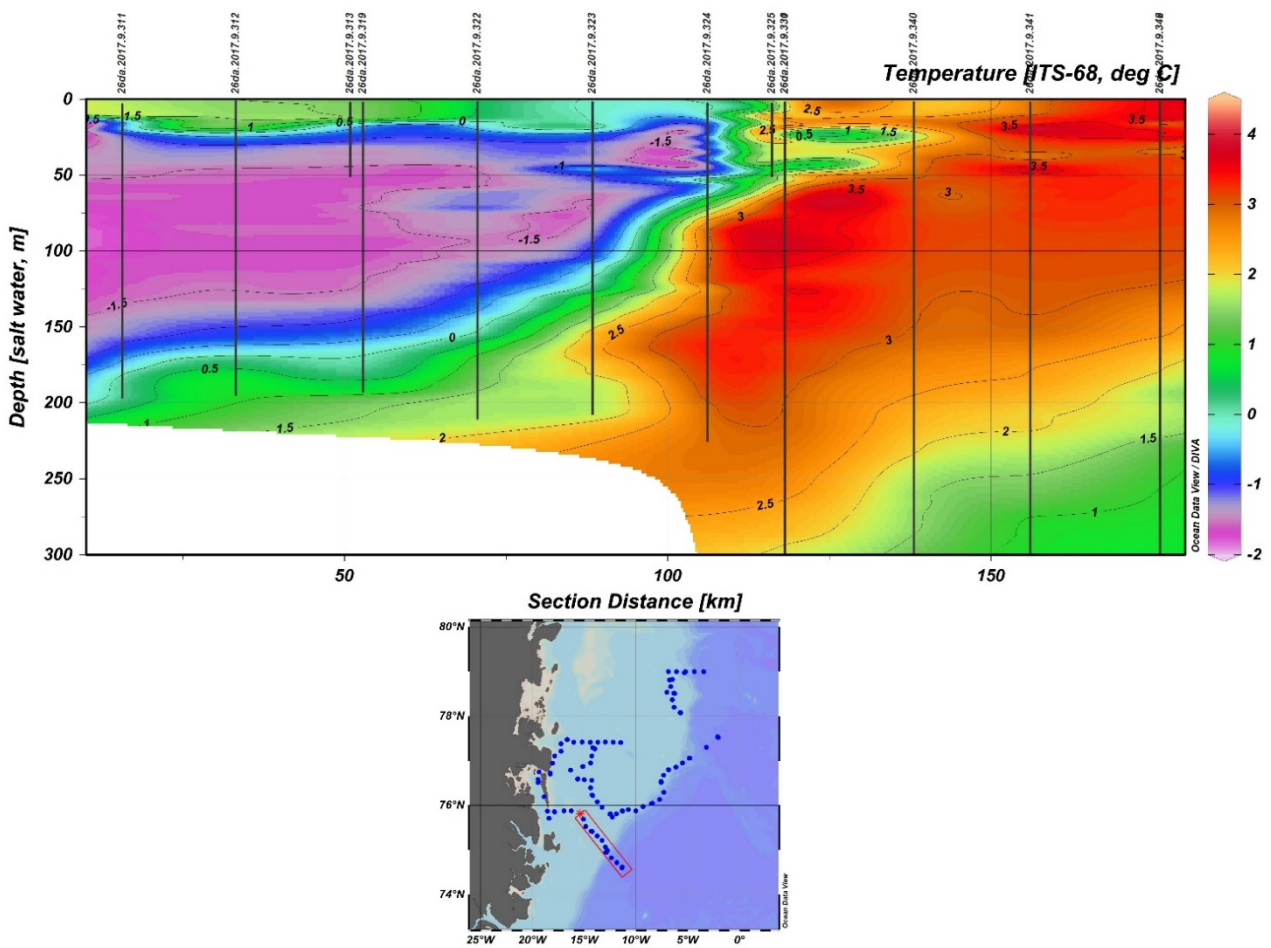


Figure 6.3. Temperature distribution along a transect crossing the East Greenland shelf break. This figure illustrates the sharp boundary between the colder waters of the East Greenland Current and warmer waters of Atlantic origin.

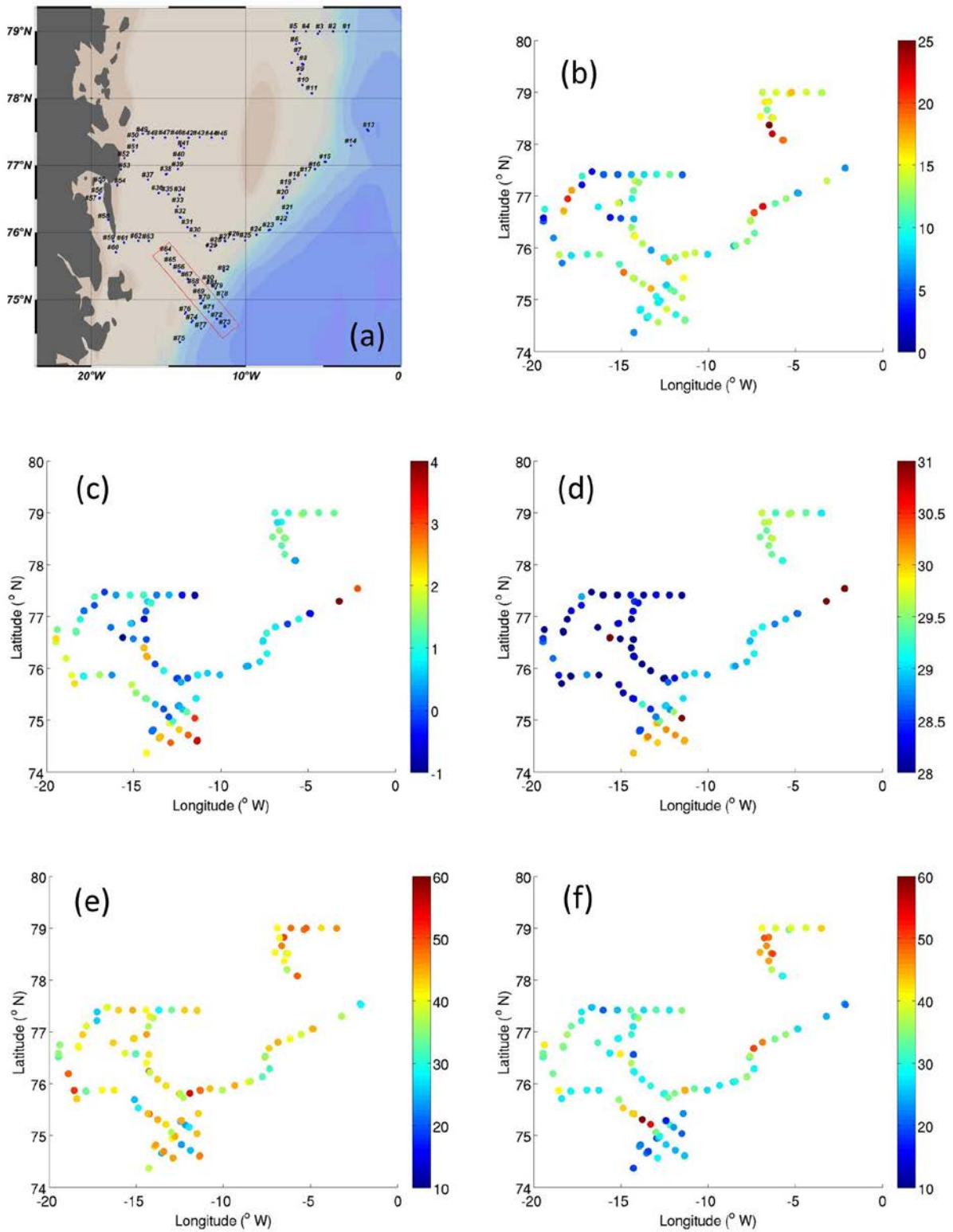


Figure 6.4. (a) Location of CTD stations, (b) mixed layer depth (MLD) calculated for all CTD stations (m), (c) mean temperature inside the MLD ($^{\circ}\text{C}$), (d) mean salinity inside the MLD, (e) depth of the chlorophyll maximum (m), (f) depth of the photic layer (m).

6.1.3 Chlorophyll maximum and depth of the photic layer

The depths of the chlorophyll-*a* maximum at each CTD station were extracted. The characteristic depth range of the chlorophyll-*a* maximum was found between 30 and 40 m. Deeper chlorophyll-*a* maxima (up to 50 m) were occasionally found along the outer shelf and individual stations at the inner shelf (*figure 6.4*). The depth of the photic layer at each station was then defined as the depth, where PAR is 1 % of the near-surface value (*figure 6.4f*). Typical depths of the photic layer varied between 20 and 40 m at inner shelf and coastal areas in the southwest of the sampling area, whereas photic layer depths >40 m were confined to the north-eastern part of the sampling area (outer shelf) and some individual stations across the inner shelf.

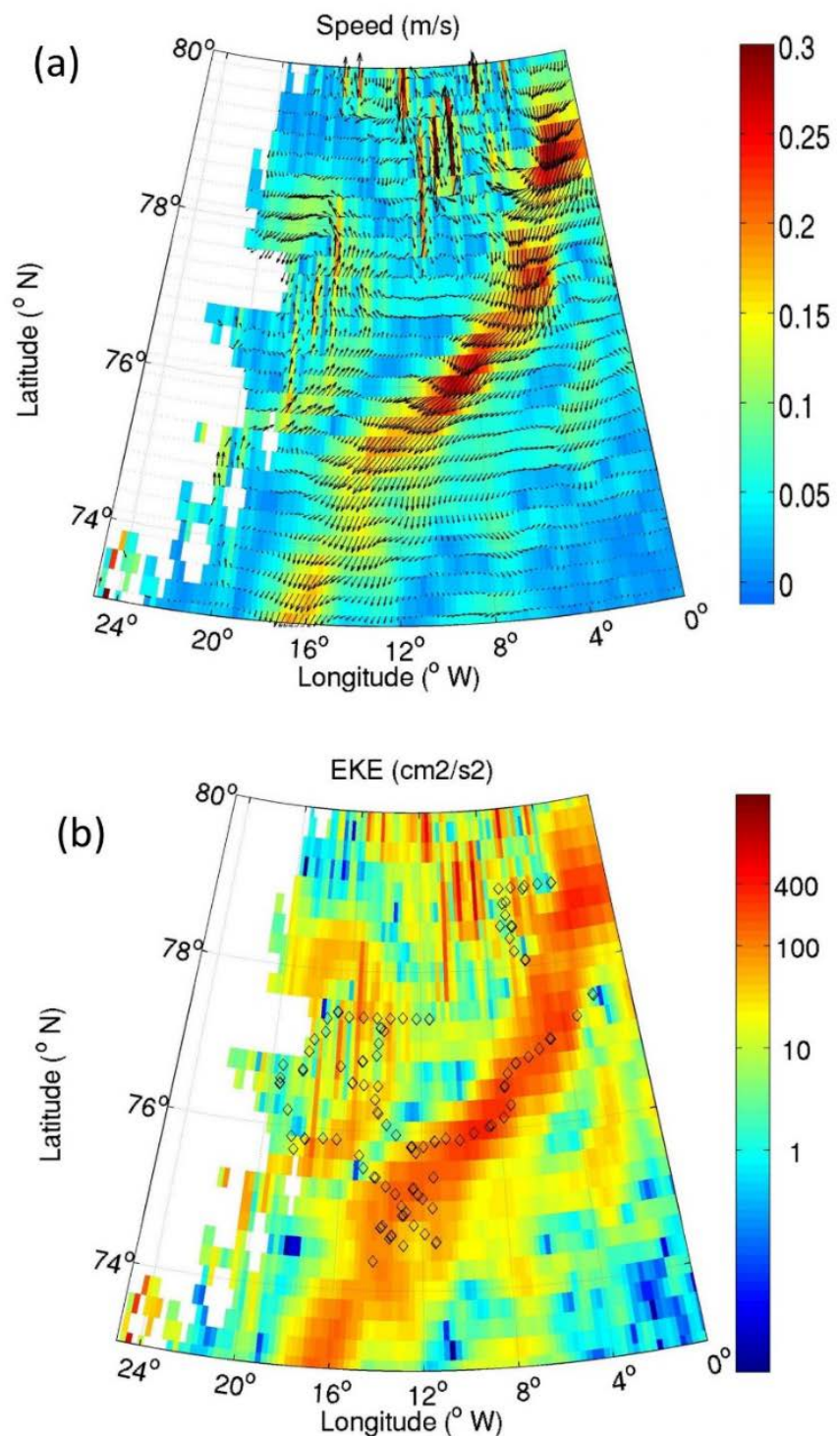
6.1.4 Currents

The Greenland Sea is an area of major water mass transformation of warmer northward flowing waters in the eastern Greenland Sea to colder and fresher waters flowing south in the western Greenland Sea (*figure 6.2*). Warmer northward flowing currents are of Atlantic origin and include the Norwegian Atlantic Frontal Current (NwAFC), the Norwegian Atlantic Slope Current (NwASC) and the West Spitsbergen Current (WSC). Water from the West Spitsbergen Current flows westward in the Northern Greenland Sea and forms the outer East Greenland Current (EGC) while the Shelfbreak East Greenland current and the Polar Surface Water Jet (PSW) are other parts of the EGC – a highly energetic and the most prominent flow feature.

The EGC flows southward along the shelf break off the east coast of Greenland from the Fram Strait (79° N) to Cape Farewell (60° N). Another prominent feature of the circulation in the Greenland Sea is the Greenland Sea eddy centred in the western Greenland Sea at 75° N (*figure 6.2*).

During the NEG cruise, average surface current speeds associated with the EGC were up to 30 cm s⁻¹ and eddy kinetic energies of up 400 cm² s⁻² (*figures 6.5a and b*). Another prominent circulation feature during the cruise was a cyclonic, northward flowing current on the East Greenland shelf centred between 75° N and 78° N (*figure 6.5*).

Figure 6.5. (a) AVISO (Archiving, Validation and Interpretation of Satellite Oceanographic data) surface currents (m/s) and (b) eddy kinetic energy EKE (cm^2s^{-2}) averaged over the period of the NEG cruise. Please note that the colour scale in (b) is logarithmic.

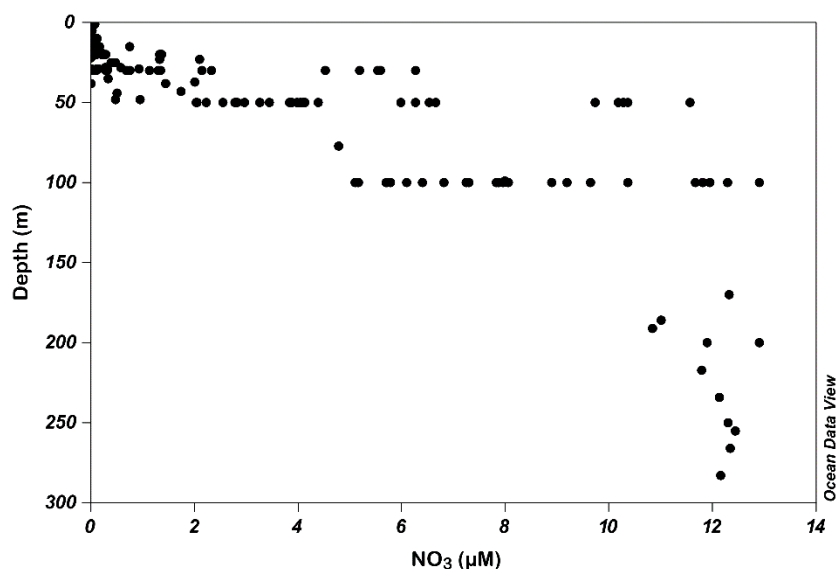


6.2 Biogeochemistry and phytoplankton

Marine primary producers synthesise organic compounds from aqueous carbon dioxide through the process of photosynthesis using light as the energy source. Primary producers are therefore the foundation of the marine food web and the energy source of all higher trophic levels. In high latitude waters experiencing seasonal or year-round ice-free conditions, phytoplankton remain the major primary producers (e.g. Carmack & Wassmann 2006), while ice algae, macroalgae and benthic diatoms may contribute significantly depending on ice conditions and water depths. Phytoplankton production is mainly regulated by environmental factors such as sea ice and light conditions, nutrient replenishment and stratification of the water column keeping

phytoplankton in the photic zone (e.g. Tremblay & Gagnon 2009). While light conditions may set the seasonal boundaries for the primary production, inorganic nutrient availability and replenishment generally determines the magnitude of production in high latitude systems experiencing seasonal or year-round ice-free conditions.

Figure 6.6. Nitrate (NO_3) concentrations (μM) in relation to sampling depths down to 300 m for all stations.



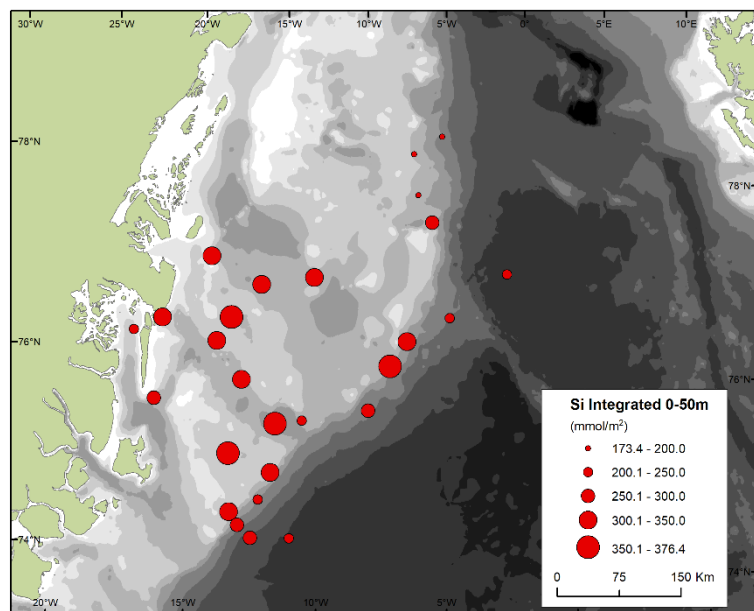
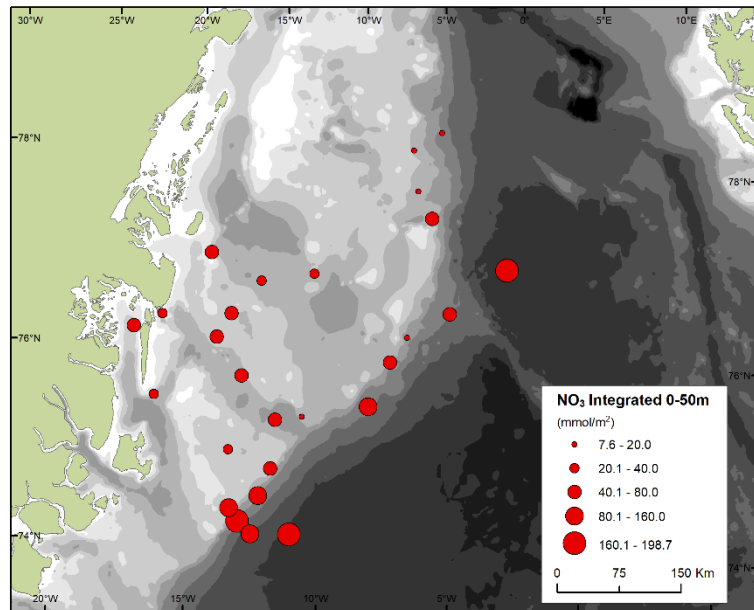
6.2.1 Nutrients

Replenishment of inorganic nutrients is essential for sustaining phytoplankton production, i.e. new production. Inorganic nutrient stocks and recycling along with advection, stratification and mixing of the water column are factors controlling the nutrient replenishment (e.g. Tremblay & Gagnon 2009). While both nitrogen, silicate, phosphate and ammonia are considered important, nitrogen and silicate are often singled out as the two main limiting factors on Arctic phytoplankton production in high latitude systems. Moreover, while silicate is essential to two important microplankton groups, i.e. diatoms and dinoflagellates, nitrogen remains vital to all groups.

A general trend in nutrient conditions throughout the study area was prevailing low concentrations in the surface waters (<20 m), particularly for nitrate (figure 6.6). Nitrate levels most often remained below or around the detection limit for the analysis in the upper sampling depths, while samples >20 m revealed increasing concentrations. Depleted nitrate levels in the surface layer, which also has the most favourable light conditions, likely was a major factor controlling phytoplankton production, as described below.

Integrated nutrient concentrations (0-50 m) showed low nitrate levels at the shelf stations, while silicate levels remained high (figure 6.7). This reversed pattern between nitrate and silicate on the shelf brings further support to nitrate replenishment being a major limiting factor for primary productivity along with deteriorating light conditions during this late-season study. The highest integrated levels of nitrate were recorded along the shelf break corresponding with deeper mixing of the water column, as previously described by a deeper mixed layer depth (MLD) at the shelf break.

Figure 6.7. Integrated nitrate and silicate concentrations (mmol m^{-2}) for the 0-50 m depth strata at all biological sampling stations.



Nutrient concentrations along a transect crossing the East Greenland shelf break showed a gradually ascending nitrate cline ($>1 \mu\text{M}$) moving away from the coast, while a descending high to moderate silicate concentration cline ($>4 \mu\text{M}$) was observed in the upper 10 m (*figure 6.8*).

High silicate concentrations on the shelf and costal stations (*figure 6.7 and 6.8*) could be an indication of replenishment from either terrestrial sources or the southward flowing East Greenland Current system. The Greenland Ice Sheet has been stipulated being an important source or transporter of dissolved silicate for the fjords and surrounding coastal waters (e.g. Meire et al. 2016).

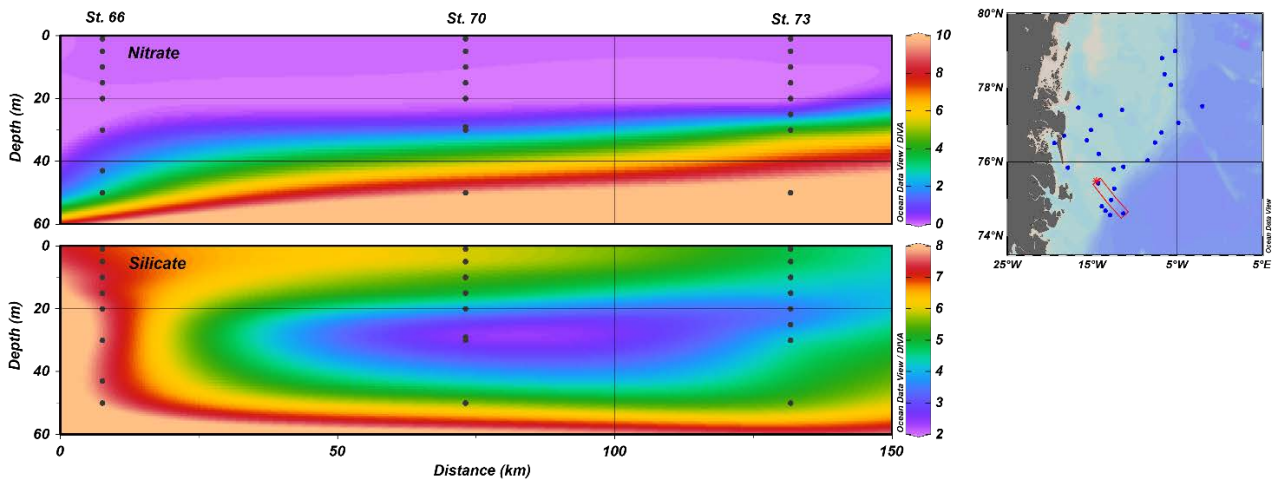


Figure 6.8. Nitrate and silicate concentrations (μM) along a transect crossing the East Greenland shelf break.

6.2.2 Phytoplankton

Phytoplankton are the main primary producers in high latitude waters experiencing seasonal or year-round ice-free conditions. The biomass of phytoplankton is often depicted as the concentration of chlorophyll-*a*, the main photosynthetic pigment in planktonic algae. In contrast, the photosynthetic productivity of phytoplankton is often described as the amount of carbon produced (i.e. ^{14}C incorporation technique) or the amount of oxygen released as a by-product of photosynthesis.

Integrated phytoplankton biomass and production within the 0-50 m depth strata across the study area revealed the highest values at or outside the East Greenland shelf break (figures 6.9, 6.10 and 6.11). The lower values on the shelf can likely be linked to nitrate limitation of the phytoplankton production, while high values at the shelf break correspond with the previously described boundary between the colder waters of the East Greenland Current and warmer waters of Atlantic origin resulting in elevated mixing of the water column.

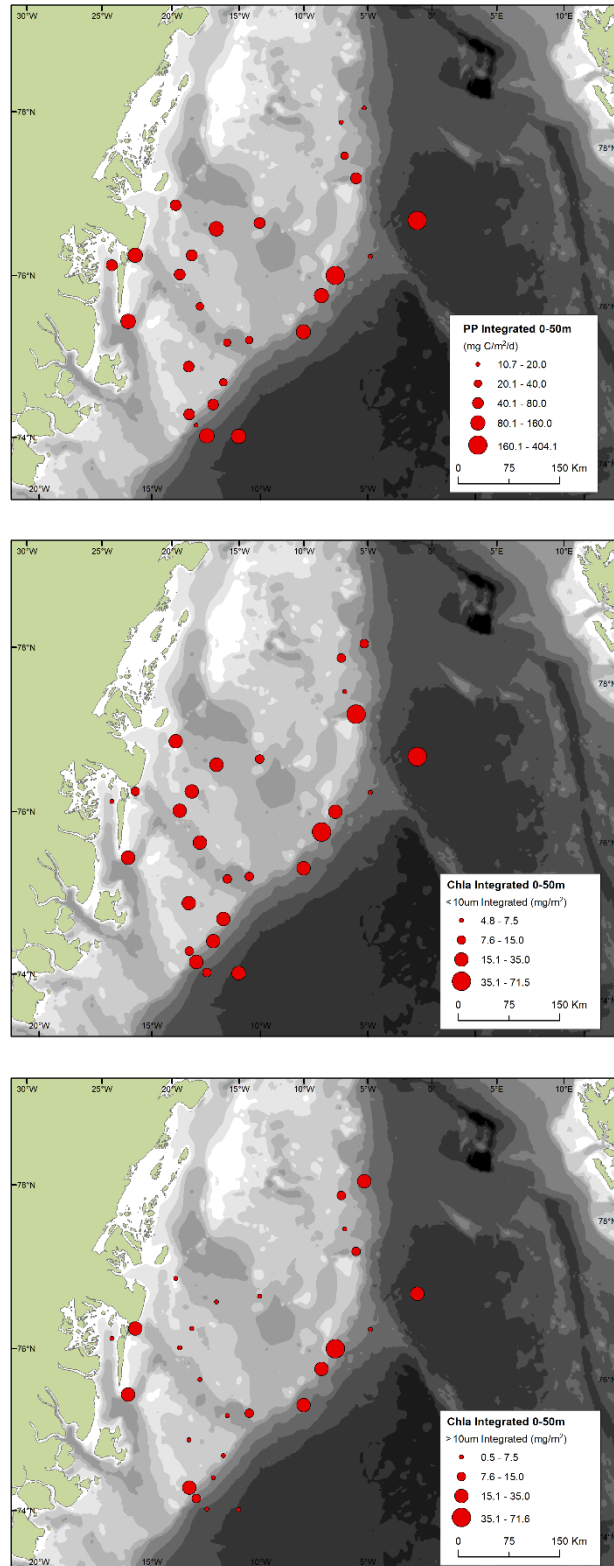
In situ fluorescence measurements (e.g. CTD profiler equipped with a fluorometer) are *in vivo* measurements, thus considered relative estimates of chlorophyll-*a*, while the chlorophyll-*a* extraction method represents an *in vitro* quantitative measurement. Nonetheless, CTD profilers equipped with a fluorometer often provide more detailed depth profiles of the relative phytoplankton biomass.

A transect crossing the East Greenland shelf break showed a layer of high fluorescence (relative chlorophyll-*a* concentration) from 30-50 m on the shelf, while the high biomass layer was observed somewhat higher in the water column (20-40 m) outside the shelf break (figure 6.10). Peak phytoplankton biomass (fluorescence) observed at the shelf break correspond to the boundary between the colder waters of the East Greenland Current and warmer waters of Atlantic origin. Primary production along the same transect revealed low rates on the shelf, while the highest production was observed at or outside the shelf break (figure 6.9). Comparing the primary production rates and the chlorophyll-*a* (GF/F) concentrations in the upper 50 m along the transect also revealed that the layer of chlorophyll-*a* maxima does not account for the highest production, but more moderate phytoplankton biomasses in the upper 20 m depicted the highest production. Decreasing incoming irradiance and solar angle this late in the season likely resulted in deteriorating light levels in the

water column, thus concentrating production to the uppermost part of the water column (<20 m) despite low nitrate levels.

The deep layer of chlorophyll-*a* maxima characterized by low productivity across the shelf may represent a stressed phytoplankton biomass, which is settling (sinking) towards the bottom. High concentrations of phaeopigments (ca 1 mg m⁻³) compared to chlorophyll-*a* (ca 1.5 mg m⁻³) support a deteriorating phytoplankton community likely stressed by the diminishing seasonal light conditions and nitrate depletion.

Figure 6.9. Integrated primary production (mg C m⁻² d⁻¹) and total chlorophyll-*a* concentration and Chl-*a* larger than 10 μm (mg Chl-*a* m⁻²) for the 0-50 m depth strata at all biological sampling stations.



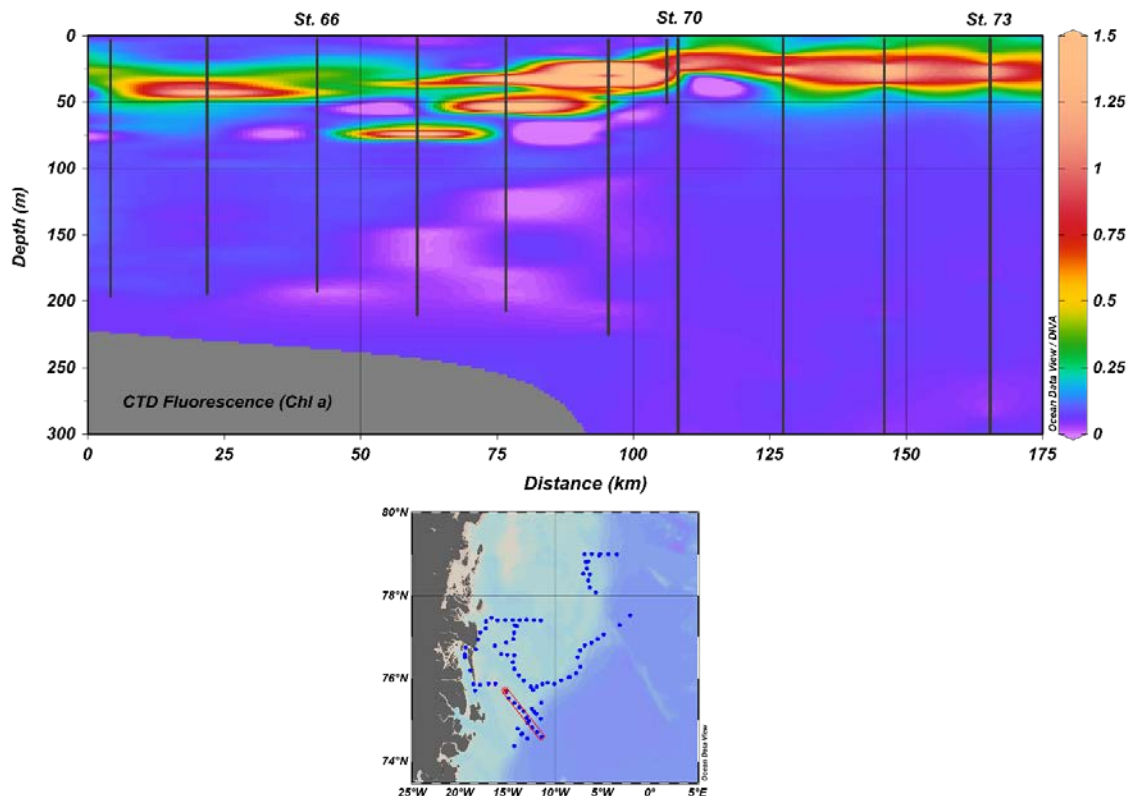


Figure 6.10. Fluorescence (relative chlorophyll-*a* concentration) along a transect crossing the East Greenland shelf break. Selected station numbers serve for comparison with the in vitro quantitative measurement of chlorophyll-*a* along the same transect (figure 6.9).

Size-fractionated pigment analysis revealed that a higher proportion of the biomass comes from larger phytoplankton, i.e. chlorophyll-*a* >10 μm , compared to the smaller phytoplankton biomass (i.e. <10 μm) at the shelf break, while on the shelf and outside the shelf break the larger phytoplankton contributed less to the biomass (figure 6.9). This is of particular interest for the energy transfer to the higher trophic levels, as the large filter feeding copepods *Calanus* spp. are limited to food particles >10 μm . The shelf break therefore seems to comprise an abundant food supply for the important copepods during this late season study.

6.3 Zooplankton

The mesozooplankton (size 0.05-20 mm) biomass and community composition were clearly associated to the oceanography and bathymetry of the area. The biomass was highest along the shelf break area (figure 6.12) where the North Atlantic water mass meets the Arctic (figure 6.2) and the surface current speeds and eddy kinetic energies were highest (figure 6.5) and the highest primary production was found (figure 6.9). Large *Calanus* dominated the biomass (figure 6.13). Other abundant species of the copepods were *Pseudocalanus* spp., *Microcalanus* spp., *Oithona similis*, *Oncaea borealis* and *Metridia longa*. Copepods dominated the mesozooplankton biomass. Other abundant groups were Larvaceans (*Oikopleura* spp, *Fritillaria borealia*), Chaetognatha (*Eukhronia hamata*, *Sagitta* spp.) and meroplankton larvae.

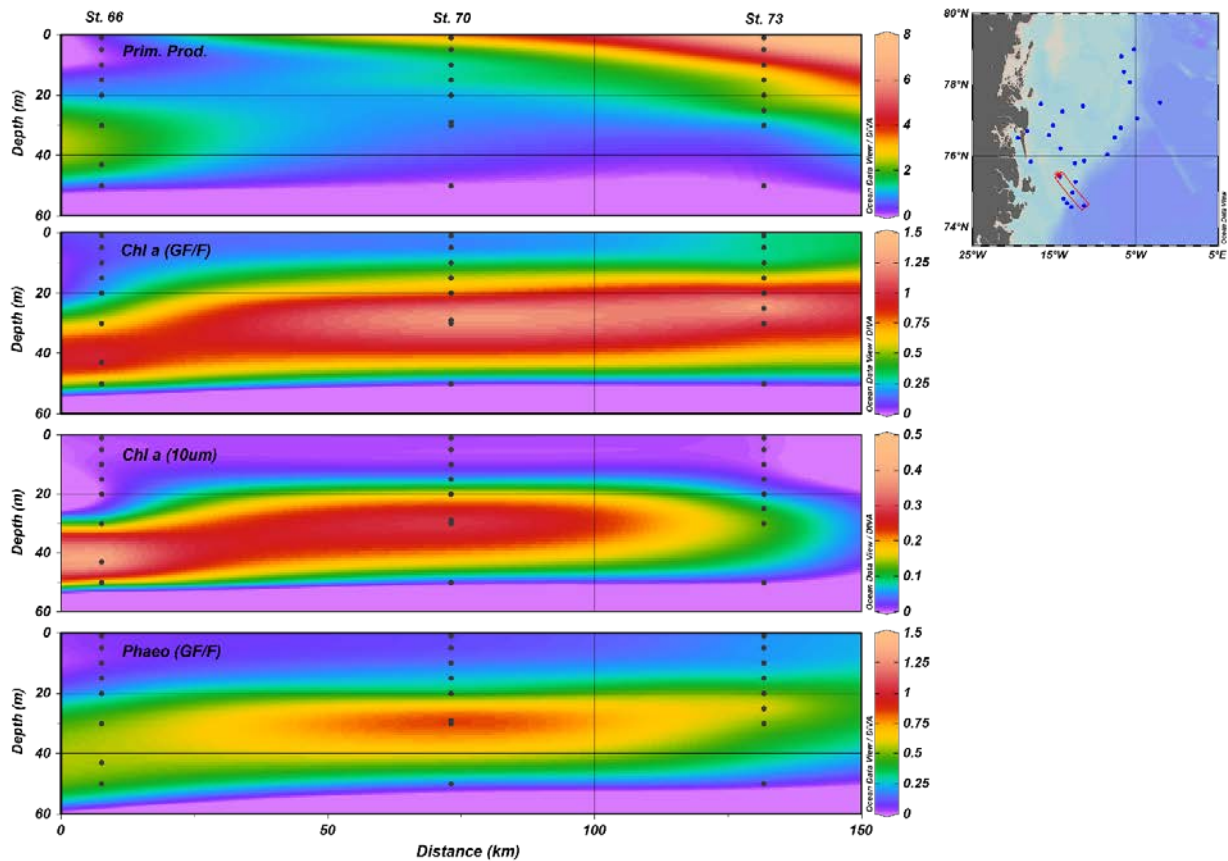


Figure 6.11. Primary production rates (Prim prod; mg C m⁻³ d⁻¹) and concentrations of chlorophyll-a (Chl-a (GF/F); mg m⁻³), chlorophyll-a larger than 10 µm (Chl-a (10 µm); mg m⁻³) and phaeopigments (Phaeo (GF/F); mg m⁻³) along a transect crossing the East Greenland shelf break.

The North Atlantic *Calanus finmarchicus* was present at all stations, but much more abundant at the stations off the shelf in the Greenland Sea. The Arctic *Calanus* species *C. glacialis* and *C. hyberboreus*, on the other hand, had the opposite patterns, and were not found at all in the upper 50 m in the Greenland Sea (figure 6.13). A large part of the dominant *Calanus* was still present in the surface water, which are important for visual predators and predators feeding from the surface, e.g. seabirds like little auk. Compared to the west coast of Greenland at similar latitude in the same period, the biomass of mesozooplankton was much lower both in the upper and deeper part of the water column (Møller et al. 2018).

The macrozooplankton (size >20 mm) like the mesozooplankton had elevated biomass in the shelf break area, but also at the near-shore stations. There were dominated by krill (*Meganyctiphanes norvegica*, *Thysanoëssa inermis*, *Thysanoëssa longicaudata*), amphipods (*Themisto libellula*, *Themisto abyssorum*) and Chaetognatha.

Figure 6.12. The biomass of copepods in a) the upper 50 m of the water column and b) from 50 m to the bottom (although never deeper than 1,000 m) sampled by a Multinet.

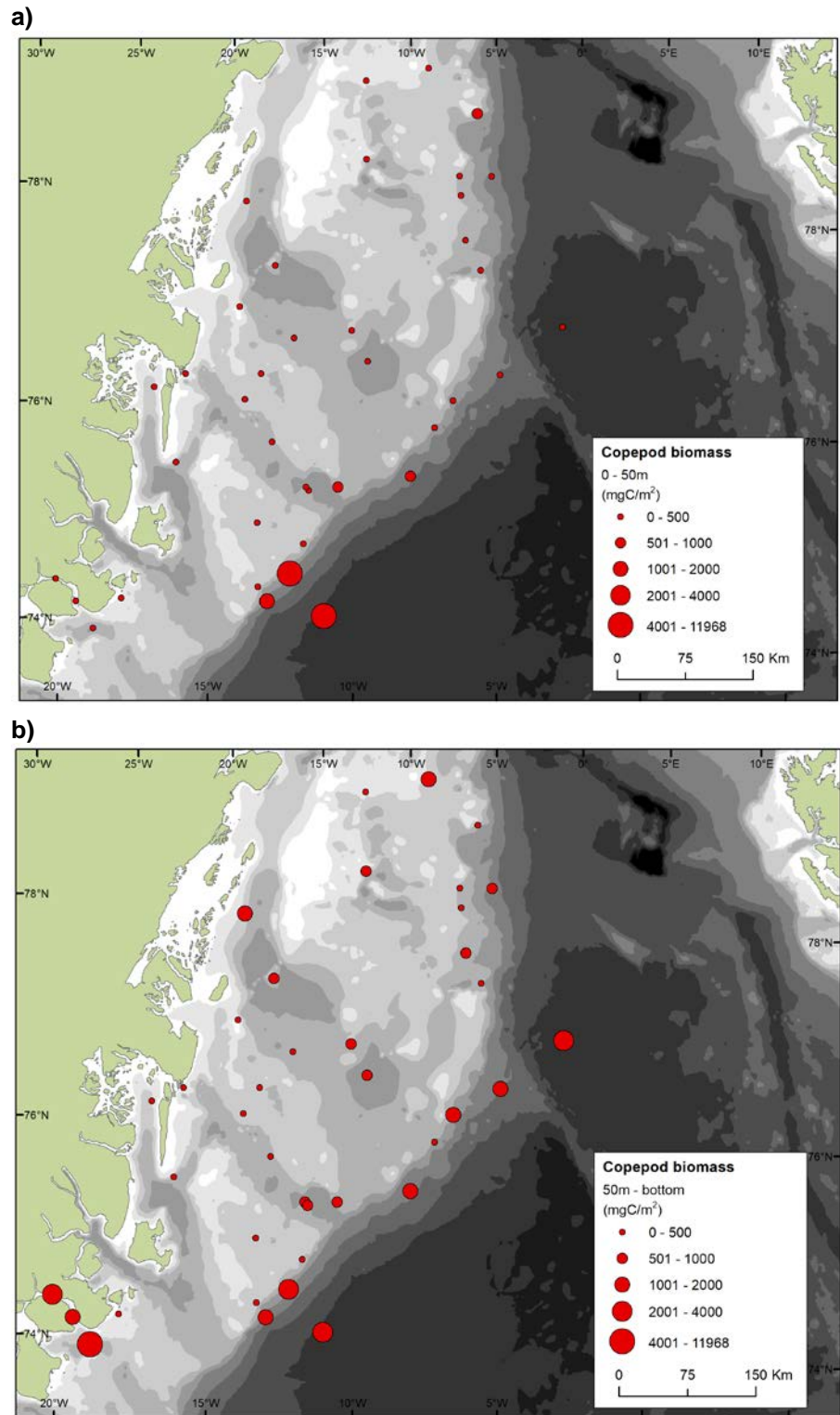


Figure 6.13. The species composition of the copepod community in the upper 50 m of the water column.

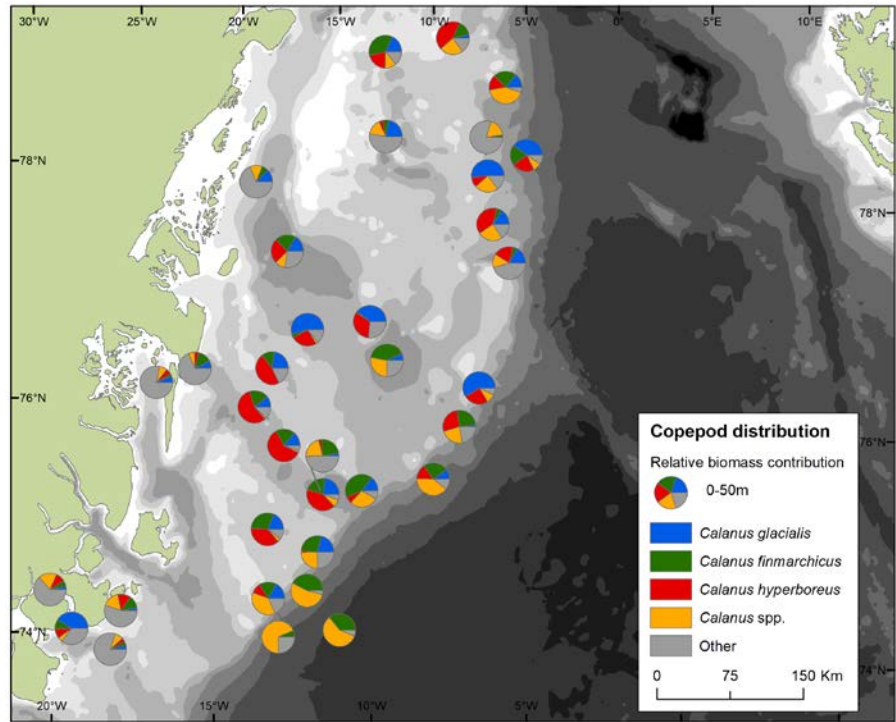
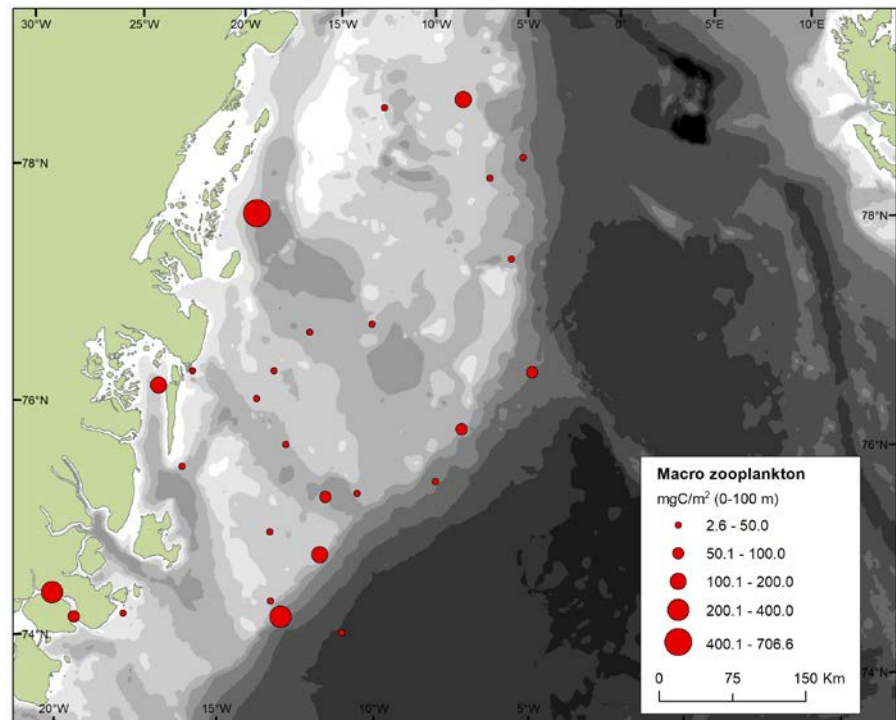


Figure 6.14. The biomass of macrozooplankton in the upper 100 m of the water column sampled by the MIK-net.



6.4 Acoustic measurements

The acoustic measurements gave a high-resolution distribution of the density of organisms along the cruise track. The relative abundance (sA values) of the three different groups (plankton, krill/amphipods and “others” (stronger scatterers)) showed the same pattern as the samples obtained with the Multi-net and MIK-net; the highest densities were found along the shelf break and in coastal areas (figure 6.15). Data are presented for the whole water column

(sA total, although for plankton only for the upper 100 metres), although data is also available for the different depth strata for the large organisms (0-50, 50-100, 100-150, 150-200 and 200 m-bottom).

The WBAT data were used to get an idea of the vertical distribution of targets >2 mm in size (like *Calanus* spp., krill, amphipods, and fish larvae, i.e. larger meso- and macroplankton) at a finer scale than what is provided by the Multinet (figure 6.16). Broadly, the vertical distribution follows the vertical distribution of phytoplankton, i.e. the highest density is found in the layers with much phytoplankton. However, for st. 73, where there is a high primary production (figure 6.11), it could seem that the vertical zooplankton distribution follows the primary production more closely than the phytoplankton biomass, peaking at greater depth, which could be an indication that the zooplankton prefer healthy productive phytoplankton cells. Sometimes, a deep peak of zooplankton is also seen, which could be individuals avoiding the surface layers during daylight.

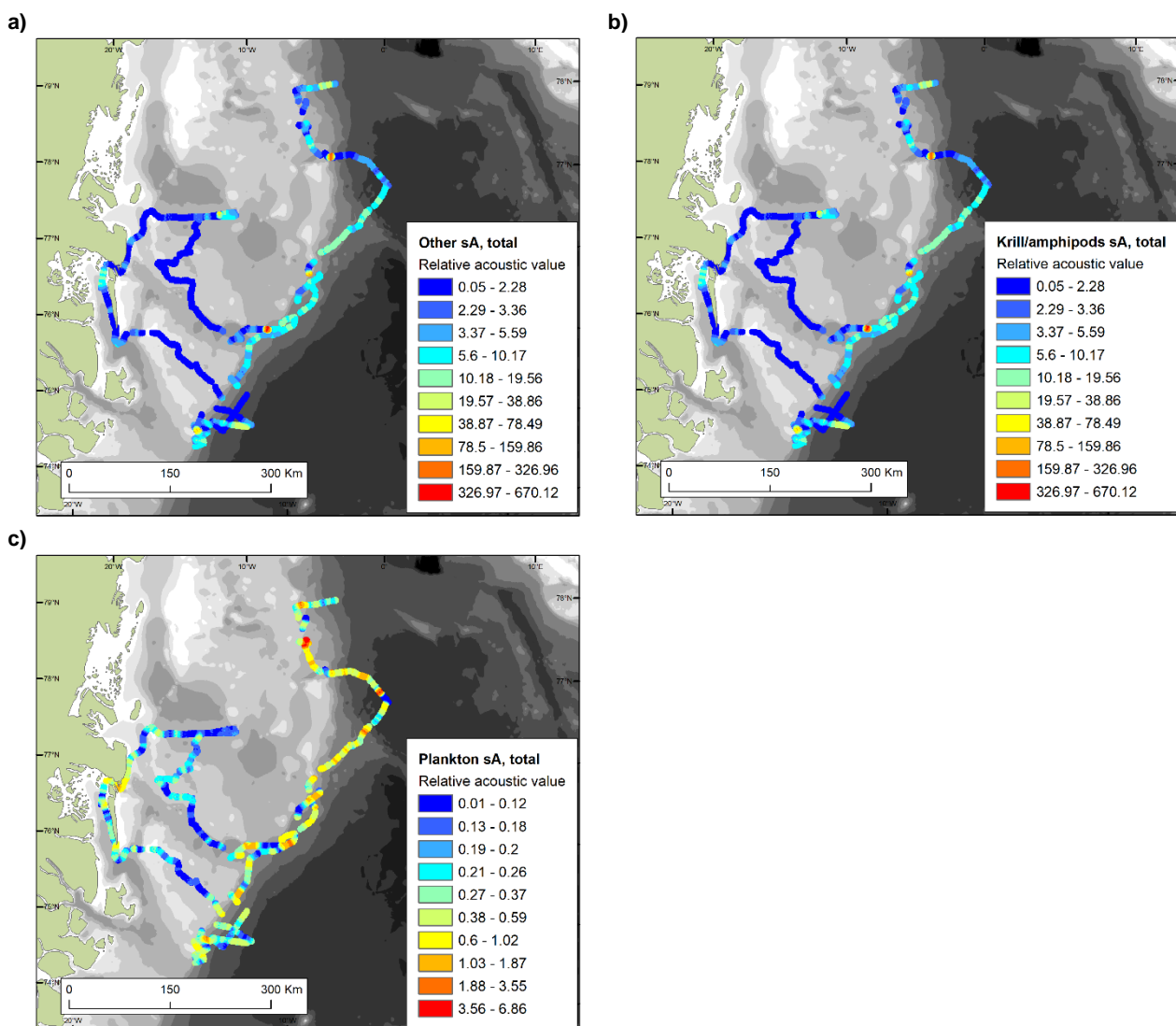


Figure 6.15. The total backscatter divided into three different groups: a) fish and stronger scatterers, b) macroplankton (i.e. krill-like organisms) and c) smaller zooplankton, and mean volume backscattering strength (Sv, dB) thresholds of -82 dB, -85 dB and -90 dB, respectively, were used to separate the three groups.

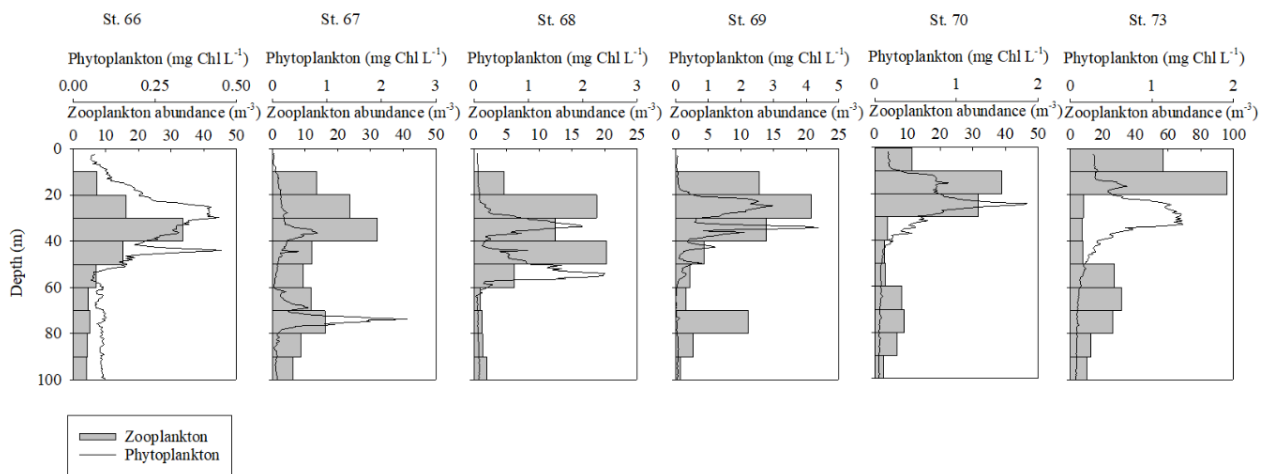


Figure 6.16. The vertical distribution of phytoplankton and zooplankton measured by the CTD fluorometer and the WBAT, respectively, along the transect plotted in *figure 6.3* and *figure 6.10*.

6.5 Seabirds and marine mammals

The survey showed in general low diversity and abundance of seabirds and marine mammals in the area. 22 bird species and 9 species of marine mammals were observed. Total numbers recorded have been summarized in *table 6.1*. The most abundant species recorded on the 1,988 km transect within the 300 m wide transect bands were little auk, kittiwake and fulmar, and for these species as well as for thick-billed murre density maps have been produced. Little auks were the most numerous seabird with highest densities observed along the shelf break and in the open pack ice. During the last days of the cruise, a remarkable number of little auks flying north was observed. The observations of little auks confirm the tracking results of little auks from the colony near Scoresby Sund (Mosbech et al. 2012) which identified a postbreeding staging area in the Greenland Sea region. Relatively large numbers of fulmars followed the ship during most of the cruise and kittiwakes also followed the ship and were observed especially in the open pack ice. Ivory gulls were seen regularly, mostly in small flocks in connection with pack ice. Small numbers of black guillemot, Arctic tern, thick-billed murre, Arctic skua, pomarine skua and long-tailed skua were also observed. Data on skuas, ivory gull and Arctic tern are presented (*figure 6.23*, *figure 6.29*, *figure 6.30*) but not discussed in further detail.

At the shelf break, some fin whales and northern bottlenose whales were observed as well as two orcas and two blue whales (*figure 6.17* and *figure 6.18*). At the shelf, one bowhead whale and a few seals were observed (*table 6.1*).

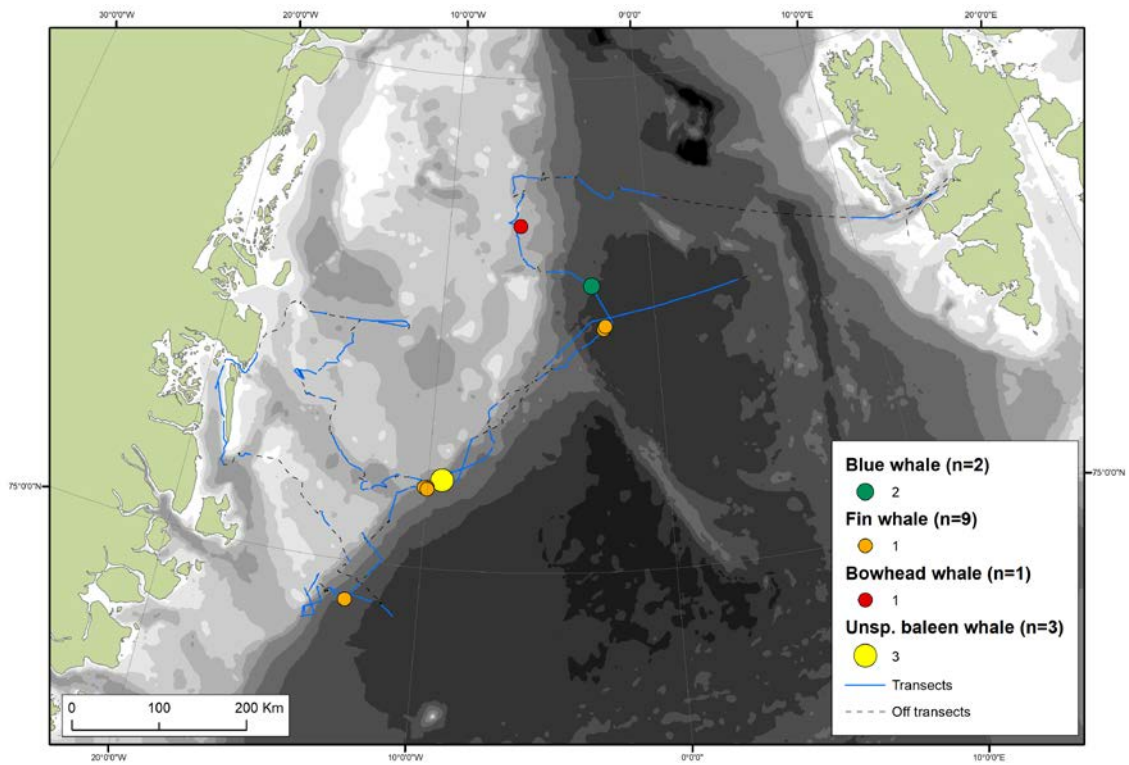


Figure 6.17. Baleen whale observations and ice cover on the transects.

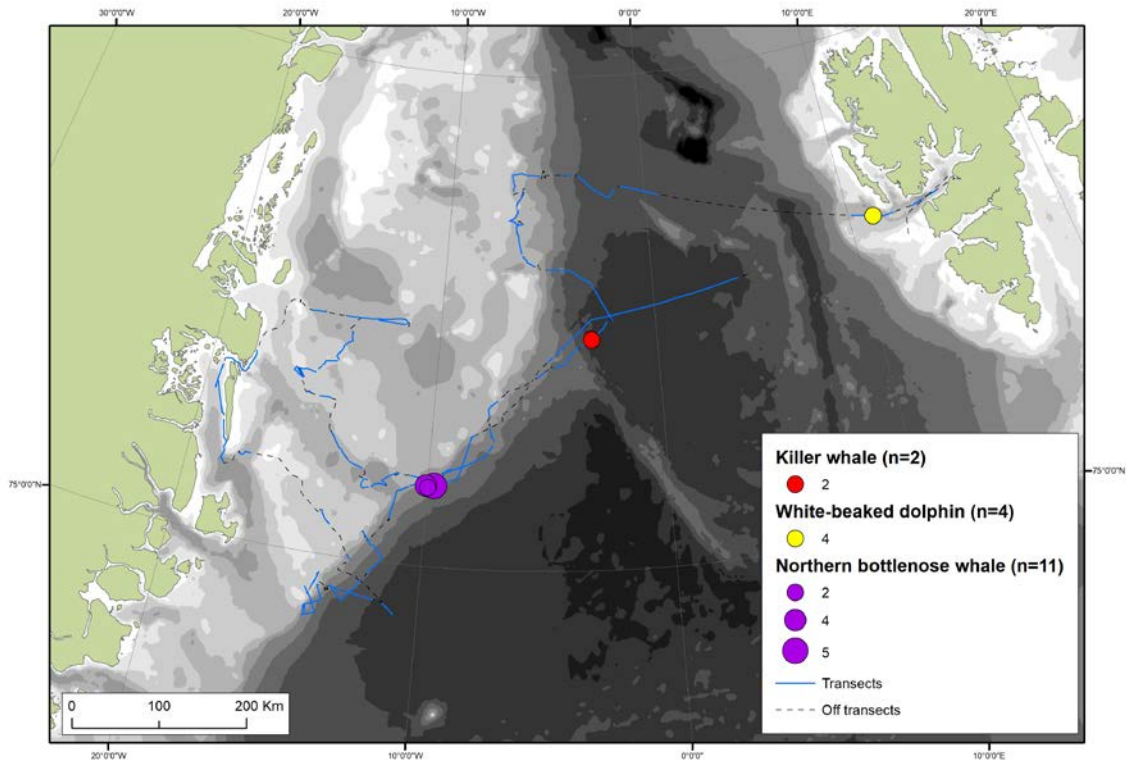


Figure 6.18. Toothed whales and ice cover recorded on the transects.

6.5.1 Seabird species account

Northern Fulmar

Fulmars were widespread in low numbers (*figure 6.19* and *figure 6.20*). They often followed the ship, and we compensated for ship-followers in the density estimation. It appears that we observed higher densities than the average of the previous surveys in the Greenland Seabird at Sea database (*figure 6.21*).

Interestingly, from the SEATRACK maps (*figure 6.22*) it is seen that the post-breeding fulmars tracked from four North Atlantic colonies do not in any of the three years tracked use the western Greenland Sea north of 70° N and west of 10° W. Therefore, most likely the fulmars observed on the DANA cruise (*figure 6.19* and *figure 6.20*) west of 10° W were mainly non-breeders and birds from the Greenland colonies.

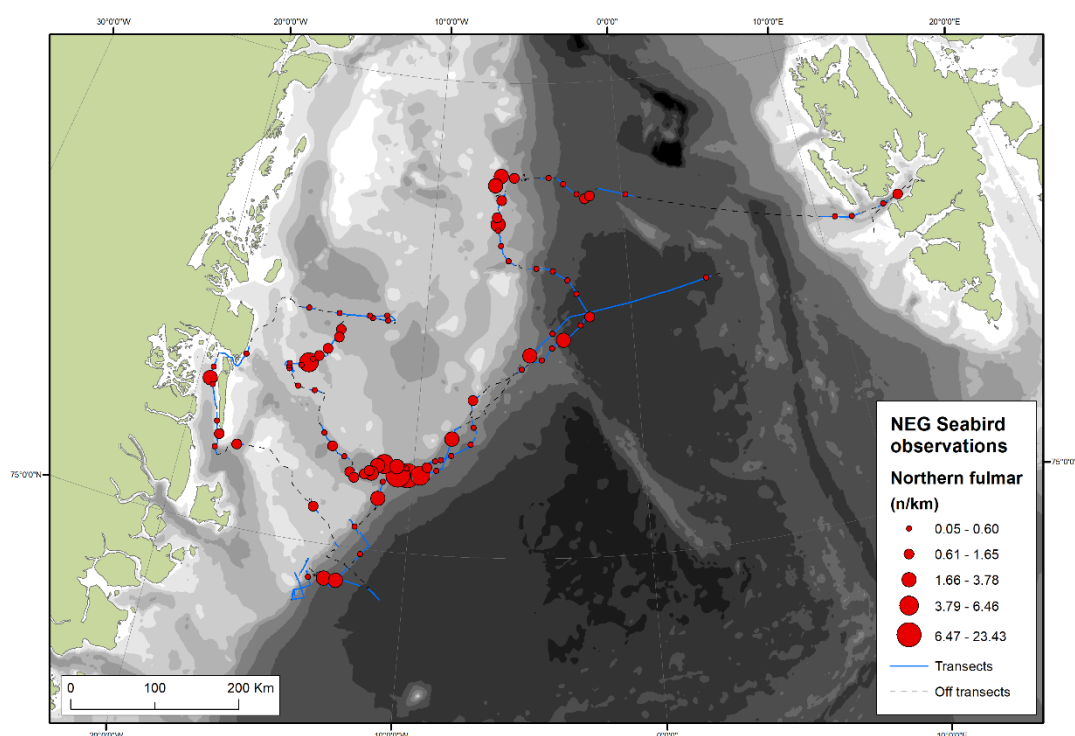


Figure 6.19. The fulmar observations (n/km transect) overlaying the observed ice cover on the transects.

Table 6.1. Seabirds and marine mammals recorded during the DANA cruise 22 August to 11 September 2017. Bird numbers are given as birds recorded on water or flying within the 300 m wide transect, and birds recorded outside the transect.

Species	Total obs.	Transect, birds on water	Transect, flying birds (snapshot)	Total on transect	Obs. outside transect
Red-throated diver/loon	2	0		0	2
Northern fulmar	1548	191	50	241	1307
Long-tailed duck	4	1		1	3
Ringed plover	5	0		0	5
Purple sandpiper	1	0		0	1
Unspecified sandpiper	3	0		0	3
Ruddy turnstone	1	0		0	1
Red-necked phalarope	1	0	1	1	
Pomarine skua/jaeger	26	1	8	9	17
Pomarine or arctic skua/jaeger	2	0		0	2
Arctic skua/parasitic jaeger	3	0		0	3
Long-tailed skua/jaeger	8	0		0	8
Great skua	4	1		1	3
Unspecified skua/jaeger	1	0		0	1
Sabine Gull	1	0		0	1
Lesser black-backed gull	1	1		1	
Iceland gull	2	0		0	2
Glaucous gull	43	7	8	15	28
Black-legged kittiwake	1108	222	85	307	800
Ivory gull	95	12	20	32	63
Arctic tern	149	6	21	27	122
Thick-billed murre	30	11	3	14	16
Black guillemot	4	1		1	3
Little auk/Dovekie	19555	3120	12030	15150	4405
Atlantic puffin	65	19	5	24	41
Northern wheatear	2	1	1	2	
Hooded seal	1	0		0	1
Harp seal	1	0		0	1
Ringed seal	4	1		1	3
Unidentified seal	2	1		1	1
Bowhead whale	1	0		0	2
Blue whale	2	0		0	2
Fin whale	9	0		0	9
Unidentified baleen whale	3	0		0	3
Northern bottlenose whale	11	0		0	11
White-beaked dolphin	4	0		0	4
Orca/Killer whale	2	0		0	2
Unspecified whale	1	0		0	1

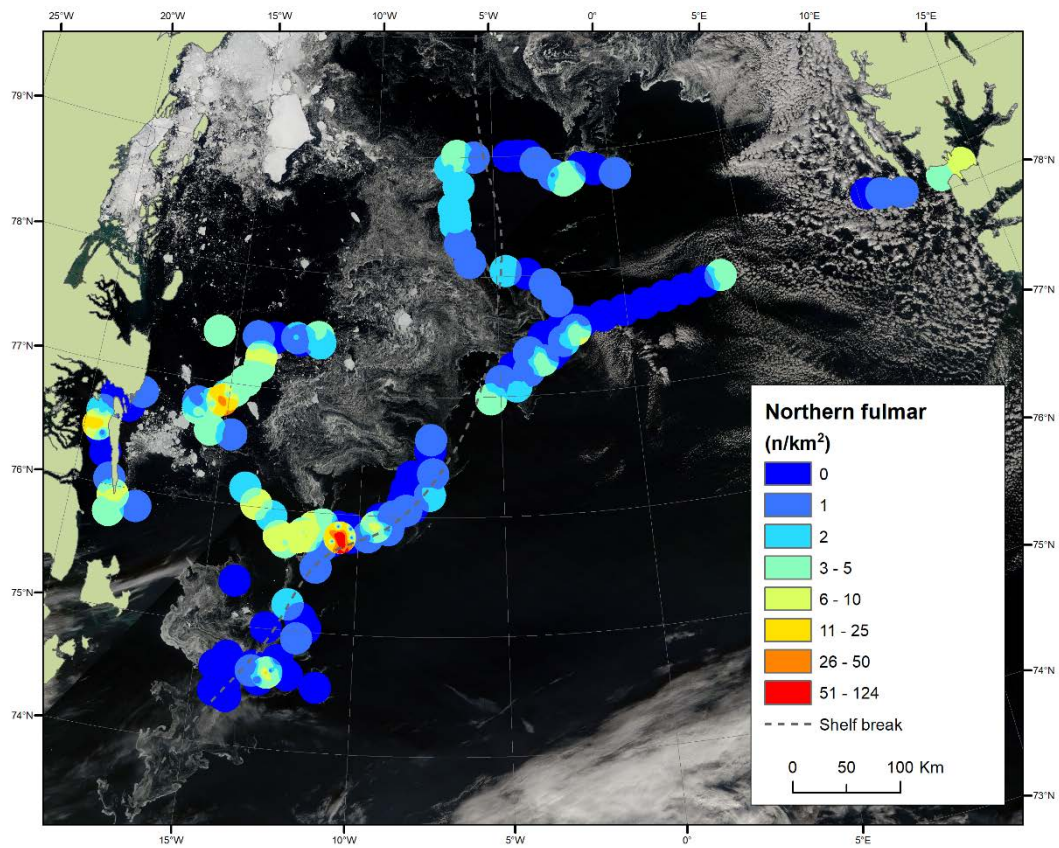


Figure 6.20. Density of fulmars on the Dana transects overlaying a satellite image with sea ice distribution from 26 August 2017.

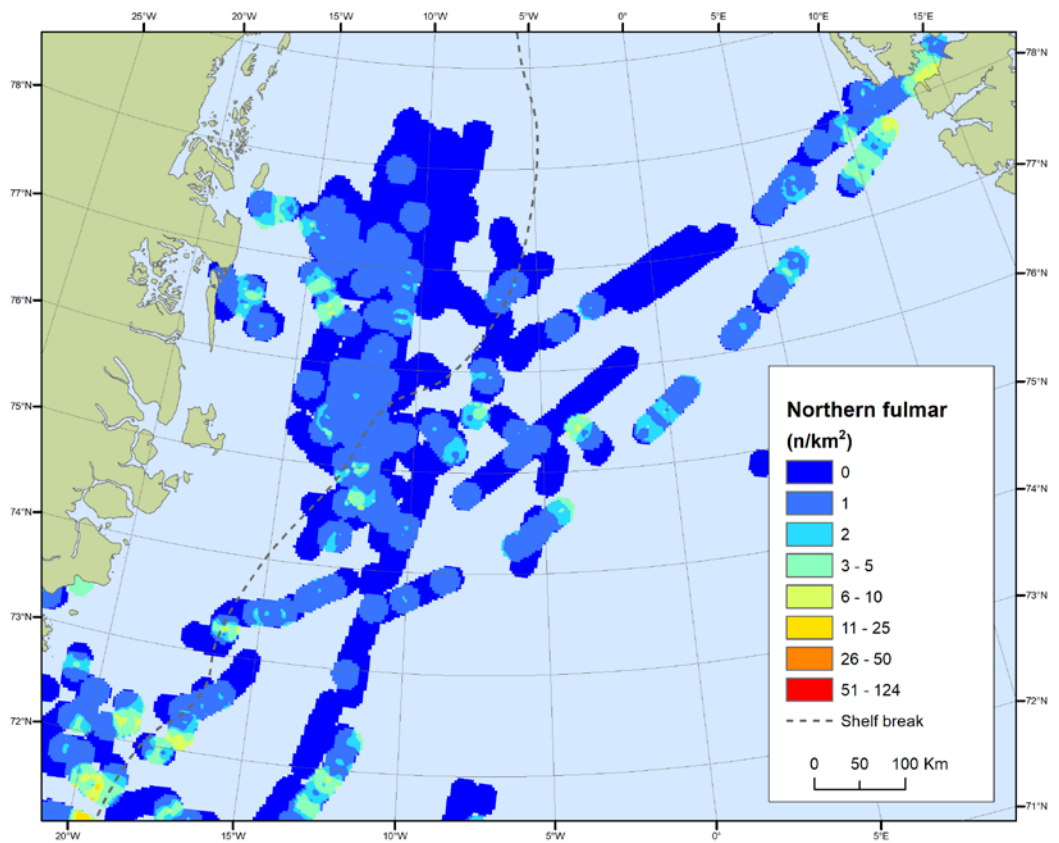


Figure 6.21. Fulmar density in the Greenland Sea calculated from the Greenland Seabirds at Sea database based on six individual summer surveys in 1994, 1995, 2006, 2007, 2009 and 2010.

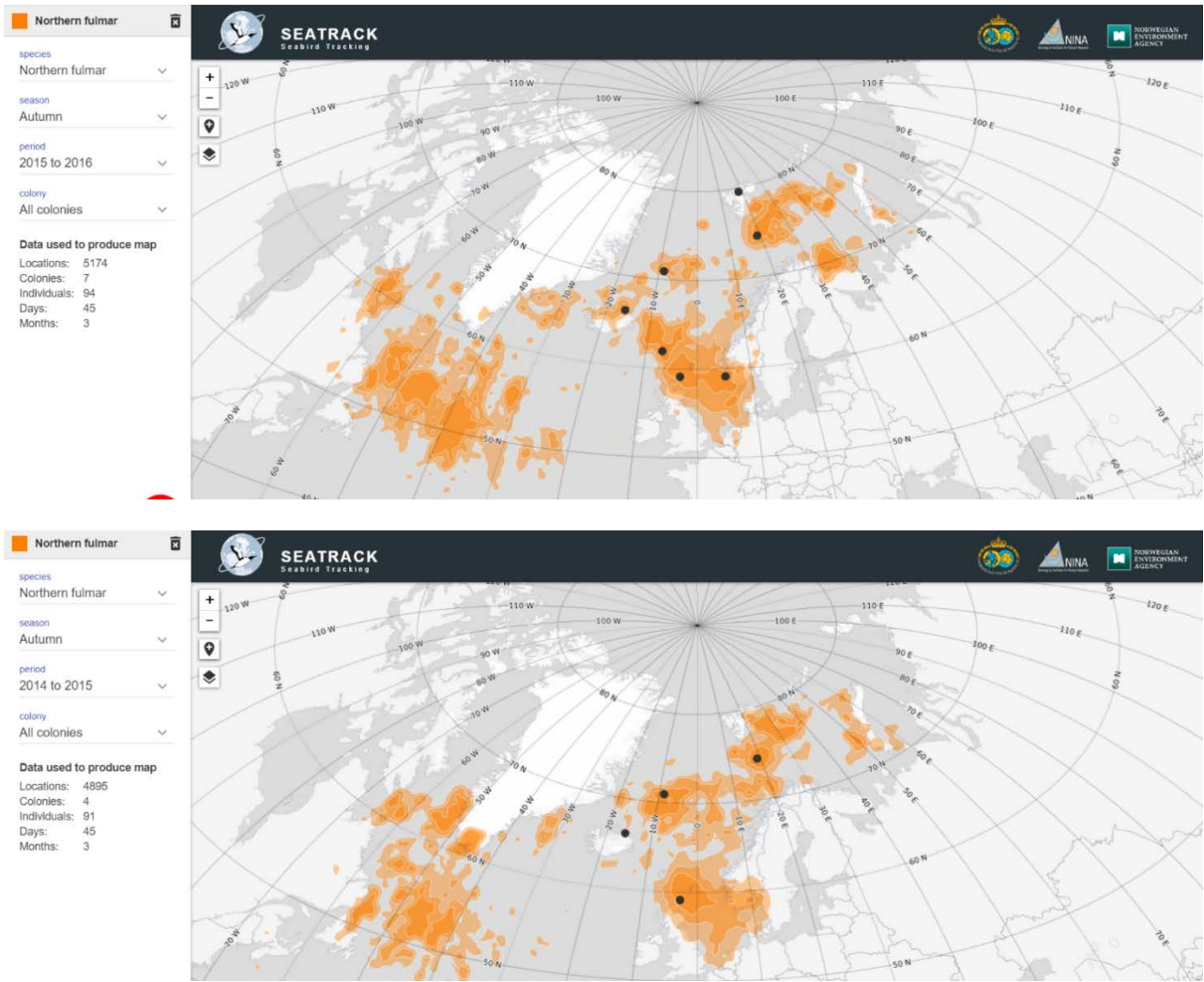


Figure 6.22. The distribution of fulmar in the Greenland Sea during autumn (August-October) in 2014, 2015 and 2016 based on tracking with geolocators from the breeding colonies (black dots) (screen dumps from the SEATRACK programme, <http://seatrack.seapop.no>).

Skuas

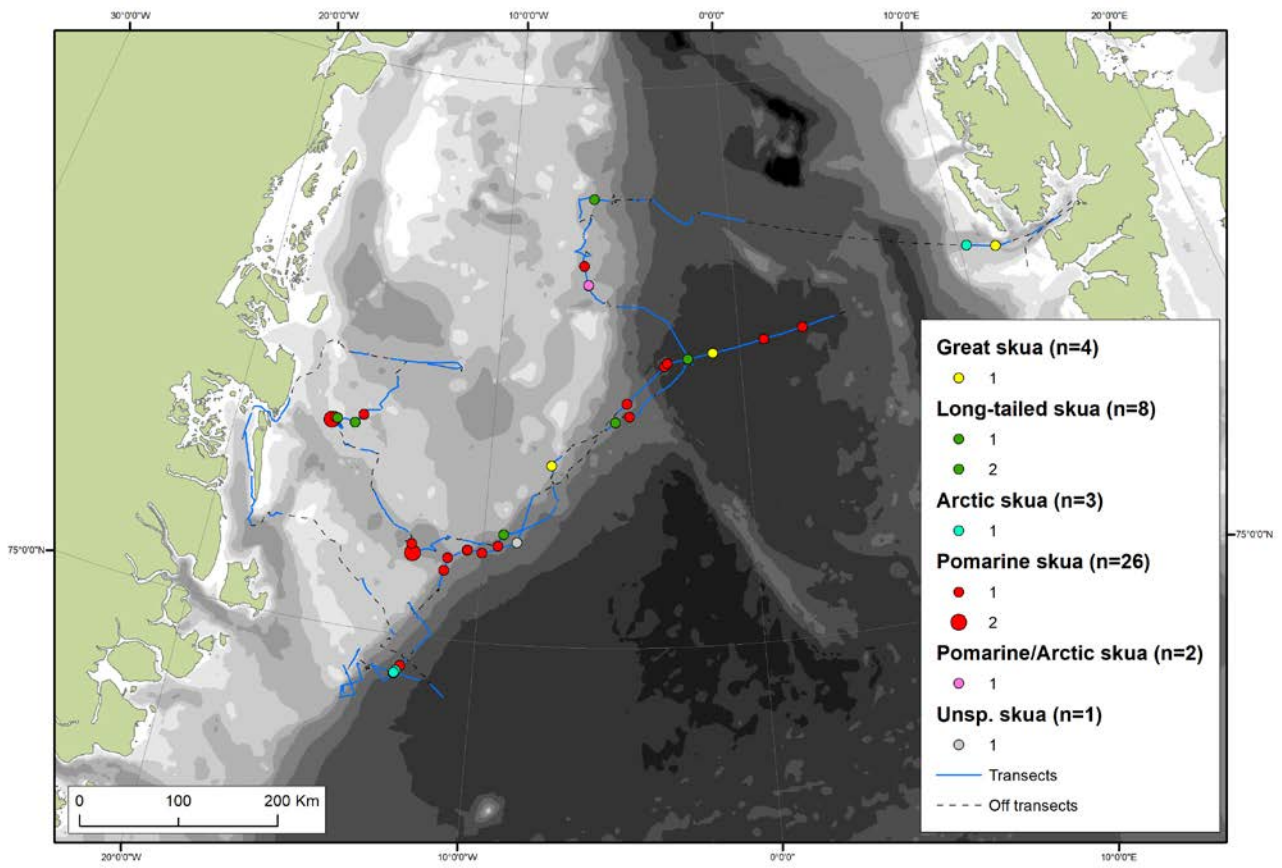


Figure 6.23. Observations of skuas overlaying the observed ice cover on the transects.

Black-legged kittiwake

Kittiwakes were widespread in low numbers (*figure 6.24* and *figure 6.25*). They often followed the ship, and we omitted the ship-followers from the transect records. The abundance of kittiwakes on the Dana cruise in 2017 seems to be relatively high compared to the average density in the area from previous surveys (*figure 6.26*).

It is seen from the SEATRACK maps that the western Greenland Sea also was an important postbreeding area for kittiwakes from a number of North Atlantic colonies in 2014, 2015, 2016 (*figure 6.27*). Remarkably, the distribution of tracked birds from each colony separately reveals that all four colonies studied had birds visiting the western Greenland Sea during autumn (*figure 6.28*). However, the discrete analysis clearly revealed that colonies in mainland Norway (Røst), Iceland and Svalbard contributed most with birds to the western Greenland Sea.

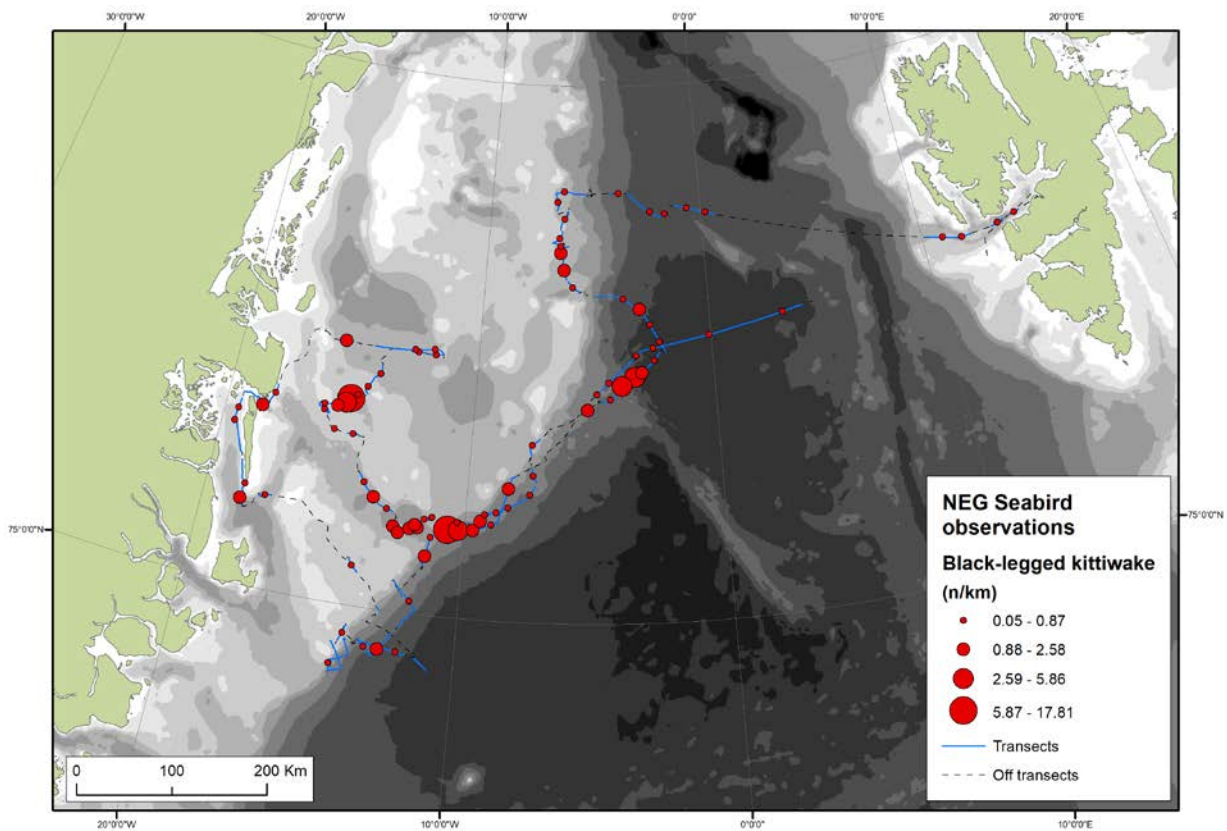


Figure 6.24. The black-legged kittiwake observations (n/km transect) overlaying the observed ice cover on the transects.

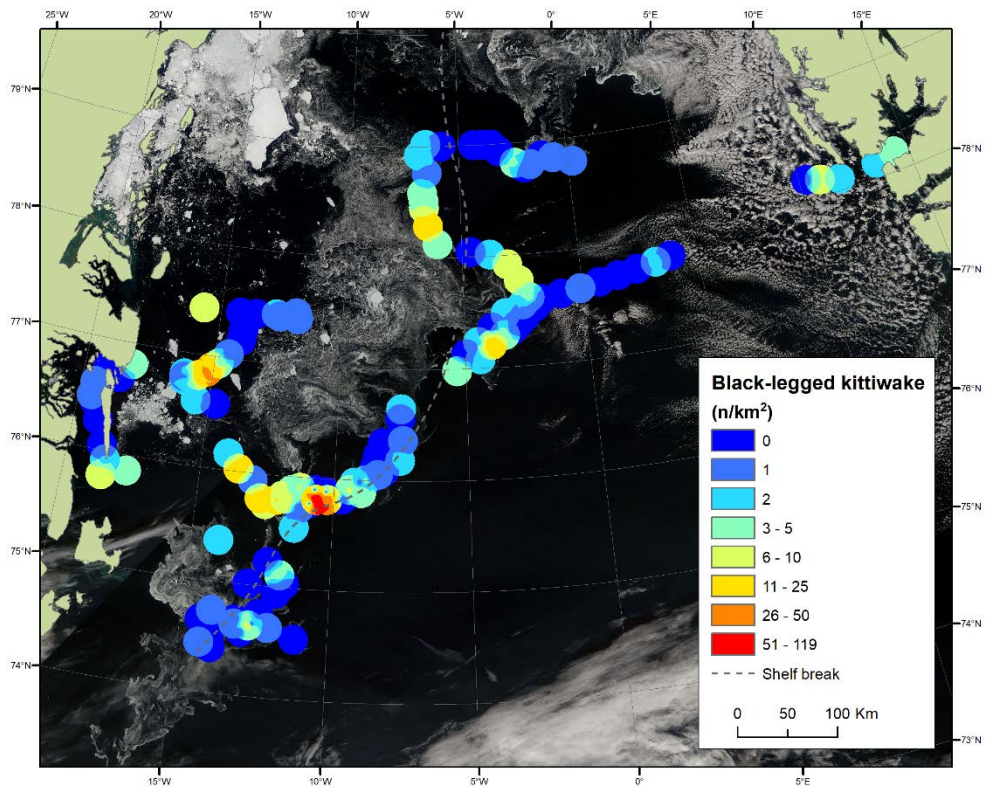


Figure 6.25. Density of black-legged kittiwake on the Dana transects, overlaying a satellite image with sea ice distribution from 26 August 2017 (effective search width = 150 m).

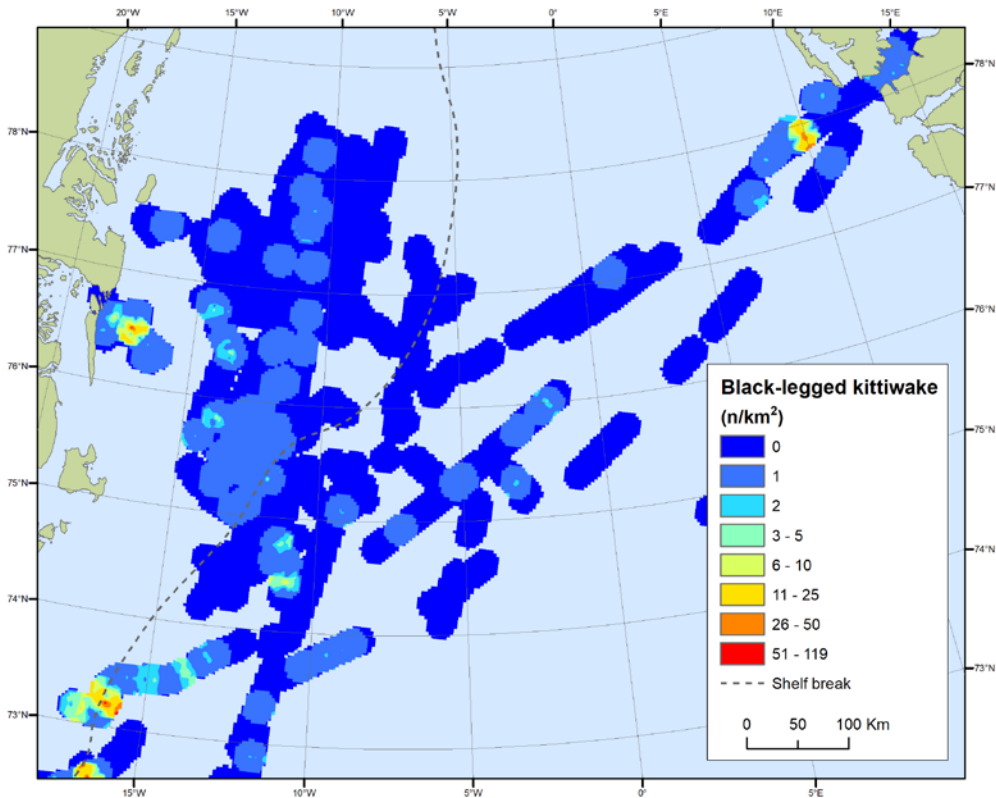


Figure 6.26. Black-legged kittiwake density in the Greenland Sea calculated from the Greenland Seabirds at Sea database based on six individual summer surveys in 1994, 1995, 2006, 2007, 2009 and 2010.

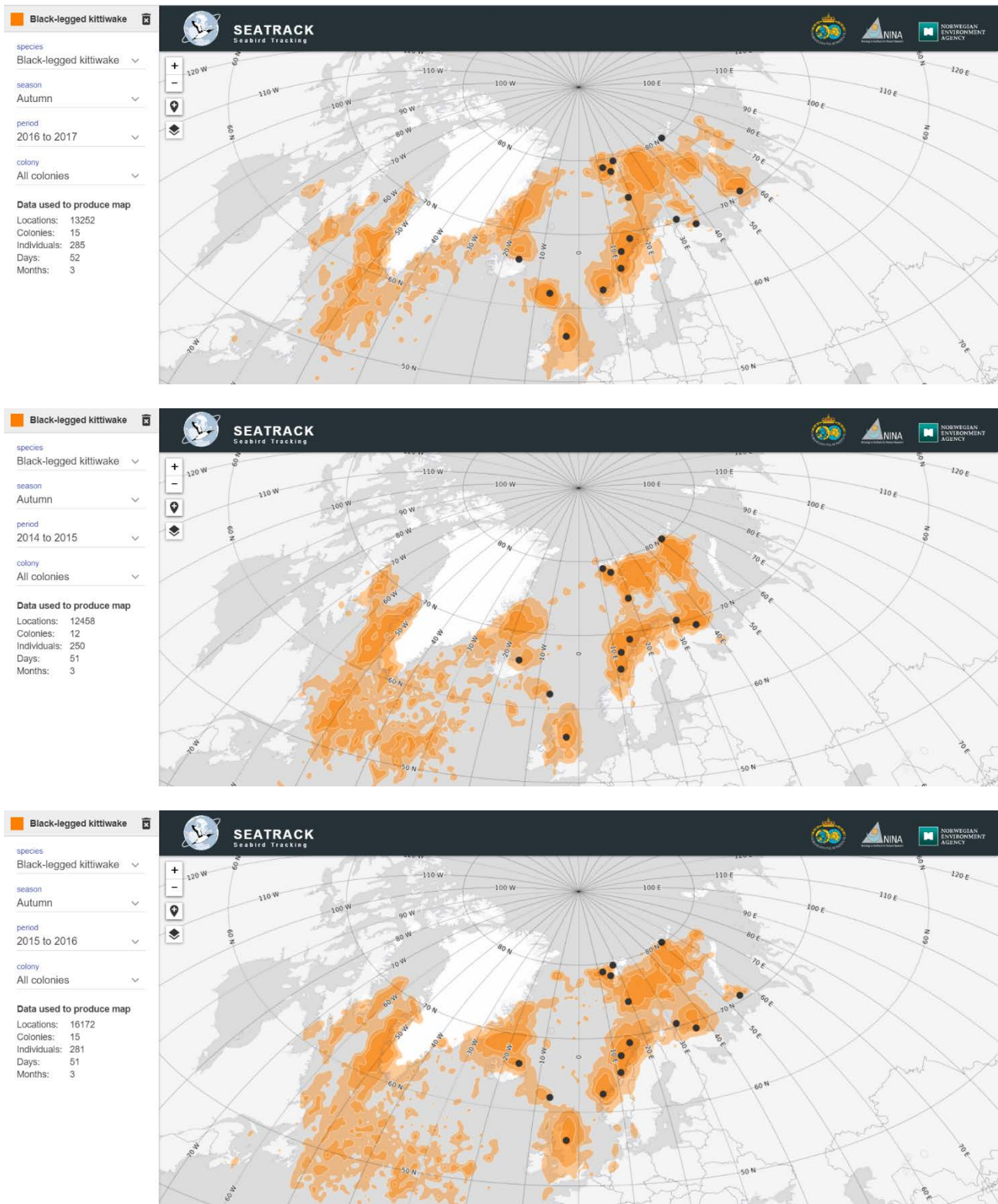


Figure 6.27. The distribution of black-legged kittiwake in the Greenland Sea during autumn (August-October) in 2014, 2015 and 2016 based on tracking with geolocators from the breeding colonies (black dots) (screen dumps from the SEATRACK programme).

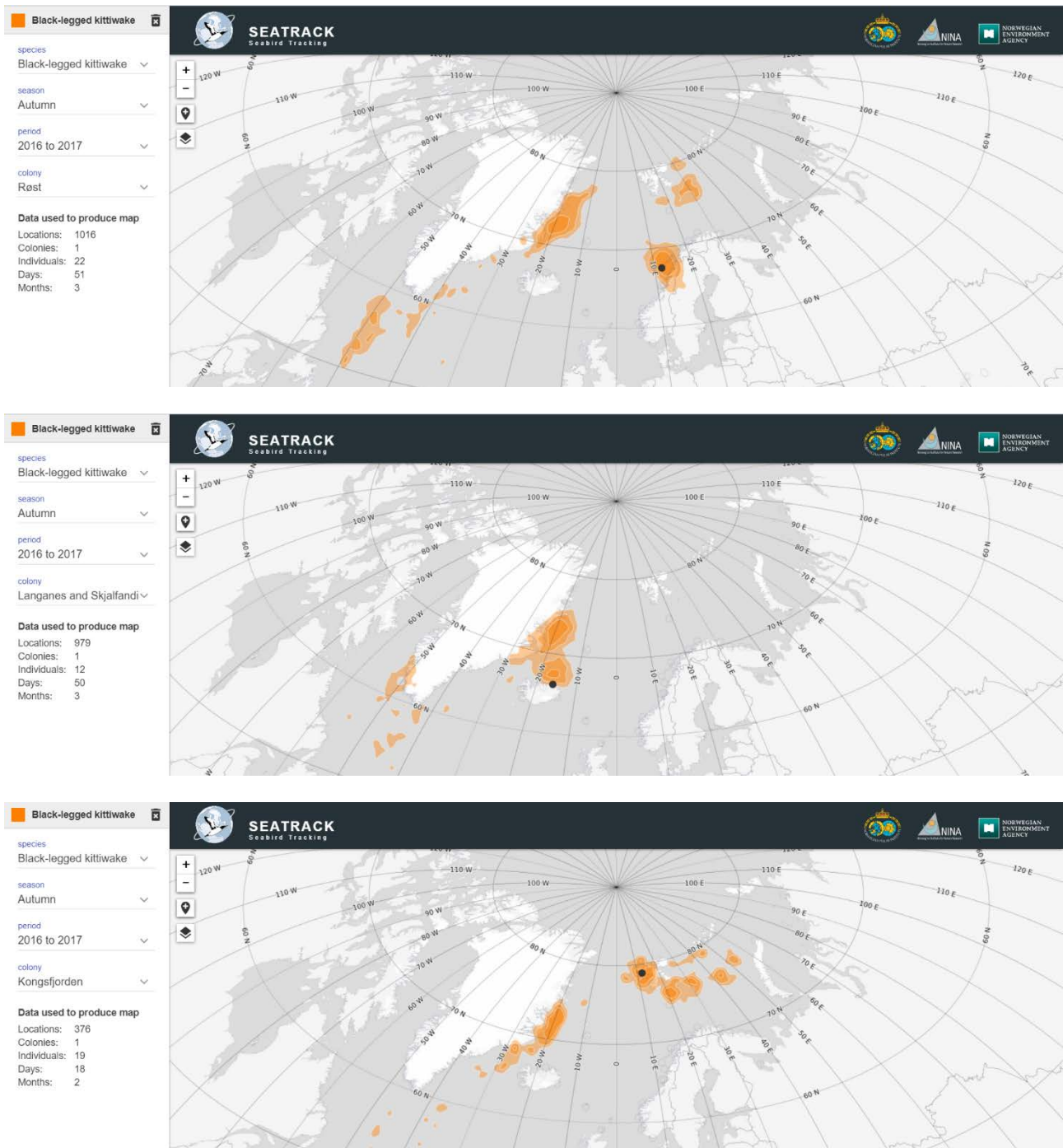


Figure 6.28. The distribution of black-legged kittiwake in the Greenland Sea during autumn (August-October) in 2016 based on tracking with geolocators from the breeding colonies (black dots) on mainland Norway, Iceland and Svalbard, respectively (screen dumps from the SEATRACK programme, <http://seatrack.seapop.no>).

Ivory gull

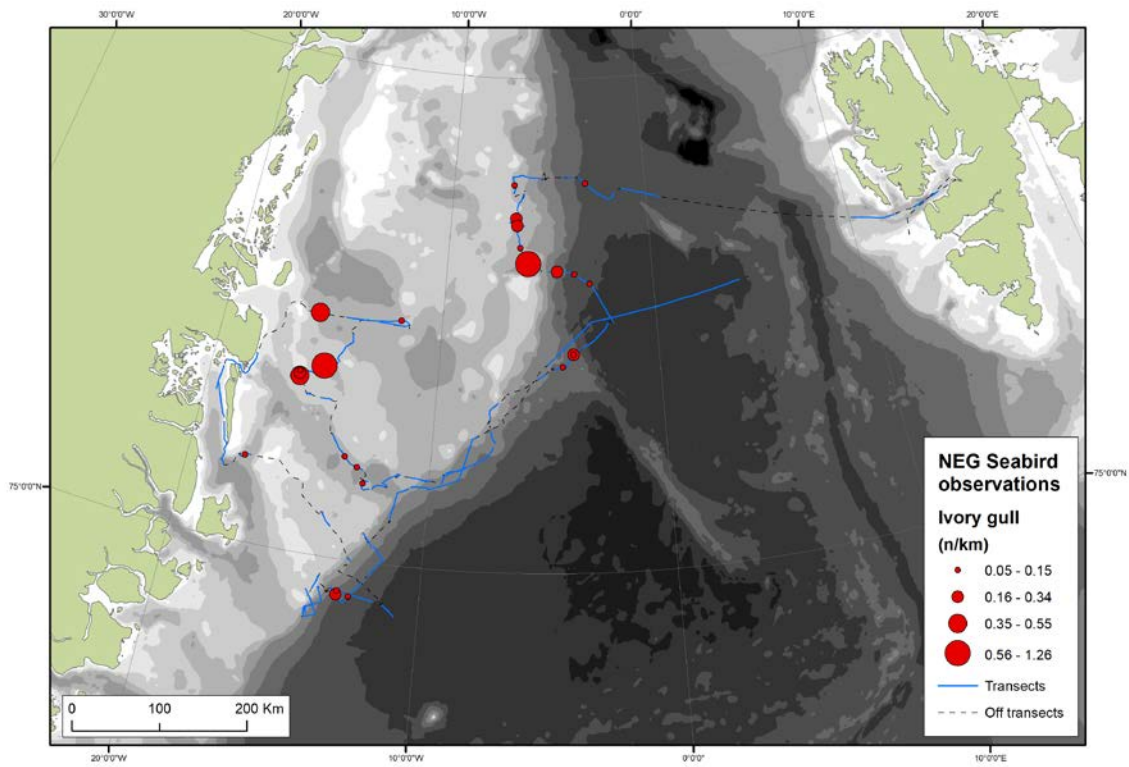


Figure 6.29. The ivory gull observations (n/km transect) overlaying the observed ice cover on the transects.

Arctic tern

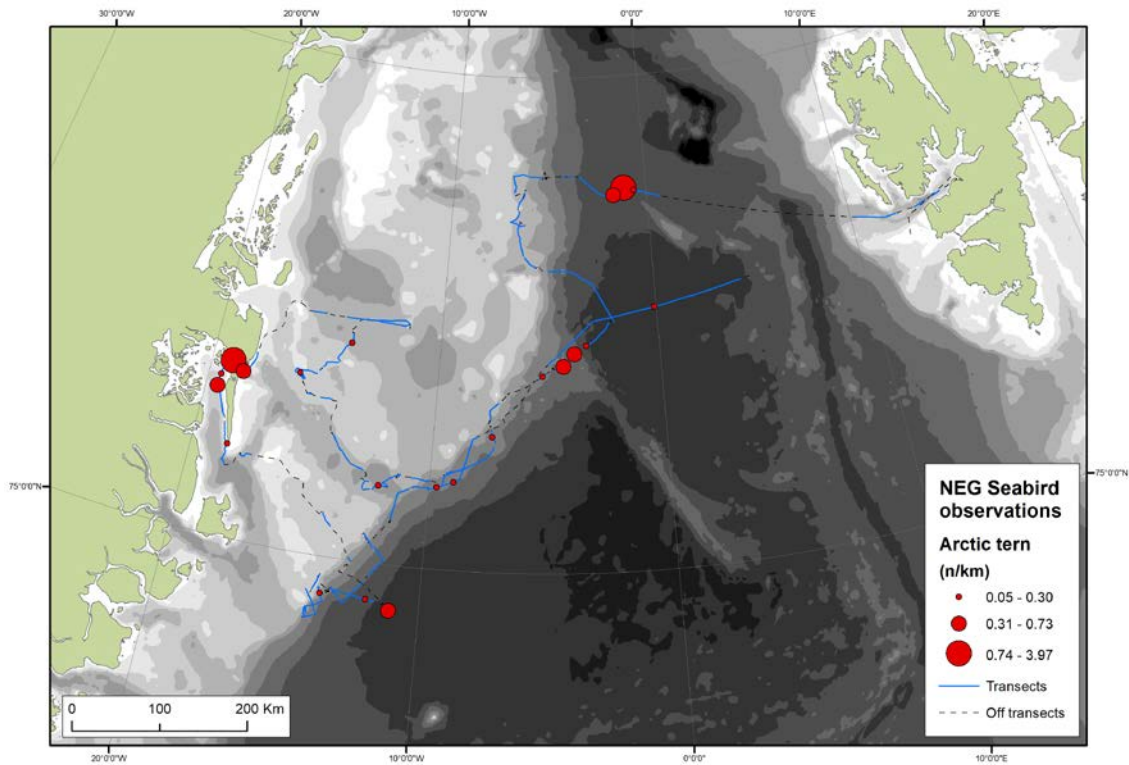


Figure 6.30. The Arctic tern observations (n/km transect) overlaying the observed ice cover on the transects. The high numbers at Danmarkshavn (the coast) reflect the vicinity of an Arctic tern colony.

Little Auk

Little auks were the most numerous seabirds on the Dana cruise (*table 6.1*) with the highest densities observed along the shelf break, and lower densities on the shelf in the open pack ice (*figure 6.31, figure 6.32*). The same distributional pattern is seen in the older data from the Greenland Seabirds at Sea database (*figure 6.33*). The subsequent survey (12 September - 1 October 2017) did not cover the shelf break, but data from the shelf indicate low densities on the shelf (average density 2.7 bird/km²) continuing during the last half of September (*figure 6.32*).

From the SEATRACK maps (*figure 6.34*), it is clear that the central Greenland Sea is an important area for the tracked little auks, with some variation in distribution between years. It can be seen that the little auk colonies at Svalbard and Bjørnøya contributed most with birds to the western Greenland Sea (*figure 6.35*), while birds from the colony at Franz Josef Land to a much lesser extent visited the western Greenland sea during autumn. Also, little auks from the Scoresby Sund colonies contribute to the little auks in the Greenland Sea in a north going postbreeding migration (Mosbech et al. 2012) (data not included on the SEATRACK maps).

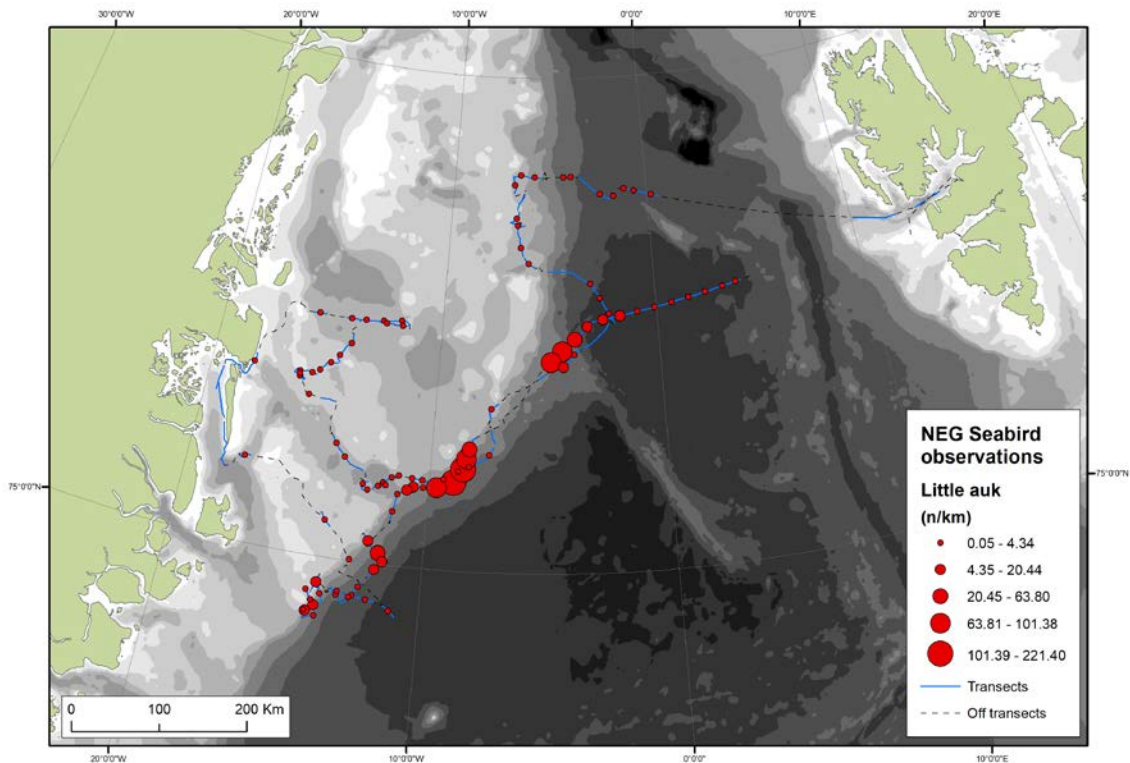
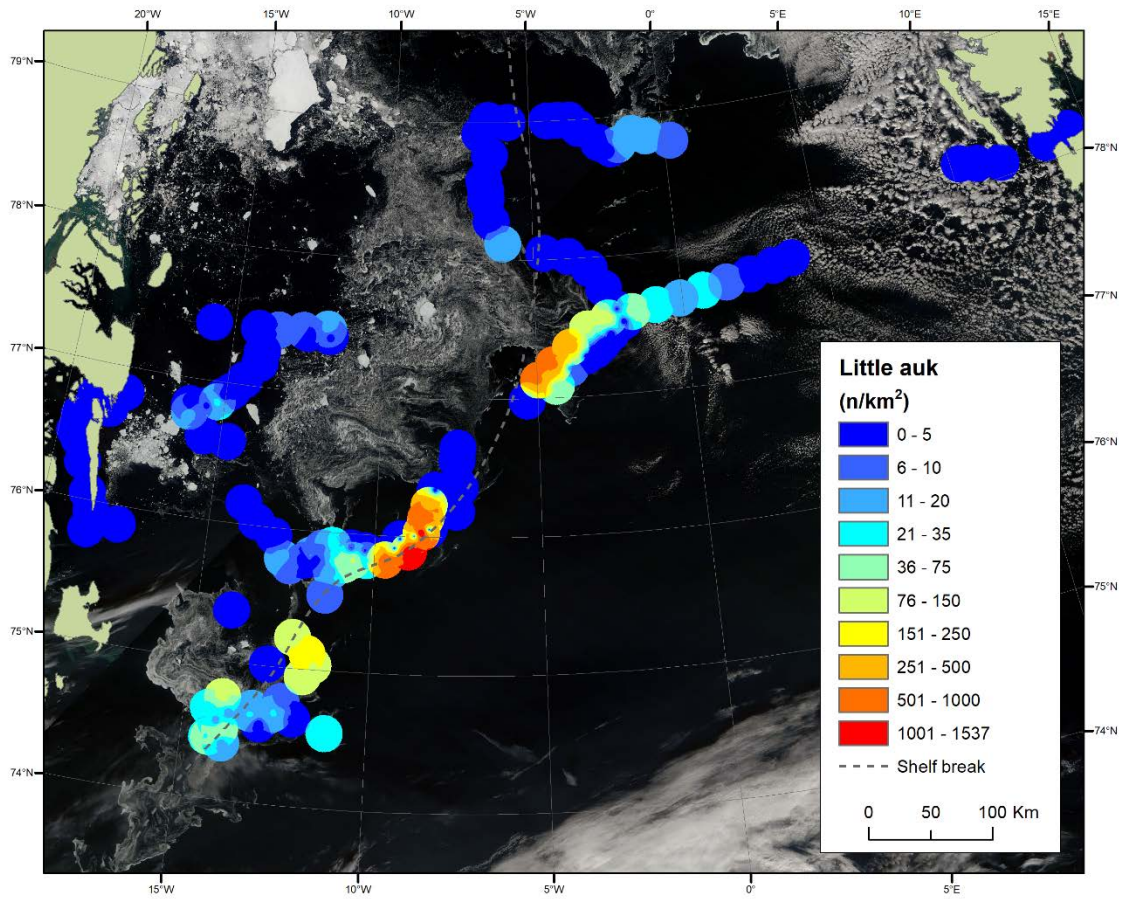


Figure 6.31. The little auk observations (n/km transect) overlaying the observed ice cover on the transects.

a)



b)

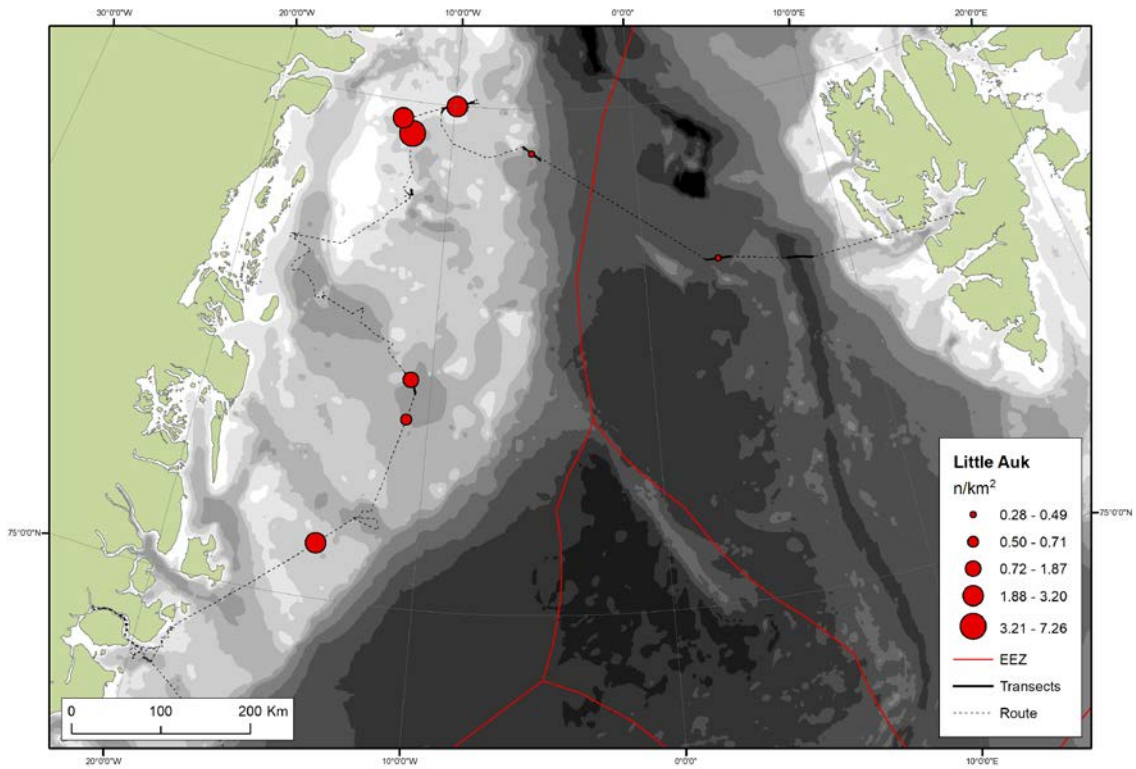


Figure 6.32. (a) Density of little auk on the transects, overlaying a satellite image with sea ice distribution from 26 August 2017. (b) Density of little auk on the shelf recorded on a few small transects during the subsequent survey (12 September to 1 October).

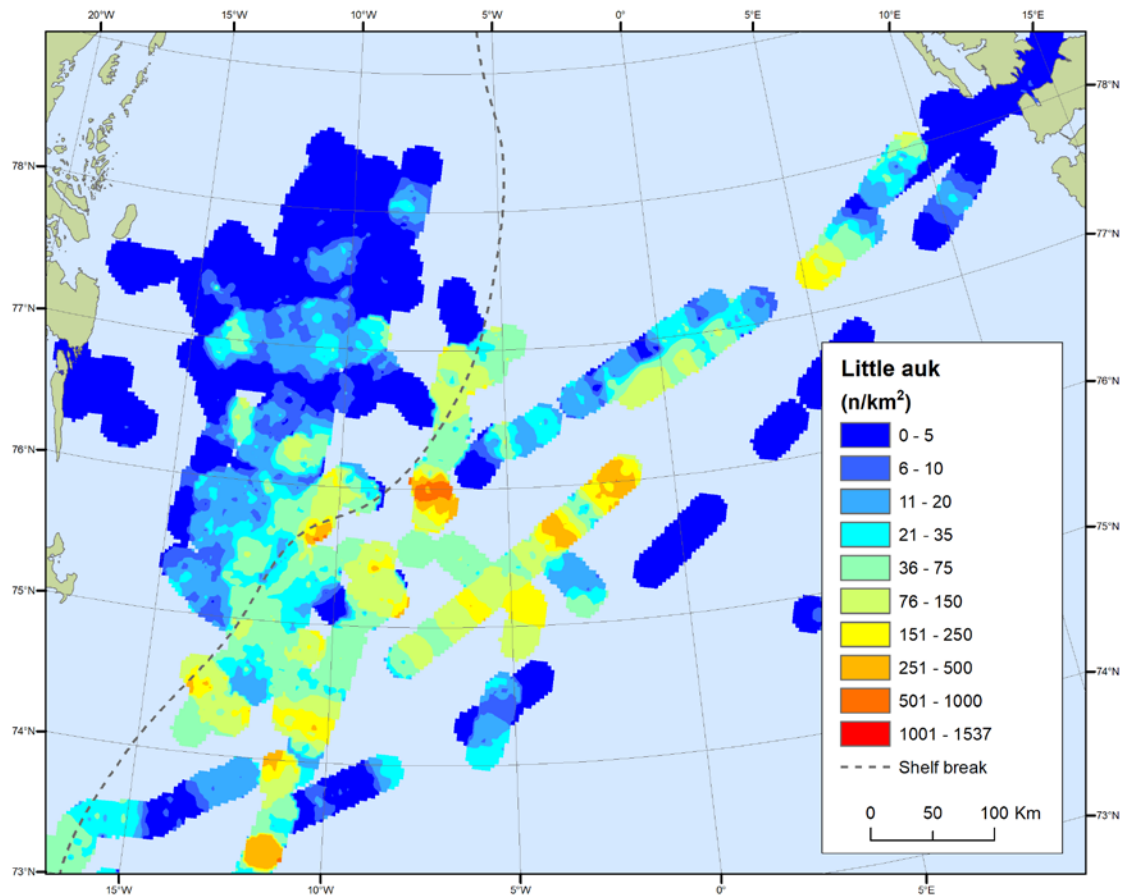


Figure 6.33. Little auk density in the Greenland Sea calculated from the Greenland Seabirds at Sea database based on six individual summer surveys in 1994, 1995, 2006, 2007, 2009 and 2010.

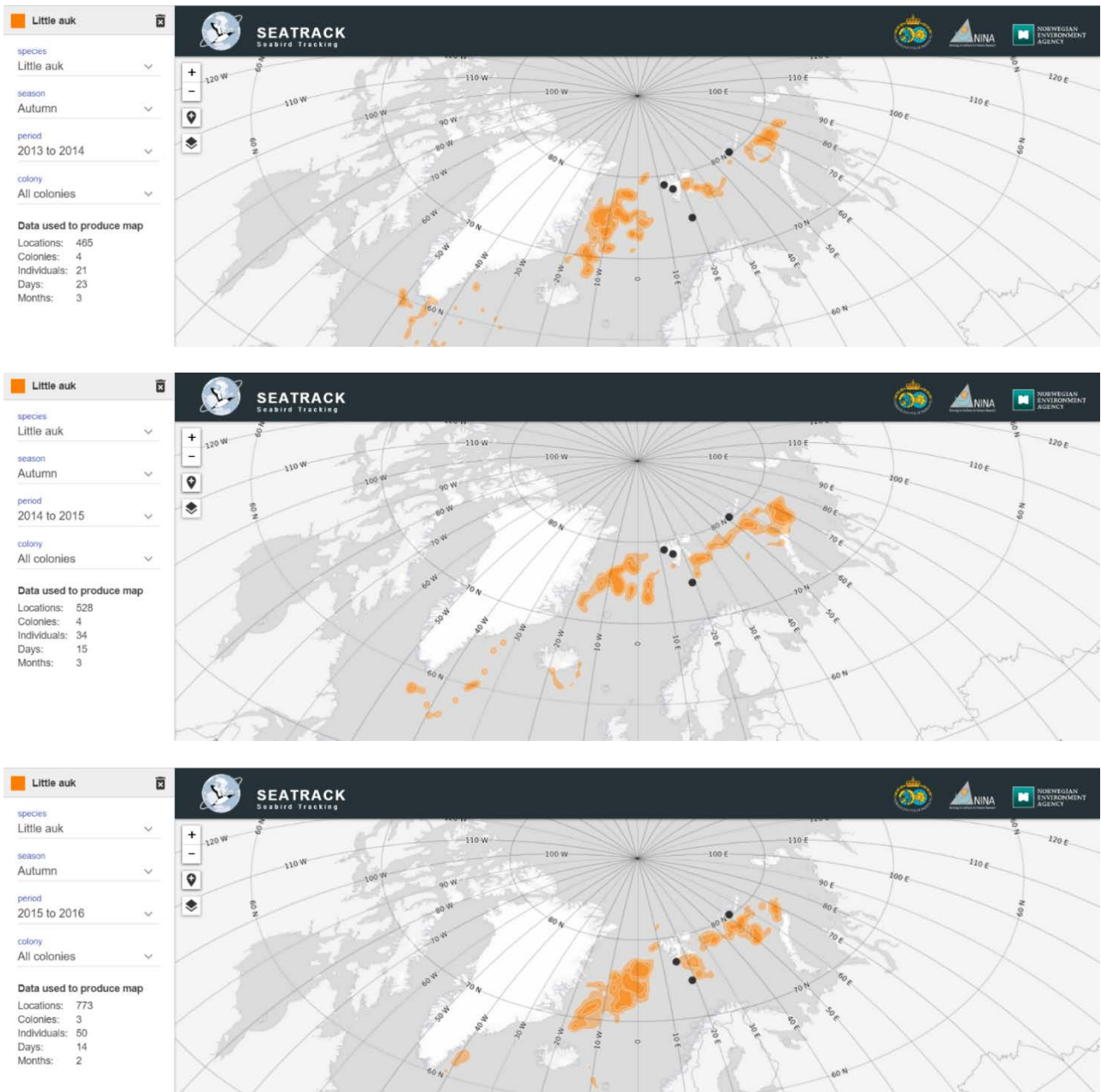


Figure 6.34. The distribution of little auk in the Greenland Sea during autumn (August-October) in 2014, 2015 and 2016 based on tracking with geolocators from the breeding colonies in Norway and Franz Josef Land (black dots) (screen dumps from the SEATRACK programme).

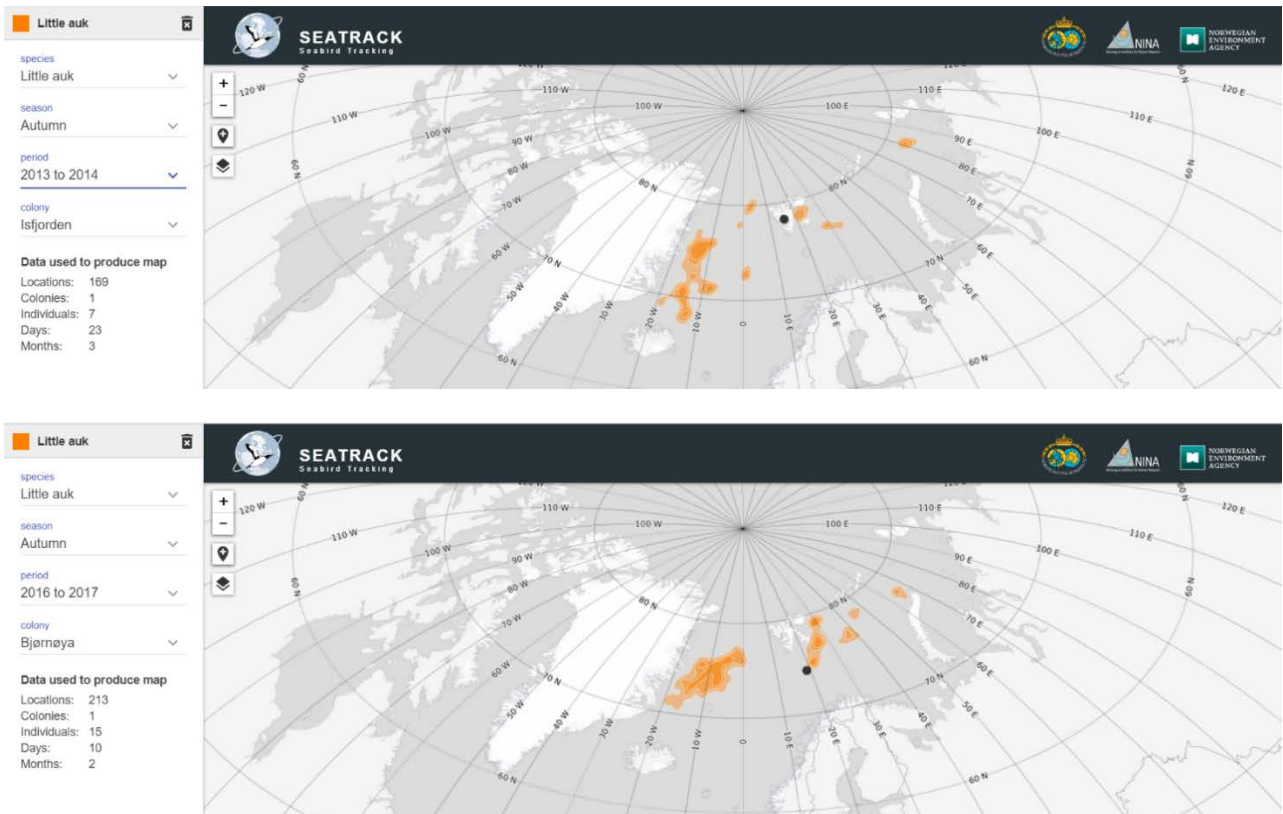


Figure 6.35. The distribution of tracked little auks in the Greenland Sea during autumn (August-October) based on tracking with geolocators from the breeding colonies in Svalbard and Bjørnøya, respectively (black dots) (screen dumps from the SEATRACK programme, <http://seatrack.seapop.no>).

Thick-billed murre

Very few thick-billed murres were observed during the Dana cruise 22 August to 11 September (*table 6.1, figure 6.36 and figure 6.37*) and thick-billed murres were nearly absent during the subsequent survey 12 September to 1 October. This is consistent with the records in the Greenland Seabirds at Sea database (*figure 6.38*) where thick-billed murres mainly have been observed further to the east.

Also the SEATRACK data (*figure 6.39*) indicate that the thick-billed murre swimming migration is only passing through the southernmost part of the western Greenland Sea. However, there is some variability between years (*figure 6.39*) which may be caused by variability in ice conditions, oceanographic conditions or simply the wind conditions during the swimming migration. The tracked thick-billed murres occurring in the southern part of the western Greenland Sea during autumn were tracked from the colonies Isfjorden (Svalbard), Jan Mayen, and Langanes and Skjalfandi (Iceland).

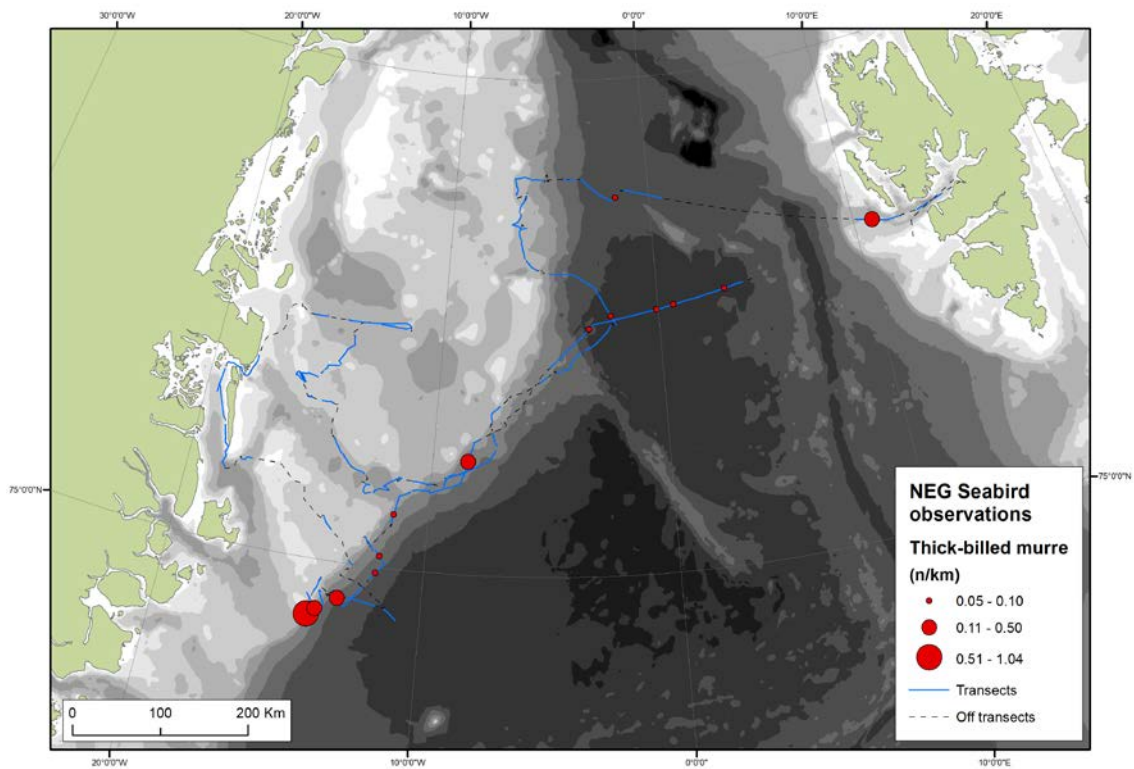


Figure 6.36. The thick-billed murre observations (n/km transect) overlaying the observed ice cover on the Dana transects.

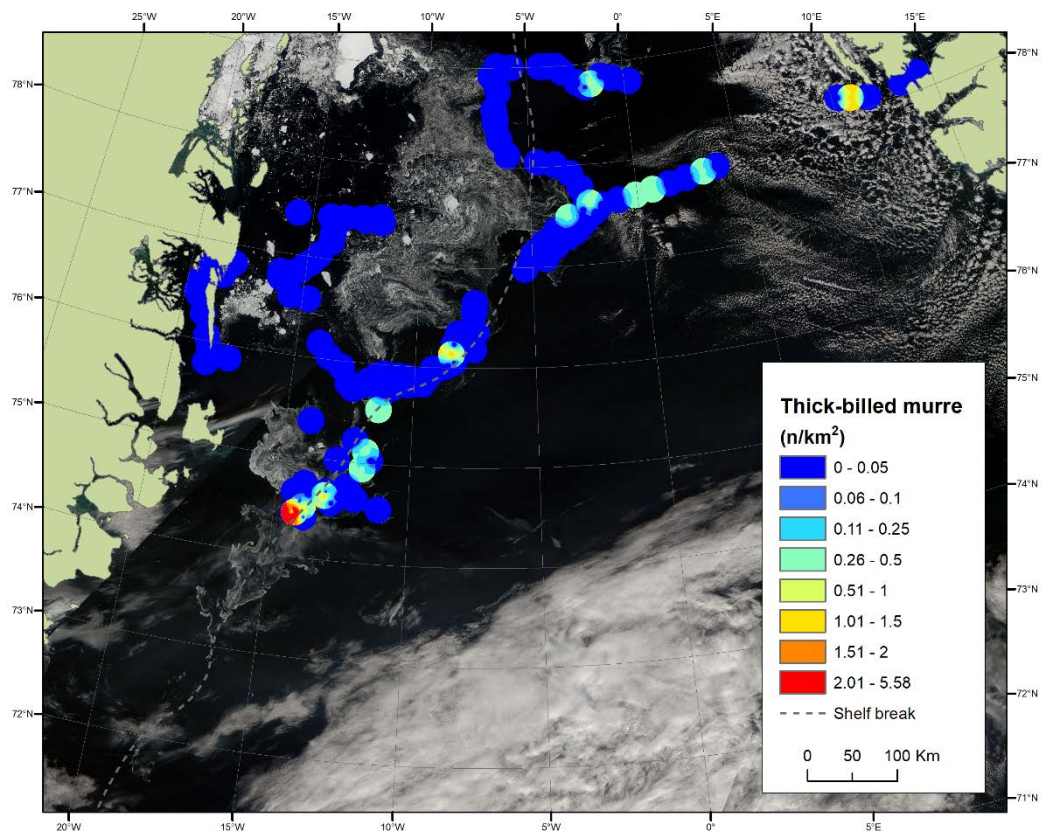


Figure 6.37. Density of thick-billed murre on the transects, overlaying a satellite image with sea ice distribution from 26 August 2017.

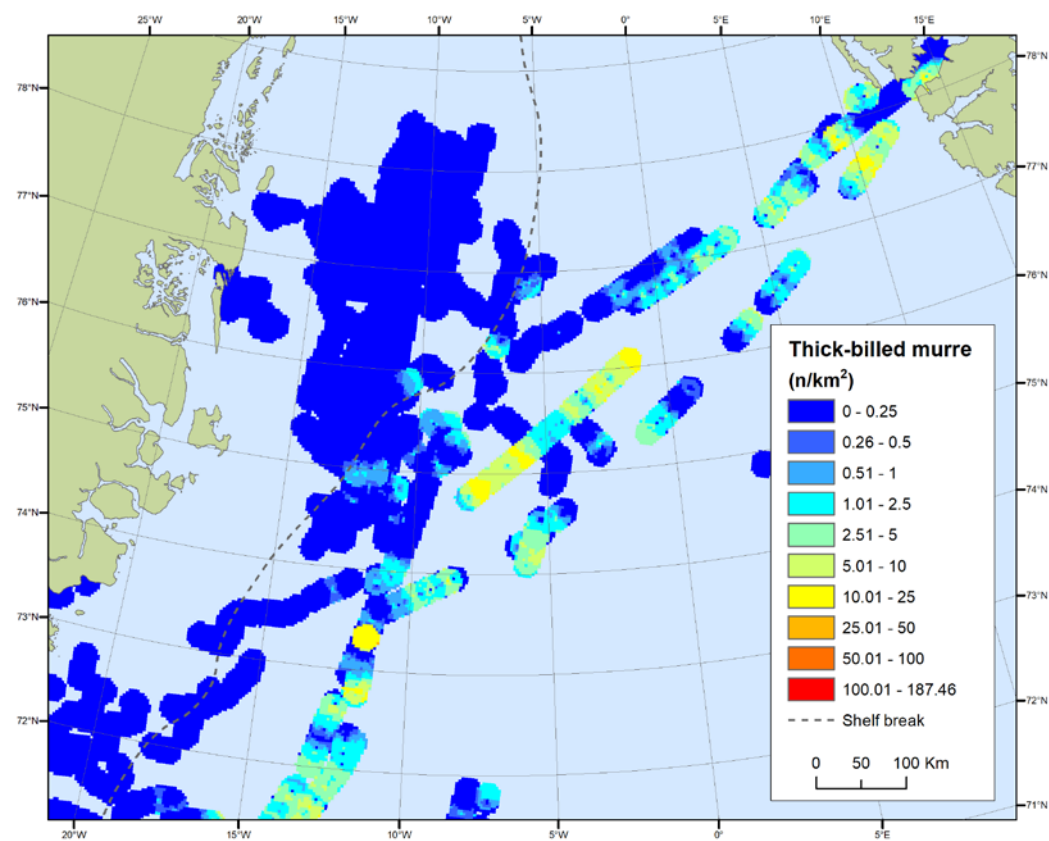


Figure 6.38. Thick-billed murre density in the Greenland Sea calculated from the Greenland Seabirds at Sea database based on six individual summer surveys in 1994, 1995, 2006, 2007, 2009 and 2010.

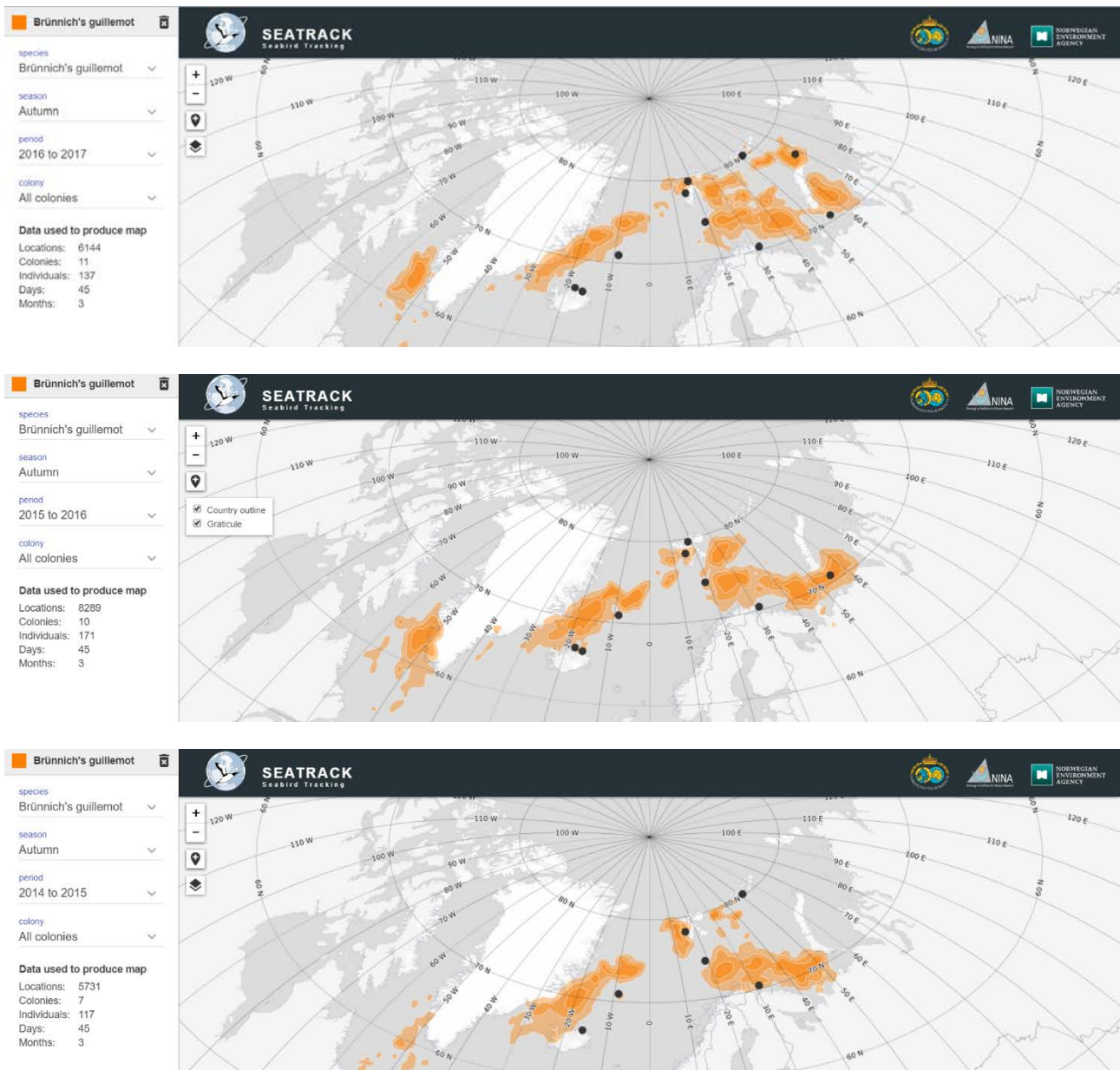


Figure 6.39. The distribution of tracked thick-billed murre (Brunnich's guillemot) in the Greenland Sea during autumn (August–October) in 2014, 2015 and 2016 based on tracking with geolocators from the breeding colonies (black dots) (screen dumps from the SEATRACK programme, <http://seatrack.seapop.no>). The tracked birds occurring in the western Greenland Sea come from the colonies Isfjorden (Svalbard), Jan Mayen, and Langanes and Skjalfandi (Iceland).

7 References

Bauerfeind E, Garrity C, Krumbholz M, Ramseier RO, Voss M (1997) Seasonal variability of sediment trap collections in the Northeast Water Polynya. Part 2. Biochemical and microscopic composition of sedimenting matter. *J Mar Syst* 10:371-389.

Boertmann D & Mosbech A (eds.) (2011) The western Greenland Sea, a strategic environmental impact assessment of hydrocarbon activities. Aarhus University, DCE – Danish Centre for Environment and Energy, 268 pp. - Scientific Report from DCE – Danish Centre for Environment and Energy no. 22.

Carmack E, Wassmann P (2006) Food webs and physical-biological coupling on pan-Arctic shelves: unifying concepts and comprehensive perspectives. *Prog Oceanogr* 71:446-477.

Fauchald P, Anker-Nilssen T, Barrett RT, Bustnes JO, Bårdsen B-J, Christensen-Dalsgaard S, Descamps S, Engen S, Erikstad KE, Hanssen SA, Lorentsen S-H, Moe B, Reiertsen TK, Strøm H, Systad GH (2015) The status and trends of seabirds breeding in Norway and Svalbard – NINA Report 1151. 84pp.

Fort J, Moe B, Strøm H, Grémillet D, Welcker J, Schultner J, Jerstad K, Johansen KL, Phillips RA, Mosbech A (2013) Multicolony tracking reveals potential threats to little auks wintering in the North Atlantic from marine pollution and shrinking sea ice cover. *Diversity and Distributions* 19:1322-1332.

Hansen HP, Koroleff F (1999) Determination of nutrients. In: Grasshoff K, Kremling K, Ehrhardt M (eds) *Methods of seawater analysis*, 3rd edn. Wiley-VCH.

Hirche H, Mumm N (1992) Distribution of dominant copepods in the Nansen Basin, Arctic Ocean, in summer. *Deep Sea Res* 39:485-505.

Hirche HJ, Hagen W, Mumm N, Richter C (1994) The Northeast Water polynya, Greenland Sea - III. Meso- and macrozooplankton distribution and production of dominant herbivorous copepods during spring. *Polar Biol* 14:491-503.

Holding JM, Markager S, Juul-Pedersen T, Paulsen ML, Møller EF, Meire L, Sejr MK (2019) Seasonal and spatial patterns of primary production in a high-latitude fjord affected by Greenland Ice Sheet run-off. *Biogeosciences Discuss*:1-28.

Hygum B, Rey C, Hansen B, Carlotti F (2000) Rearing cohorts of *Calanus finmarchicus* (Gunnerus) in mesocosms. *ICES J Mar Sci* 57:1740-1751.

ICES (2017) Manual for the Midwater Ring Net sampling during IBTS Q1. Series of ICES Survey Protocols SISP 2. 25 pp. <http://doi.org/10.17895/ices.pub.3434>

Isaksen K, Bakken V (1995) Estimation of the breeding density of little auks (*Alle alle*). I: Isaksen K & Bakken V (eds.): Seabird populations in the northern Barents Sea. Source data for the impact assessment of the effects of oil drilling activity. Norsk Polarinstitutt Meddelelser 135, pp. 37-47. Tromsø: Norwegian Polar Institute.

Jespersen AM, Christoffersen K (1987) Measurements of chlorophyll a from phytoplankton using ethanol as extraction solvent. Arch Hydrobiol 109:445-445.

Johansen KL, Boertmann D, Mosbech A, Hansen TB (2015) Manual for seabird and marine mammal survey on seismic vessels in Greenland. 4th revised edition, April 2015. Aarhus University, DCE - Danish Centre for Environment and Energy, 74 pp. Scientific Report from DCE - Danish Centre for Environment and Energy No. 152.

Klein Breteler WCM, Fransz HG, Gonzalez SR (1982) Growth and development of four calanoid copepod species under experimental and natural conditions. Netherlands J Sea Res 16:195-207.

Madsen SD, Nielsen TG, Hansen BW (2001) Annual population development and production by *Calanus finmarchicus*, *C. glacialis* and *C. hyperboreus* in Disko Bay, western Greenland. Mar Biol 139:75-93.

Meire L, Meire P, Struyf E, Krawczyk DW, Arendt KE, Yde JC, Juul-Pedersen T, Hopwood MJ, Rysgaard S, Meysman FJR (2016) High export of dissolved silica from the Greenland Ice Sheet. Geophys. Res. Lett. 43:9173-9182. doi:10.1002/2016GL070191

Middelbo AB, Sejr MK, Arendt KE, Møller EF (2018) Impact of glacial meltwater on spatiotemporal distribution of copepods and their grazing impact in Young Sound NE, Greenland. Limnol Oceanogr 63:322-336.

Møller EF, Johansen KL, Agersted MD, Rigét F, Clausen DS, Larsen J, Lyngs P, Middelbo A, Mosbech A (2018) Zooplankton phenology may explain the North Water polynya's importance as a breeding area for little auks. MEPS 605:207-223.

Møller EF, Nielsen TG, Richardson K (2006) The zooplankton community in the Greenland Sea: Composition and role in carbon turnover. Deep Sea Res Part I Oceanogr Res Pap 53:76-93.

Mosbech A, Johansen KL, Bech NI, Lyngs P, Harding AM, Egevang C, et al. (2012) Inter-breeding movements of little auks *Alle alle* reveal a key post-breeding staging area in the Greenland Sea. Polar Biology 35(2):305-311.

Nielsen TG, Kjellerup S, Smolina I, Hoarau G, Lindeque P (2014) Live discrimination of *Calanus glacialis* and *C. finmarchicus* females: Can we trust phenological differences? Mar Biol 161:1299-1306.

Pesant S, Legendre L, Gosselin M, Bauerfeind E, Budéus G (2002) Wind-triggered events of phytoplankton downward flux in the Northeast Water Polynya. J Mar Syst 31:261-278.

- Qu B, Gabric AJ, Lu Z, Li H, Zhao L (2016) Unusual phytoplankton bloom phenology in the northern Greenland Sea during 2010. *J Mar Syst* 164:144-150.
- Richardson K, Markager S, Buch E, Lassen MF, Kristensen AS (2005) Seasonal distribution of primary production, phytoplankton biomass and size distribution in the Greenland Sea. *Deep Sea Res Part I Oceanogr Res Pap* 52:979-999.
- Rudels B, Fahrbach E., Meincke J, Budéus G, Eriksson P (2002) The East Greenland Current and its contribution to the Denmark Strait overflow. *ICES Journal of Marine Science* 59:1133-1154.
- Rysgaard S, Glud RN (2007) Carbon cycling in Arctic marine ecosystems: Case study Young Sound. *Medd Greenland, Bioscience*. 216.
- Sabatini M, Kiørboe T (1994) Egg production, growth and development of the cyclopoid copepod *Oithona similis*. *J Plankton Res* 16:1329-1351.
- Satapoomin S (1999) Carbon content of some common tropical Andaman Sea copepods. *J Plankton Res* 21:2117-2123.
- Steeman-Nielsen E (1952) The use of radio-active carbon (^{14}C) for measuring organic production in the sea. *J Cons Int Explor Mer* 18:117-140.
- Swalethorp R, Kjellerup S, Dünweber M, Nielsen TG, Møller EF, Rysgaard S, Hansen BW (2011) Grazing, egg production, and biochemical evidence of differences in the life strategies of *Calanus finmarchicus*, *C. glacialis* and *C. hyperboreus* in Disko Bay, Western Greenland. *Mar Ecol Prog Ser* 429:125-144.
- Tremblay J-E, Gagnon J (2009) The effects of irradiance and nutrient supply on the productivity of Arctic waters: A perspective on climate. In: Nihoul JCJ & Kostianoy AG (eds.) *Influence of Climate Change on the Changing Arctic and Sub-Arctic Conditions - 2009*. Springer Science + Business Media B.V.

Appendix 1

List of samplings on R/V Dana 24-8-2017 to 9-9-2017

Gear code	Parameter
BONGO	Zooplankton
FOTÁ	Pelagic trawl
HAPS	Bottom sample
MIK	Macrozooplankton
MULTI	Zooplankton
SEA	CTD (Seabird)
TV3	Benthic trawl
VGRAB	Bottom sample
WP 3	Zooplankton
WP2	Zooplankton

Station	Time	Gear code	Position latitude start	Position longitude start	Bottom depth start
1	2017-08-24T13:04:13+00:00	SEA	78.59.856 N	003.29.802 W	2265
1	2017-08-24T13:28:41+00:00	SEA	78.59.748 N	003.30.125 W	2263
2	2017-08-24T16:02:18+00:00	SEA	78.59.915 N	004.22.924 W	1707
3	2017-08-24T18:43:34+00:00	WP2	78.59.911 N	005.13.563 W	20
3	2017-08-24T19:15:30+00:00	SEA	78.59.910 N	005.14.762 W	1114
3	2017-08-24T20:04:24+00:00	MULTI	78.59.940 N	005.16.175 W	1097
3	2017-08-24T22:05:25+00:00	BONGO	78.59.620 N	005.19.338 W	1049
3	2017-08-24T22:43:13+00:00	SEA	78.58.112 N	005.21.523 W	993
3	2017-08-25T00:58:57+00:00	TV3	79.00.729 N	005.20.999 W	20
3	2017-08-25T02:36:24+00:00	MIK	79.02.116 N	005.15.880 W	11
3	2017-08-25T03:26:18+00:00	MIK	78.59.542 N	005.13.888 W	41
3	2017-08-25T04:14:08+00:00	HAPS	78.58.731 N	005.14.016 W	185
3	2017-08-25T07:23:58+00:00	VGRAB	78.59.136 N	005.10.782 W	1148
4	2017-08-25T10:05:04+00:00	SEA	78.59.924 N	006.07.492 W	425
5	2017-08-25T11:52:40+00:00	SEA	78.59.959 N	006.53.998 W	267
6	2017-08-25T14:03:14+00:00	WP2	78.50.089 N	006.51.624 W	243
6	2017-08-25T14:43:46+00:00	WP 3	78.50.250 N	006.51.036 W	245
6	2017-08-25T15:05:43+00:00	BONGO	78.49.957 N	006.50.493 W	246
6	2017-08-25T16:37:16+00:00	MULTI	78.48.376 N	006.48.131 W	241
6	2017-08-25T17:01:22+00:00	SEA	78.48.515 N	006.46.761 W	247
6	2017-08-25T18:46:54+00:00	SEA	78.49.449 N	006.32.063 W	267
6	2017-08-25T19:48:03+00:00	TV3	78.50.603 N	006.25.980 W	285
6	2017-08-25T21:08:40+00:00	VGRAB	78.51.638 N	006.17.604 W	301
6	2017-08-25T21:57:54+00:00	MIK	78.50.951 N	006.20.668 W	293
6	2017-08-25T22:52:03+00:00	MIK	78.48.004 N	006.23.697 W	274
6	2017-08-25T23:34:49+00:00	HAPS	78.47.807 N	006.28.929 W	274
6	2017-08-26T00:05:23+00:00	HAPS	78.48.756 N	006.23.998 W	286
6	2017-08-26T00:20:52+00:00	VGRAB	78.48.900 N	006.23.993 W	285
6	2017-08-26T00:36:21+00:00	VGRAB	78.49.068 N	006.23.944 W	287

Station	Time	Gear code	Position latitude start	Position longitude start	Bottom depth start
6	2017-08-26T00:49:41+00:00	VGRAB	78.49.242 N	006.23.738 W	290
6	2017-08-26T01:17:02+00:00	VGRAB	78.49.510 N	006.19.851 W	299
6	2017-08-26T01:32:35+00:00	VGRAB	78.49.699 N	006.19.819 W	299
6	2017-08-26T01:52:57+00:00	VGRAB	78.49.905 N	006.19.652 W	296
6	2017-08-26T02:01:12+00:00	VGRAB	78.50.002 N	006.19.304 W	303
7	2017-08-26T04:11:47+00:00	CTD	78.39.647 N	006.39.280 W	247
7	2017-08-26T05:51:28+00:00	CTD	78.32.001 N	007.02.139 W	268
8	2017-08-26T07:56:20+00:00	SEA	78.30.554 N	006.17.660 W	302
8	2017-08-26T08:24:44+00:00	SEA	78.30.619 N	006.18.342 W	304
8	2017-08-26T09:13:24+00:00	MULTI	78.30.817 N	006.20.613 W	301
8	2017-08-26T09:47:21+00:00	SEA	78.30.986 N	006.22.421 W	303
8	2017-08-26T10:30:16+00:00	WP2	78.31.188 N	006.23.984 W	302
8	2017-08-26T10:40:33+00:00	WP2	78.31.244 N	006.24.345 W	308
9	2017-08-26T12:48:34+00:00	SEA	78.22.090 N	006.30.380 W	281
10	2017-08-26T14:53:34+00:00	SEA	78.12.201 N	006.21.498 W	335
11	2017-08-26T17:14:35+00:00	SEA	78.04.812 N	005.45.786 W	331
12	2017-08-26T17:42:37+00:00	WP2	78.04.761 N	005.45.118 W	331
12	2017-08-26T17:55:02+00:00	WP2	78.04.732 N	005.44.837 W	331
11	2017-08-26T18:28:44+00:00	MULTI	78.04.730 N	005.43.774 W	338
11	2017-08-26T18:42:21+00:00	SEA	78.04.741 N	005.43.369 W	339
12	2017-08-26T19:29:38+00:00	HAPS	78.04.847 N	005.41.744 W	328
12	2017-08-26T20:08:00+00:00	HAPS	78.04.898 N	005.40.507 W	334
12	2017-08-26T20:29:11+00:00	HAPS	78.04.987 N	005.39.617 W	334
12	2017-08-26T20:54:35+00:00	VGRAB	78.04.983 N	005.39.510 W	335
12	2017-08-26T21:09:08+00:00	VGRAB	78.05.004 N	005.39.379 W	335
12	2017-08-26T21:25:05+00:00	VGRAB	78.05.015 N	005.39.366 W	335
12	2017-08-26T21:37:58+00:00	VGRAB	78.05.039 N	005.39.241 W	339
12	2017-08-26T21:52:02+00:00	VGRAB	78.05.053 N	005.39.192 W	339
12	2017-08-26T22:11:43+00:00	HAPS	78.05.113 N	005.38.779 W	337
12	2017-08-26T22:29:39+00:00	HAPS	78.05.155 N	005.38.551 W	341
12	2017-08-26T22:45:10+00:00	HAPS	78.05.199 N	005.38.347 W	340
12	2017-08-26T23:09:07+00:00	MIK	78.05.419 N	005.37.528 W	338
13	2017-08-27T06:22:23+00:00	MULTI	77.30.573 N	002.01.771 W	384
13	2017-08-27T07:34:57+00:00	SEA	77.31.110 N	002.05.337 W	2999
13	2017-08-27T09:23:11+00:00	WP2	77.32.105 N	002.09.066 W	2987
13	2017-08-27T10:04:38+00:00	SEA	77.32.313 N	002.09.700 W	2984
13	2017-08-27T10:41:43+00:00	MIK	77.32.112 N	002.10.667 W	2985
13	2017-08-27T11:15:06+00:00	WP2	77.31.287 N	002.14.014 W	2996
13	2017-08-27T11:25:21+00:00	WP2	77.31.280 N	002.13.944 W	2997
14	2017-08-27T13:43:01+00:00	SEA	77.17.976 N	003.13.012 W	2968
14	2017-08-27T15:26:15+00:00	FOTÃ	77.17.379 N	003.20.547 W	2977
15	2017-08-27T20:26:38+00:00	WP2	77.03.443 N	004.49.931 W	1482
15	2017-08-27T20:35:48+00:00	WP2	77.03.435 N	004.50.304 W	1479
15	2017-08-27T20:47:35+00:00	SEA	77.03.436 N	004.50.719 W	1475
15	2017-08-27T21:19:04+00:00	MULTI	77.03.462 N	004.51.772 W	1462
15	2017-08-27T22:34:41+00:00	SEA	77.03.596 N	004.54.112 W	1440

Station	Time	Gear code	Position latitude start	Position longitude start	Bottom depth start
15	2017-08-28T00:06:19+00:00	MIK	77.03.916 N	004.55.121 W	1430
15	2017-08-28T00:51:27+00:00	MIK	77.02.472 N	004.54.826 W	1438
15	2017-08-28T01:19:46+00:00	HAPS	77.03.770 N	004.53.855 W	1442
15	2017-08-28T02:24:34+00:00	VGRAB	77.04.407 N	004.51.105 W	1461
15	2017-08-28T03:20:24+00:00	VGRAB	77.04.489 N	004.50.368 W	1460
15	2017-08-28T04:16:24+00:00	VGRAB	77.04.426 N	004.49.403 W	1471
16	2017-08-28T06:25:10+00:00	SEA	76.57.096 N	005.31.576 W	1246
17	2017-08-28T08:38:41+00:00	SEA	76.51.641 N	006.09.273 W	1066
18	2017-08-28T11:47:13+00:00	MULTI	76.48.013 N	006.52.416 W	846
18	2017-08-28T12:17:49+00:00	WP2	76.48.071 N	006.52.653 W	412
18	2017-08-28T12:27:36+00:00	WP2	76.48.045 N	006.52.917 W	398
18	2017-08-28T12:40:27+00:00	SEA	76.48.011 N	006.53.197 W	390
18	2017-08-28T13:32:33+00:00	MIK	76.47.897 N	006.53.971 W	375
18	2017-08-28T13:59:40+00:00	MIK	76.46.523 N	006.57.712 W	362
18	2017-08-28T14:31:33+00:00	WP 3	76.45.652 N	007.00.329 W	351
18	2017-08-28T14:59:11+00:00	WP 3	76.45.594 N	007.01.016 W	345
18	2017-08-28T16:25:55+00:00	TV3	76.44.196 N	007.05.818 W	333
19	2017-08-28T17:43:39+00:00	SEA	76.40.838 N	007.22.201 W	325
20	2017-08-28T19:21:29+00:00	WP2	76.32.215 N	007.34.623 W	581
20	2017-08-28T19:35:44+00:00	SEA	76.32.086 N	007.35.082 W	576
20	2017-08-28T20:10:16+00:00	MULTI	76.31.725 N	007.36.309 W	576
20	2017-08-28T21:03:19+00:00	SEA	76.31.067 N	007.36.586 W	620
20	2017-08-28T22:18:08+00:00	HAPS	76.30.153 N	007.38.992 W	618
20	2017-08-28T23:04:36+00:00	MIK	76.29.531 N	007.39.065 W	641
20	2017-08-28T23:53:13+00:00	MIK	76.27.619 N	007.32.748 W	36
20	2017-08-29T00:25:59+00:00	HAPS	76.28.524 N	007.34.770 W	757
20	2017-08-29T01:26:38+00:00	VGRAB	76.27.936 N	007.35.775 W	774
20	2017-08-29T01:56:35+00:00	VGRAB	76.27.629 N	007.36.490 W	781
1	2017-08-29T03:45:39+00:00	SEA	76.17.633 N	007.20.536 W	788
22	2017-08-29T06:02:25+00:00	SEA	76.08.129 N	007.44.320 W	31
23	2017-08-29T08:20:58+00:00	SEA	76.02.870 N	008.25.457 W	1352
23	2017-08-29T09:00:04+00:00	MULTI	76.02.521 N	008.29.358 W	1313
23	2017-08-29T10:02:57+00:00	SEA	76.02.440 N	008.31.975 W	1286
23	2017-08-29T11:52:53+00:00	MIK	76.01.794 N	008.36.117 W	1269
23	2017-08-29T12:52:39+00:00	WP 3	76.01.439 N	008.35.917 W	1284
23	2017-08-29T13:47:15+00:00	WP2	76.01.133 N	008.38.075 W	1279
24	2017-08-29T14:58:49+00:00	SEA	75.58.387 N	009.19.586 W	974
24	2017-08-29T17:35:07+00:00	FOTÁ	75.54.830 N	009.24.903 W	1092
25	2017-08-29T19:15:56+00:00	SEA	75.52.925 N	010.03.118 W	723
26	2017-08-29T21:33:06+00:00	SEA	75.54.298 N	010.46.652 W	300
27	2017-08-29T23:08:45+00:00	MIK	75.53.481 N	011.24.131 W	298
27	2017-08-29T23:58:33+00:00	MIK	75.55.122 N	011.19.326 W	202
27	2017-08-30T00:55:34+00:00	HAPS	75.53.134 N	011.24.175 W	298
27	2017-08-30T01:33:29+00:00	HAPS	75.53.168 N	011.23.400 W	300
27	2017-08-30T01:47:30+00:00	VGRAB	75.53.138 N	011.23.057 W	297
27	2017-08-30T02:17:44+00:00	VGRAB	75.53.004 N	011.22.695 W	298

Station	Time	Gear code	Position latitude start	Position longitude start	Bottom depth start
27	2017-08-30T02:30:53+00:00	VGRAB	75.53.033 N	011.22.592 W	299
27	2017-08-30T02:44:00+00:00	VGRAB	75.53.022 N	011.22.494 W	299
27	2017-08-30T03:10:32+00:00	VGRAB	75.53.041 N	011.22.119 W	297
27	2017-08-30T03:24:48+00:00	VGRAB	75.53.016 N	011.21.795 W	293
27	2017-08-30T03:41:33+00:00	HAPS	75.52.942 N	011.21.398 W	293
27	2017-08-30T03:59:15+00:00	SEA	75.52.844 N	011.21.281 W	294
27	2017-08-30T04:31:49+00:00	MULTI	75.52.583 N	011.20.858 W	293
27	2017-08-30T05:13:20+00:00	SEA	75.52.433 N	011.20.049 W	291
27	2017-08-30T06:14:09+00:00	TV3	75.53.352 N	011.17.783 W	267
27	2017-08-30T07:23:51+00:00	WP2	75.54.710 N	011.12.830 W	228
27	2017-08-30T07:37:32+00:00	WP2	75.54.777 N	011.12.638 W	229
27	2017-08-30T07:57:44+00:00	WP 3	75.54.846 N	011.12.392 W	231
28	2017-08-30T09:30:36+00:00	SEA	75.48.853 N	011.55.031 W	357
29	2017-08-30T13:00:19+00:00	SEA	75.44.418 N	012.17.788 W	355
29	2017-08-30T17:31:13+00:00	SEA	75.48.564 N	012.29.035 W	402
29	2017-08-30T18:18:11+00:00	SEA	75.48.558 N	012.29.448 W	402
29	2017-08-30T18:58:16+00:00	MULTI	75.48.546 N	012.30.214 W	402
29	2017-08-30T19:39:02+00:00	WP2	75.48.446 N	012.31.800 W	399
29	2017-08-30T19:52:24+00:00	WP2	75.48.436 N	012.32.077 W	393
29	2017-08-30T20:09:03+00:00	SEA	75.48.442 N	012.32.428 W	388
29	2017-08-30T21:34:53+00:00	TV3	75.49.305 N	012.42.173 W	394
29	2017-08-30T23:05:59+00:00	HAPS	75.49.635 N	012.46.308 W	397
29	2017-08-30T23:50:00+00:00	MIK	75.49.920 N	012.45.378 W	389
29	2017-08-31T00:29:49+00:00	MIK	75.51.264 N	012.39.809 W	396
29	2017-08-31T00:56:36+00:00	HAPS	75.52.114 N	012.36.564 W	402
29	2017-08-31T01:16:37+00:00	VGRAB	75.52.235 N	012.36.665 W	400
29	2017-08-31T01:37:55+00:00	VGRAB	75.52.326 N	012.36.876 W	406
29	2017-08-31T01:55:36+00:00	VGRAB	75.52.366 N	012.37.169 W	404
29	2017-08-31T02:15:22+00:00	VGRAB	75.52.505 N	012.37.407 W	405
29	2017-08-31T02:35:07+00:00	VGRAB	75.52.631 N	012.37.679 W	406
30	2017-08-31T04:07:58+00:00	SEA	75.57.443 N	013.17.313 W	278
31	2017-08-31T05:50:04+00:00	SEA	76.04.970 N	013.46.646 W	257
32	2017-08-31T07:43:38+00:00	SEA	76.13.506 N	014.13.772 W	269
32	2017-08-31T07:58:15+00:00	MULTI	76.13.635 N	014.14.356 W	278
32	2017-08-31T08:50:25+00:00	SEA	76.14.146 N	014.16.075 W	270
32	2017-08-31T09:35:02+00:00	MIK	76.14.814 N	014.18.016 W	271
32	2017-08-31T10:18:53+00:00	WP2	76.13.177 N	014.20.737 W	271
32	2017-08-31T10:31:53+00:00	WP2	76.13.279 N	014.20.653 W	275
32	2017-08-31T10:46:05+00:00	WP 3	76.13.392 N	014.20.585 W	277
33	2017-08-31T12:19:13+00:00	SEA	76.23.751 N	014.24.750 W	249
34	2017-08-31T14:04:11+00:00	SEA	76.33.854 N	014.16.796 W	215
35	2017-08-31T15:29:08+00:00	SEA	76.34.491 N	015.01.581 W	215
36	2017-08-31T16:49:29+00:00	SEA	76.35.730 N	015.37.948 W	191
36	2017-08-31T17:51:17+00:00	TV3	76.36.043 N	015.33.255 W	208
36	2017-08-31T19:12:16+00:00	MIK	76.34.997 N	015.26.588 W	243
36	2017-08-31T20:06:11+00:00	SEA	76.35.371 N	015.39.133 W	190

Station	Time	Gear code	Position latitude start	Position longitude start	Bottom depth start
36	2017-08-31T21:06:46+00:00	WP2	76.35.507 N	015.39.419 W	190
36	2017-08-31T21:23:41+00:00	WP2	76.35.563 N	015.39.361 W	189
36	2017-08-31T21:40:23+00:00	HAPS	76.35.656 N	015.39.334 W	189
36	2017-08-31T22:04:58+00:00	HAPS	76.35.715 N	015.39.074 W	191
36	2017-08-31T22:15:56+00:00	VGRAB	76.35.765 N	015.38.978 W	191
36	2017-08-31T22:27:28+00:00	VGRAB	76.35.841 N	015.39.001 W	193
36	2017-08-31T22:38:45+00:00	VGRAB	76.35.855 N	015.39.035 W	192
36	2017-08-31T22:50:15+00:00	VGRAB	76.35.919 N	015.39.012 W	190
36	2017-08-31T23:00:31+00:00	VGRAB	76.35.993 N	015.39.034 W	192
36	2017-08-31T23:28:04+00:00	VGRAB	76.37.256 N	015.43.759 W	189
36	2017-08-31T23:38:56+00:00	VGRAB	76.37.296 N	015.43.755 W	187
36	2017-08-31T23:49:50+00:00	VGRAB	76.37.339 N	015.43.809 W	187
36	2017-08-31T23:59:40+00:00	VGRAB	76.37.388 N	015.43.790 W	189
36	2017-09-01T00:10:05+00:00	VGRAB	76.37.428 N	015.43.732 W	192
37	2017-09-01T04:26:23+00:00	SEA	76.47.509 N	016.19.560 W	194
38	2017-09-01T08:44:36+00:00	MULTI	76.51.932 N	015.10.316 W	242
38	2017-09-01T09:06:26+00:00	SEA	76.52.190 N	015.10.583 W	246
38	2017-09-01T09:47:47+00:00	WP2	76.52.216 N	015.09.526 W	243
38	2017-09-01T10:00:32+00:00	WP2	76.52.232 N	015.09.118 W	241
38	2017-09-01T10:20:16+00:00	WP 3	76.52.320 N	015.08.464 W	247
38	2017-09-01T10:37:31+00:00	WP 3	76.52.353 N	015.08.051 W	247
38	2017-09-01T11:00:08+00:00	SEA	76.52.467 N	015.07.467 W	251
38	2017-09-01T12:04:24+00:00	MIK	76.52.919 N	015.07.044 W	247
39	2017-09-01T14:11:16+00:00	SEA	76.57.064 N	014.23.875 W	210
40	2017-09-01T15:53:47+00:00	SEA	77.06.269 N	014.18.398 W	256
41	2017-09-01T17:37:10+00:00	WP2	77.15.878 N	014.00.290 W	256
41	2017-09-01T17:48:28+00:00	WP2	77.15.883 N	014.00.325 W	252
41	2017-09-01T18:02:09+00:00	SEA	77.15.870 N	014.00.479 W	249
41	2017-09-01T18:38:31+00:00	MULTI	77.15.760 N	014.01.238 W	258
41	2017-09-01T19:02:43+00:00	MIK	77.15.898 N	014.01.997 W	253
41	2017-09-01T19:23:20+00:00	MIK	77.16.641 N	014.05.459 W	253
41	2017-09-01T20:08:42+00:00	SEA	77.17.716 N	014.12.255 W	265
41	2017-09-01T21:14:04+00:00	SEA	77.17.591 N	014.13.068 W	269
41	2017-09-01T22:02:37+00:00	HAPS	77.17.430 N	014.13.483 W	270
41	2017-09-01T22:38:35+00:00	HAPS	77.17.403 N	014.12.661 W	271
41	2017-09-01T22:51:43+00:00	VGRAB	77.17.449 N	014.12.082 W	268
41	2017-09-01T23:04:35+00:00	VGRAB	77.17.433 N	014.11.695 W	263
41	2017-09-01T23:16:10+00:00	VGRAB	77.17.385 N	014.11.408 W	267
41	2017-09-01T23:28:31+00:00	VGRAB	77.17.344 N	014.11.050 W	262
41	2017-09-01T23:42:10+00:00	VGRAB	77.17.311 N	014.10.553 W	261
42	2017-09-02T01:12:08+00:00	SEA	77.24.995 N	013.42.544 W	264
43	2017-09-02T02:42:23+00:00	SEA	77.25.446 N	012.59.226 W	259
44	2017-09-02T04:11:06+00:00	SEA	77.25.115 N	012.13.644 W	401
45	2017-09-02T06:01:13+00:00	SEA	77.24.719 N	011.30.256 W	463
45	2017-09-02T06:28:53+00:00	MULTI	77.24.660 N	011.30.589 W	465
45	2017-09-02T07:13:21+00:00	SEA	77.24.472 N	011.30.692 W	467

Station	Time	Gear code	Position latitude start	Position longitude start	Bottom depth start
45	2017-09-02T08:34:21+00:00	WP2	77.24.828 N	011.30.543 W	463
45	2017-09-02T08:46:06+00:00	WP2	77.24.857 N	011.30.478 W	463
45	2017-09-02T08:59:49+00:00	WP 3	77.25.014 N	011.30.360 W	451
45	2017-09-02T09:18:03+00:00	VGRAB	77.25.217 N	011.30.263 W	442
45	2017-09-02T09:36:24+00:00	VGRAB	77.25.330 N	011.30.055 W	437
45	2017-09-02T09:53:39+00:00	VGRAB	77.25.410 N	011.29.813 W	435
45	2017-09-02T10:41:36+00:00	MIK	77.26.012 N	011.32.323 W	444
46	2017-09-02T14:48:22+00:00	SEA	77.25.071 N	014.27.071 W	291
47	2017-09-02T16:31:17+00:00	SEA	77.25.115 N	015.13.495 W	318
48	2017-09-02T18:15:48+00:00	SEA	77.24.956 N	016.02.344 W	274
49	2017-09-02T19:57:54+00:00	SEA	77.28.472 N	016.41.708 W	82
49	2017-09-02T20:32:36+00:00	WP2	77.28.131 N	016.40.494 W	81
49	2017-09-02T20:59:46+00:00	MULTI	77.28.070 N	016.40.010 W	71
49	2017-09-02T21:15:31+00:00	MULTI	77.28.022 N	016.40.070 W	71
49	2017-09-02T21:32:57+00:00	SEA	77.28.427 N	016.39.104 W	80
49	2017-09-02T22:02:41+00:00	MIK	77.28.518 N	016.38.979 W	84
49	2017-09-02T22:28:29+00:00	HAPS	77.29.502 N	016.40.401 W	120
49	2017-09-02T23:00:12+00:00	HAPS	77.29.446 N	016.40.271 W	117
49	2017-09-02T23:08:49+00:00	VGRAB	77.29.455 N	016.40.288 W	117
49	2017-09-02T23:17:41+00:00	VGRAB	77.29.444 N	016.40.317 W	116
49	2017-09-02T23:26:07+00:00	VGRAB	77.29.418 N	016.40.212 W	115
49	2017-09-02T23:34:04+00:00	VGRAB	77.29.375 N	016.40.079 W	117
49	2017-09-02T23:41:45+00:00	VGRAB	77.29.366 N	016.40.042 W	117
50	2017-09-03T01:05:04+00:00	SEA	77.23.032 N	017.15.454 W	168
51	2017-09-03T02:32:15+00:00	SEA	77.12.913 N	017.16.462 W	196
52	2017-09-03T04:04:15+00:00	SEA	77.06.569 N	017.51.506 W	245
53	2017-09-03T05:28:49+00:00	SEA	76.57.002 N	018.04.962 W	162
54	2017-09-03T07:12:31+00:00	SEA	76.43.339 N	018.19.224 W	151
54	2017-09-03T07:49:47+00:00	MULTI	76.42.830 N	018.19.800 W	150
54	2017-09-03T08:32:34+00:00	SEA	76.42.173 N	018.19.104 W	205
54	2017-09-03T09:11:58+00:00	MIK	76.41.934 N	018.18.212 W	233
54	2017-09-03T09:49:18+00:00	WP2	76.43.233 N	018.17.346 W	211
54	2017-09-03T10:02:18+00:00	WP2	76.43.159 N	018.17.591 W	213
54	2017-09-03T10:18:48+00:00	WP 3	76.43.001 N	018.17.966 W	214
55	2017-09-03T12:33:28+00:00	SEA	76.44.934 N	019.23.163 W	198
56	2017-09-03T14:01:48+00:00	SEA	76.35.001 N	019.28.172 W	249
57	2017-09-03T16:33:57+00:00	FOTÃ	76.28.300 N	019.29.725 W	387
57	2017-09-03T17:48:37+00:00	SEA	76.30.817 N	019.28.578 W	333
57	2017-09-03T18:18:08+00:00	MULTI	76.31.059 N	019.29.282 W	327
57	2017-09-03T18:45:16+00:00	WP2	76.31.239 N	019.29.786 W	325
57	2017-09-03T18:54:47+00:00	WP2	76.31.295 N	019.29.879 W	322
57	2017-09-03T20:00:53+00:00	WP 3	76.30.963 N	019.28.605 W	329
57	2017-09-03T20:13:05+00:00	SEA	76.31.035 N	019.28.465 W	320
57	2017-09-03T21:32:16+00:00	SEA	76.31.322 N	019.27.490 W	318
57	2017-09-03T22:18:24+00:00	TV3	76.29.827 N	019.29.634 W	361
57	2017-09-03T23:30:54+00:00	MIK	76.27.182 N	019.29.078 W	402

Station	Time	Gear code	Position latitude start	Position longitude start	Bottom depth start
57	2017-09-03T23:57:48+00:00	MIK	76.27.765 N	019.29.099 W	397
57	2017-09-04T01:00:47+00:00	HAPS	76.31.246 N	019.28.492 W	322
57	2017-09-04T01:41:36+00:00	HAPS	76.31.387 N	019.28.635 W	318
57	2017-09-04T01:56:18+00:00	VGRAB	76.31.439 N	019.28.798 W	320
57	2017-09-04T02:11:26+00:00	VGRAB	76.31.467 N	019.28.822 W	321
57	2017-09-04T02:25:29+00:00	VGRAB	76.31.480 N	019.28.808 W	319
58	2017-09-04T05:08:44+00:00	SEA	76.11.589 N	018.54.375 W	326
59	2017-09-04T08:10:56+00:00	SEA	75.52.429 N	018.34.565 W	268
60	2017-09-04T09:59:48+00:00	SEA	75.42.862 N	018.24.991 W	457
61	2017-09-04T12:32:04+00:00	SEA	75.51.480 N	017.53.830 W	61
61	2017-09-04T13:04:42+00:00	MULTI	75.51.291 N	017.53.488 W	71
61	2017-09-04T13:25:09+00:00	WP2	75.51.162 N	017.53.162 W	89
61	2017-09-04T13:36:31+00:00	WP2	75.51.166 N	017.52.948 W	86
61	2017-09-04T13:47:23+00:00	WP2	75.51.118 N	017.52.796 W	89
61	2017-09-04T13:56:17+00:00	WP2	75.51.081 N	017.52.594 W	92
61	2017-09-04T14:15:12+00:00	SEA	75.51.001 N	017.52.197 W	101
61	2017-09-04T15:04:37+00:00	HAPS	75.51.456 N	017.54.958 W	61
61	2017-09-04T15:48:16+00:00	HAPS	75.51.558 N	017.54.920 W	56
61	2017-09-04T15:52:09+00:00	HAPS	75.51.528 N	017.55.015 W	57
61	2017-09-04T15:58:26+00:00	VGRAB	75.51.514 N	017.55.116 W	57
61	2017-09-04T16:05:45+00:00	VGRAB	75.51.500 N	017.55.283 W	59
61	2017-09-04T16:12:22+00:00	VGRAB	75.51.424 N	017.55.330 W	62
61	2017-09-04T16:28:34+00:00	VGRAB	75.51.313 N	017.55.696 W	83
61	2017-09-04T16:35:32+00:00	VGRAB	75.51.325 N	017.55.872 W	81
61	2017-09-04T17:18:10+00:00	MIK	75.50.810 N	017.42.109 W	171
62	2017-09-04T18:58:00+00:00	SEA	75.52.652 N	016.57.880 W	71
63	2017-09-04T20:37:52+00:00	SEA	75.52.681 N	016.16.651 W	101
63	2017-09-04T21:04:29+00:00	HAPS	75.52.524 N	016.15.679 W	99
63	2017-09-04T21:11:29+00:00	HAPS	75.52.520 N	016.15.522 W	98
63	2017-09-04T21:29:17+00:00	HAPS	75.52.485 N	016.14.963 W	99
63	2017-09-04T21:59:28+00:00	VGRAB	75.52.444 N	016.13.958 W	111
63	2017-09-04T22:09:57+00:00	VGRAB	75.52.425 N	016.13.662 W	108
63	2017-09-04T22:16:23+00:00	VGRAB	75.52.413 N	016.13.461 W	104
63	2017-09-04T22:23:25+00:00	VGRAB	75.52.398 N	016.13.247 W	105
63	2017-09-04T22:30:39+00:00	VGRAB	75.52.380 N	016.13.038 W	107
63	2017-09-04T22:38:29+00:00	VGRAB	75.52.310 N	016.12.744 W	111
63	2017-09-04T22:45:17+00:00	VGRAB	75.52.297 N	016.12.416 W	115
63	2017-09-04T22:52:32+00:00	VGRAB	75.52.288 N	016.12.105 W	118
64	2017-09-05T01:39:00+00:00	SEA	75.41.485 N	015.06.800 W	199
65	2017-09-05T03:25:31+00:00	SEA	75.31.942 N	014.53.165 W	197
66	2017-09-05T04:58:09+00:00	SEA	75.31.942 N	014.53.161 W	197
66	2017-09-05T05:38:05+00:00	MULTI	75.25.509 N	014.18.795 W	209
66	2017-09-05T06:02:24+00:00	WP2	75.25.413 N	014.17.870 W	200
66	2017-09-05T06:17:47+00:00	WP2	75.25.299 N	014.17.124 W	196
66	2017-09-05T06:34:05+00:00	SEA	75.25.194 N	014.16.322 W	196
66	2017-09-05T07:09:23+00:00	MIK	75.25.109 N	014.14.828 W	193

Station	Time	Gear code	Position latitude start	Position longitude start	Bottom depth start
66	2017-09-05T08:23:24+00:00	TV3	75.26.183 N	014.12.657 W	217
67	2017-09-05T10:28:46+00:00	SEA	75.18.796 N	013.45.927 W	213
68	2017-09-05T12:03:46+00:00	SEA	75.12.954 N	013.17.966 W	212
69	2017-09-05T13:48:13+00:00	SEA	75.05.835 N	013.04.451 W	218
70	2017-09-05T15:02:21+00:00	SEA	75.05.835 N	013.04.451 W	218
70	2017-09-05T15:34:56+00:00	MULTI	74.58.987 N	012.47.375 W	565
70	2017-09-05T16:12:01+00:00	WP2	74.58.447 N	012.48.596 W	570
70	2017-09-05T16:26:35+00:00	WP2	74.58.281 N	012.49.057 W	573
70	2017-09-05T17:09:54+00:00	WP 3	74.57.714 N	012.50.721 W	559
70	2017-09-05T17:58:01+00:00	SEA	74.57.235 N	012.51.927 W	555
70	2017-09-05T19:54:29+00:00	SEA	74.56.880 N	012.56.294 W	475
70	2017-09-05T20:19:01+00:00	WP 3	74.56.518 N	012.58.710 W	460
70	2017-09-05T21:12:52+00:00	HAPS	74.55.619 N	013.01.289 W	453
70	2017-09-05T21:38:58+00:00	HAPS	74.55.168 N	013.03.141 W	450
70	2017-09-05T22:00:09+00:00	VGRAB	74.54.754 N	013.04.443 W	459
70	2017-09-05T22:25:53+00:00	VGRAB	74.54.231 N	013.05.862 W	460
70	2017-09-05T22:41:48+00:00	VGRAB	74.53.897 N	013.06.779 W	462
70	2017-09-05T23:01:51+00:00	VGRAB	74.53.445 N	013.07.974 W	462
70	2017-09-05T23:23:58+00:00	VGRAB	74.52.956 N	013.09.335 W	465
71	2017-09-06T01:11:46+00:00	SEA	74.49.701 N	012.24.688 W	1243
72	2017-09-06T03:37:01+00:00	SEA	74.43.309 N	011.52.710 W	1158
73	2017-09-06T06:06:36+00:00	SEA	74.37.061 N	011.20.619 W	762
73	2017-09-06T06:36:07+00:00	MULTI	74.36.840 N	011.21.138 W	324
73	2017-09-06T07:49:16+00:00	WP2	74.36.336 N	011.22.166 W	2938
73	2017-09-06T08:01:00+00:00	WP2	74.36.263 N	011.22.371 W	2938
73	2017-09-06T08:12:47+00:00	SEA	74.36.186 N	011.22.490 W	2940
73	2017-09-06T10:20:44+00:00	BONGO	74.34.770 N	011.18.581 W	2969
73	2017-09-06T14:52:20+00:00	FOTÃ	74.33.912 N	011.13.448 W	3002
73	2017-09-06T16:24:56+00:00	MIK	74.36.170 N	011.26.044 W	2935
73	2017-09-06T17:06:10+00:00	MIK	74.36.152 N	011.34.712 W	2889
74	2017-09-06T20:16:57+00:00	SEA	74.41.751 N	013.25.646 W	914
74	2017-09-06T20:42:20+00:00	SEA	74.41.467 N	013.27.304 W	896
74	2017-09-06T21:10:38+00:00	MULTI	74.41.120 N	013.28.741 W	878
74	2017-09-06T22:05:49+00:00	WP2	74.40.438 N	013.31.679 W	831
74	2017-09-06T22:15:19+00:00	WP2	74.40.271 N	013.31.878 W	846
74	2017-09-06T22:30:43+00:00	SEA	74.40.023 N	013.32.186 W	874
74	2017-09-06T23:59:19+00:00	MIK	74.38.915 N	013.32.449 W	1049
74	2017-09-07T00:43:00+00:00	MIK	74.40.084 N	013.27.606 W	1079
74	2017-09-07T00:58:25+00:00	VGRAB	74.40.386 N	013.26.226 W	1091
74	2017-09-07T01:43:00+00:00	VGRAB	74.39.862 N	013.26.568 W	1178
75	2017-09-07T02:43:40+00:00	VGRAB	74.40.389 N	013.26.358 W	1085
75	2017-09-07T03:38:06+00:00	HAPS	74.40.366 N	013.25.857 W	1434
75	2017-09-07T10:46:43+00:00	SEA	74.22.470 N	014.16.234 W	611
76	2017-09-07T14:42:11+00:00	FOTÃ	74.37.903 N	014.15.749 W	170
76	2017-09-07T17:24:13+00:00	SEA	74.49.202 N	013.52.599 W	188
76	2017-09-07T18:05:12+00:00	MULTI	74.48.695 N	013.54.000 W	191

Station	Time	Gear code	Position latitude start	Position longitude start	Bottom depth start
76	2017-09-07T18:28:48+00:00	WP2	74.48.499 N	013.55.032 W	183
76	2017-09-07T18:40:26+00:00	WP2	74.48.350 N	013.55.351 W	181
76	2017-09-07T18:51:56+00:00	WP2	74.48.204 N	013.55.678 W	179
76	2017-09-07T19:13:36+00:00	SEA	74.47.948 N	013.56.334 W	179
76	2017-09-07T19:48:49+00:00	SEA	74.47.564 N	013.57.080 W	176
76	2017-09-07T20:36:51+00:00	TV3	74.48.161 N	013.55.570 W	180
76	2017-09-07T22:15:51+00:00	MIK	74.48.896 N	013.53.640 W	188
76	2017-09-07T22:33:17+00:00	MIK	74.48.125 N	013.55.222 W	188
76	2017-09-08T00:29:33+00:00	HAPS	74.40.570 N	013.31.078 W	838
76	2017-09-08T01:29:03+00:00	VGRAB	74.40.666 N	013.31.670 W	789
76	2017-09-08T02:08:16+00:00	VGRAB	74.40.653 N	013.31.170 W	817
76	2017-09-08T02:46:21+00:00	VGRAB	74.40.625 N	013.31.479 W	810
76	2017-09-08T03:26:33+00:00	HAPS	74.40.226 N	013.30.991 W	897
76	2017-09-08T05:02:06+00:00	VGRAB	74.42.996 N	013.21.331 W	906
76	2017-09-08T05:36:02+00:00	VGRAB	74.42.611 N	013.21.474 W	951
76	2017-09-08T06:13:19+00:00	VGRAB	74.42.158 N	013.21.612 W	1023
77	2017-09-08T09:41:48+00:00	SEA	74.34.247 N	012.53.898 W	2320
78	2017-09-08T14:48:32+00:00	SEA	75.02.742 N	011.30.417 W	2070
79	2017-09-08T17:18:19+00:00	SEA	75.10.206 N	011.57.429 W	1100
80	2017-09-08T19:48:07+00:00	SEA	75.17.396 N	012.24.295 W	244
80	2017-09-08T20:22:22+00:00	MULTI	75.17.311 N	012.25.707 W	238
80	2017-09-08T20:43:55+00:00	WP2	75.17.184 N	012.26.422 W	238
80	2017-09-08T20:54:11+00:00	WP2	75.17.129 N	012.26.692 W	235
80	2017-09-08T21:07:31+00:00	WP 3	75.17.045 N	012.27.018 W	237
80	2017-09-08T21:20:24+00:00	WP 3	75.16.967 N	012.27.263 W	235
80	2017-09-08T21:40:25+00:00	SEA	75.16.850 N	012.27.527 W	236
80	2017-09-08T22:28:37+00:00	MIK	75.16.452 N	012.26.870 W	238
0	2017-09-08T23:12:48+00:00	MIK	75.14.968 N	012.20.285 W	291
81	2017-09-09T00:30:30+00:00	SEA	75.12.634 N	012.11.155 W	518
81	2017-09-09T02:00:02+00:00	TV3	75.13.301 N	012.08.447 W	555
82	2017-09-09T05:08:02+00:00	HAPS	75.26.859 N	011.24.350 W	991
82	2017-09-09T06:27:37+00:00	SEA	75.25.892 N	011.25.602 W	1007
83	2017-09-09T10:47:34+00:00	FOTÃ	75.48.074 N	010.41.912 W	408
84	2017-09-09T12:55:47+00:00	HAPS	75.48.631 N	010.01.070 W	978
86	2017-09-09T17:34:29+00:00	HAPS	76.08.924 N	008.29.528 W	1018
87	2017-09-09T22:34:11+00:00	HAPS	76.33.236 N	007.03.342 W	1091

[Blank page]

IDENTIFICATION OF OFFSHORE HOT SPOTS

An integrated biological oceanographic survey focusing on biodiversity, productivity and food chain relations

This study provides information on the marine ecosystem in the western Greenland Sea and the shelf off Northeast Greenland. The biology in the area was clearly associated with the physical-chemical environment. Integrated phytoplankton biomass and production were highest at or outside the East Greenland shelf break. Likewise, the zooplankton biomass was highest along the shelf break area, and species composition reflected the origin of the water. As expected, the survey showed low diversity and abundance of seabirds and marine mammals. In total 22 and 9 species were observed, respectively. Little auks were the most numerous seabirds with the highest densities found along the shelf break.